Title

Effects of Climate Change-Induced Low Flows on Sierra Nevada Stream Ecosystems

Permalink

https://escholarship.org/uc/item/0d9951n6

Author

Leathers, Kyle

Publication Date

2024

Peer reviewed|Thesis/dissertation

Effects of Climate Change-Induced Low Flows on Sierra Nevada Stream Ecosystems

By

Kyle Leathers

A dissertation submitted in partial satisfaction of the

requirements for the degree of

Doctor of Philosophy

in

Environmental Science, Policy, and Management

in the

Graduate Division

of the

University of California, Berkeley

Committee in charge:

Dr. Albert Ruhi, Chair
Dr. David Herbst
Dr. Mary Power
Dr. Manuela Girotto

Summer 2024

Abstract

Effects of Climate Change-Induced Low Flows on Sierra Nevada Stream Ecosystems

By

Kyle Leathers

Doctor of Philosophy in Environmental Science, Policy, and Management

University of California, Berkeley

Professor Albert Ruhi, Chair

Climate change is altering physical environments and biotic communities globally. High-elevation mountain streams are particularly at risk because rising air temperatures can reduce snowpack and extend the duration of summer low flow, consequently altering a variety of abiotic variables. In turn, populations and communities exposed to environmental change can undergo shifts in phenology, fitness, and behavior–altering the ecosystem processes that these biota control. In this dissertation, I examined how climate change-induced low flows are impacting stream water temperature, invertebrate communities, and the mechanistic pathways through which low flow acts on communities. I achieved this with three complementary approaches. First, I tested the effects of earlier low flows on organismal phenology, community composition, and resulting ecosystem processes via a mesocosm experiment that simulated flow regimes expected under end-of-the-century climate projections. Second, I assessed spatiotemporal variation in thermal vulnerability to climate change in a mid-elevation stream network in the Sierra Nevada over an extreme drought year (2020–2021). Lastly, I investigated the abiotic and biotic pathways whereby drought alters invertebrate community composition and structure in a California Sierra Nevada watershed across nested spatio-temporal scales–from microhabitat to watershed, and over two decades. I found that extended low flows will likely have diverse abiotic and biotic ramifications on stream ecosystems, but the mechanisms behind these changes are complex and require deep understanding of the ecosystem context.

In the summer of 2019, I experimentally examined how earlier snowmelt will alter the phenology of mountain stream organisms and ecosystem processes via outdoor mesocosm stream channels in the Eastern Sierra Nevada, California. Channels were assigned to three hydrograph treatments that simulated the current flow regime or a 3 to 6 week earlier return to summer baseflow conditions projected under regional climate change scenarios. I measured discharge, water temperature, primary production, benthic macroinvertebrate secondary production and phenology, macroinvertebrate emergence, and predatory behavior of a riparian bird. Water temperature increased under advanced low flow conditions, which may have played a role in biofilm production to respiration ratios declining by 32%. Additionally, the majority of the benthic and emergent invertebrate species explaining community dissimilarity changed in phenology as a consequence of the early low-flow treatment. Emergent flux pulses of the dominant insect group (Chironomidae) also nearly doubled in magnitude, benefitting riparian predators. One such riparian predator, the Brewer's Blackbird, gained access to feed on benthic macroinvertebrates under the 6 week early low flow treatment that aligned with their nesting

period. Changes in both invertebrate community structure (composition) and ecosystem processes were mostly fine-scale, and response diversity at the community level stabilized seasonally aggregated responses. My findings illustrate how climate change in mountain streams at the rain-to-snow transition is poised to alter the dynamics of stream food webs via fine-scale changes in phenology even when community structure and ecosystem processes appear stable over longer time periods.

In 2020-2021, I deployed a nested array of high-frequency sensors and used advances in time-series models to examine spatiotemporal variation in thermal vulnerability. This work took place in Bull Creek, one of the Kings River Experimental Watersheds (KREW). Stream thermal sensitivity to atmospheric warming fluctuated strongly over the year and peaked in spring and summer. I found that spatially, the reach scale (~50 m) best captured variation in summer thermal regimes. Spatial variation in summer water temperature was driven firstly by upstream water temperature, with elevation, discharge, and conductivity as local correlates. Lastly, I combined the estimated summer thermal sensitivity and downscaled projections of summer air temperature to forecast end-of-the-century stream warming. I found that 25.5% of cold-water habitat may be lost under high-emissions scenario RCP 8.5 (or 7.9% under mitigated RCP 4.5). This estimated reduction suggests that up to 27.2% of stream macroinvertebrate biodiversity could be stressed or threatened in what was previously cold-water habitat. My results support that thermal vulnerability in montane stream networks may be highly variable over space and time. Taking spatiotemporal variation into account is critical to understand how climate change will impact high mountain stream ecosystems through rising temperatures and shifts in precipitation.

Stream low flows can alter communities via multiple environmental and biological mechanisms across time and space, but support is mixed as to which mechanisms are paramount and how spatial and temporal context determines their relative importance. I investigated the mechanisms whereby low flow alters stream invertebrate community composition and structure in high-mountain streams–across space and over time. To this end, I sampled aquatic macroinvertebrates from the same 60 sites in Bull Creek where temperature sensors were deployed in 2020, using a nested sampling design. Additionally, long-term data in four reaches were sampled 11 times from 2002 to 2023. The inspected abiotic mechanisms of drought (temperature, water velocity, and fine sediment) all explained variation in a similar percentage of taxa in the community (36.8% - 47.4%), but effects differed when examined spatially vs. temporally. Total spatial variance explained by abiotic mechanisms for each species had no relationship with its temporal counterpart. Biological mechanisms also differed across space and time; community dissimilarity across space was driven by differences in fine sediment causing species *turnover* (i.e., sensitive species being replaced by tolerant ones), while temporal dissimilarity was driven by differences in temperature and water velocity causing *reordering* (i.e., shifts in relative abundance). These results challenge the key assumption of 'space-for-time' substitution that underpins abundant research on climate change ecology. I contend that space-for-time substitution approaches may be inappropriate in mountain river studies because of their hierarchical structure, high temporal variability, and mechanisms operating distinctly across space and time.

This dissertation provides evidence that climate change-induced low flows will alter Sierra Nevada stream ecosystems in a variety of ways. High elevation mountain streams will increasingly be affected by climate change, a threat that is not well understood despite extensive research efforts. My findings demonstrate that climate change effects are highly context

dependent and examining them at the appropriate spatiotemporal scale is necessary to properly assess their impact. Notably, changing abiotic conditions due to extended low flows may benefit some ecosystem processes and taxa at the upper edge of their elevation range, potentially at the cost of coldwater specialists adapted to harsh high mountain streams. High response diversity of species in this dissertation ensured that ecosystem processes often remained stable even if many individual species responded to changing flow regimes. Advances in ecological models and methodology enable finer assessment of environments and communities than ever before, but my research shows that extensive data collection and knowledge of local natural history are necessary for these methods to be effective. This dissertation expands the field of drought ecology, which is of the utmost importance in a quickly changing world.

Table of Contents

Acknowledgments

My dissertation is the combined effort of many individuals who have played large and small, but always meaningful, roles. I am grateful to everyone who has collaborated with me, supported me, and been a friend in the past six years.

I am grateful to my advisor, Albert Ruhi, who is not only one of the most talented and dedicated people I know, but also an excellent mentor who has built an encouraging and considerate lab group. I knew I could always rely on you for help. I am thankful for your support to examine a wide variety of research methods, along with your keen eye for meaningful ecological questions. You enabled me to achieve everything I wanted in graduate school.

I thank my dissertation and qualifying exam committees for pointing me in the right direction and ensuring I had the foundational knowledge to design my chapters and interpret their results. I am especially indebted to David Herbst, who has been a secondary advisor in many ways to me and generously shared his expertise on Sierra Nevada macroinvertebrates. Thank you Dave for teaching me the Lauterborn organs, mentum teeth arrangements, and dorsal tubercles needed to identify the invertebrates in my samples. Your research and support have been foundational to my dissertation, and you have significantly contributed to every chapter here within. I am also thankful to Mary Power for gently and convincingly teaching me the importance of natural history, understanding your study system holistically, and the value of realistic experiments. It was a pleasure to learn from you as a graduate student instructor for Freshwater Ecology and I appreciate your feedback on all my chapters. Lastly, I am thankful to Manuela Girotto and Steven Beissinger for helping me to understand the hydrology of the Sierra Nevada and climate change, respectively.

Thank you to my labmates, who have gone above and beyond in their research and efforts to build community. Thanks to Guillermo de Mendoza for your cheerful sincerity, friendship, and willingness to help with everything in the lab, including my research. Guillermo significantly contributed to Chapter 2 of this dissertation and had the keen eyes to notice the Brewer's Blackbirds acting differently. It was a pleasure to work with Tongbi Tu and Romain Sarremejane and learn from them. Megan Pagliaro and Jessie Moravek brightened the lab with their arrival and midwestern sensibilities. Robert Fournier, Parsa Saffarinia, and Denise Colombano brought energy and experience to the lab and this dissertation greatly benefits from their input. Travis Apgar co-led field sampling in the StreamCLIMES project and was a good fishing partner. Melissa von Mayrhauser and Rose Mohammadi have been such joyful and encouraging labmates that cheer up everyone around them. Charlotte Evangélista and Tatiana Tronel were encouraging collaborators and have done a great follow up project to Chapter 2 at SNARL. Kendall Archie has chosen the challenging task of coordinating everything in the lab and has helped smooth out the end of my PhD as a man for all seasons. Lastly, it was a pleasure to learn alongside Tim Jäger how to distinguish Chironominae wing veins and tibia combs on course to us both graduating this summer.

Thank you to the undergraduates that have helped me collect and identify tens of thousands of macroinvertebrates. Gabriela Doerschlag significantly contributed to Chapter 2 as my fieldwork partner and developed an excellent senior thesis project. Thank you, Gabby, for your positive

1

Introduction

The global environment faces threats from a myriad of anthropogenic sources like land use change, pollution, and invasive species; however, none may be as ubiquitous as climate change. Human emitted greenhouse gasses last decades to centuries in the atmosphere and trap emitted radiation from the earth, altering climates across the globe (Karl and Trenberth 2003). Air temperatures have increased as a result, along with shifts in precipitation and the frequency of extreme weather events. These climatic changes have altered body size, behavior, phenology, distributions, and ecosystem processes (Weiskopf et al. 2020). However, models of ecological responses to climate change are highly uncertain and contrast with paeloecological observations (Moritz and Agudo 2013). Improving our understanding of climate change impacts may be most important in sensitive, isolated mountain and freshwater environments (Poff et al. 2012, Bowler et al. 2017).

Mountain streams are vulnerable to climate change due to their isolated nature and expected future hydrologic change. High mountains, home to cold-adapted taxa, can be isolated akin to islands due to the ruggedness of the terrain and sharp environmental gradients that hinder dispersal (Pauli and Halloy 2019). This isolation is exacerbated in mountain streams, where species can be further constrained by movement within the river network and suitable habitat may be fragmented across the landscape (Woodward et al. 2010). Although high montane streams are resilient to warming from increases in air temperature (Isaak et al. 2016), changes in hydrological processes, particularly snowmelt, are likely. In high montane streams, snow typically accumulates in the winter, followed by large increases in discharge as a result of snowmelt. Streamflow gradually declines afterwards until baseflow (i.e., low flow) is reached, potentially after peak air temperatures have passed. The natural flow regime of these streams is threatened by increases in air temperature that are projected to advance snowmelt by up to 50 days in the future as a result of precipitation switching to rain and increased snowmelt in winter-spring (Musselman et al. 2017, Reich et al. 2018). The commencement, duration, and intensity of low flows will advance or increase as a result (Yarnell et al. 2010). Droughts are also expected to become more frequent and severe in many areas such as the American Southwest, exacerbating low flows for mountains therewithin (Cayan et al. 2010). Thus, montane stream ecosystems may be highly vulnerable to climate change as a consequence of more severe low-flow periods occurring earlier and lasting longer (Herbst et al. 2019).

Low flow events intensified by climate change will affect habitat conditions and water quality. Specifically, low-flow events are associated with increased water temperature, decreased dissolved oxygen, reduced water velocity, increased sedimentation, shallower water depth, and reduced habitat connectivity (Rolls et al. 2012). Anticipating the impacts of these often covarying factors is critical, but complex (Carlisle et al. 2016). For example, although increased air temperature alone is unlikely to increase montane water temperature, low flows reduce thermal buffering and can increase maximum daily average water temperature up to 10°C (Elliott

2000, Rolls et al. 2012). However, changes in abiotic low flow conditions are not always coupled. A low flow experiment in New Zealand found that water velocity declined by 57% but no difference was observed in water temperature (Dewson et al. 2007a). If suspended sediment levels do not decline drastically with low flow, reduced water velocity can increase fine sediment deposition which disrupts connection to groundwater and reduces habitat heterogeneity (Dewson et al. 2007b). Increased fine sediment may last long after low flows end, until flushing flows occur. These altered habitat conditions may profoundly impact populations, communities, and food webs.

Low flow is responsible for complex biotic responses that researchers are still striving to understand. Increasing maximum temperatures during the summer can push species beyond their physiological limits due to thermal stress and/or insufficient dissolved oxygen levels (Trimmel et al. 2018). Warming also alters individual growth rate, behavior, and phenology in aquatic insects and fish (Hogg and Williams 1996, Woodward et al. 2010, Ledger et al. 2013). Effects on individuals may scale up to affect whole ecosystems via changes in metabolism, decomposition, and community composition (Dewson et al. 2007b, Pyne and Poff 2017). Reduced water velocity during drought alters species' ability to avoid predators and harms filter feeders (Malmqvist and Sackmann 1996). Lastly, sedimentation can reduce macroinvertebrate abundance and species richness in streams because of homogenized habitat and reduced access to the hyporheic zone (Dewson et al. 2007b). Despite the need to understand how drought acts upon communities, study results vary as to which abiotic mechanisms of drought are most influential (Hawkins et al. 1997, Waddle and Holmquist 2013, Herbst et al. 2019). A reason for this could be that drought effects are often assessed at different scales, where both scale-dependencies and cross-scale interactions can occur [i.e., patterns that are only apparent at a particular scale, or patterns that emerge when comparing scales (Levin 1992)]. Studies comparing communities across space also may not be equivalent to those comparing communities over time (Angert 2024). Detailed study of the mechanisms and context of low-flow effects on stream communities is needed to anticipate and appropriately react to climate change-enhanced droughts in mountain streams–and more broadly, to inform river ecosystem conservation and restoration (Palmer and Ruhi 2019).

Within this dissertation, I aim to improve our understanding of how climate change-altered low flows will affect Sierra Nevada stream ecosystems. According to best available science, climate change will advance median snowmelt runoff in the Sierra Nevada up to two months by 2080 (Musselman et al. 2017, Reich et al. 2018). Changes in snowmelt timing will likely alter water temperature and low flow duration with complex ecological consequences (Rolls et al. 2012). This dissertation may help identify vulnerable mountain streams, refugia, and effective management options. For example, if increased sedimentation—not temperature—drives community assembly, then groundwater-fed streams that mitigate summer warming may not be refugia from low flow. A mechanistic understanding of responses to low flows at appropriate scales and across space and time can be integrated to generate expectations for impending effects of future climate change.

In Chapter 2, I experimentally tested how climate-induced, extended summer low flow conditions alter the phenology of mountain stream organisms and the ecosystem processes that these organisms control. Increased water temperatures during low flow often cause phenological shifts in freshwater organisms, but it is uncertain if phenological change in a multitrophic

community alters ecosystem processes (Woods et al. 2021). Ecosystem responses to low flow may be sudden (e.g., after a certain abiotic threshold is passed) or cumulative, but few studies have examined the timing of change (Rolls et al. 2012, Rosero-López et al. 2022). I predicted that extended low flows would increase water temperature, alter biofilm metabolism, and advance benthic and emergent macroinvertebrate phenology. In order to test these predictions, I subjected nine flow-through outdoor stream mesocosms in California's Sierra Nevada to three flow regime treatments and examined whether the onset of low flow caused immediate or delayed shifts in aspects of the ecosystem at fine time scales.

In Chapter 3, I examined the extent to which Sierra Nevada streams are vulnerable to warming from climate change via drivers of variation across space and time. Determining the spatial and temporal scale that variation occurs at was also valuable in this pursuit. Models predicting future stream water temperatures may fall short due to assumptions that the relationship between water and air temperature is static, along with uncertainty regarding how thermal regimes vary across spatial scales (Lisi et al. 2015, Leach and Moore 2019). Addressing these knowledge gaps, along with accounting for how water temperature propagates downstream and is mediated by local conditions, can enable watershed wide estimations of thermal conditions now and in a warmer future. I predicted that thermal sensitivity varies over time at fine scales, water temperature varies spatially at the reach scale, and that current invertebrate communities would be vulnerable to projected future warming. I carried this research out using a nested array of high-frequency sensors needed for spatial network models, and advanced time series models, in a model Sierra Nevada watershed.

In Chapter 4, I investigated the abiotic and biotic pathways whereby droughts may alter invertebrate community composition and structure. Stream low flows can alter communities via multiple environmental (abiotic) and biological (biotic) mechanisms, but their relative importance is uncertain (Hawkins et al. 1997, Waddle and Holmquist 2013, Herbst et al. 2019). Further, it is unclear whether drought-induced community change across space and over time are realized through similar environmental and biological processes (Angert 2024). This is assumed for space-for-time substitution, where, for example, a warm site at the base of a mountain can 'preview' the community at higher elevations if temperatures increase. Addressing the accuracy of space-for-time approaches is critical, as they underpin much of the literature on climate change ecology (Lovell et al. 2023). I predicted that different abiotic mechanisms of drought would all affect species in unique ways, and the way they affect species and biotic mechanisms of community change would differ across space and time. I monitored a river network in California's Sierra Nevada encompassing 60 sites following a nested spatial structure combined with long-term data in four reaches that were sampled 11 times from 2002 to 2023. This allowed me to compare spatial and temporal ecological pathways of drought.

Discovering how low flows mechanistically affect Sierra Nevada stream ecosystems requires integrating results across approaches, scales, contexts, and end points. In this pursuit, I combined experimental, observational, and modeling methods to incorporate causation with realism and foresight. This dissertation seeks to further our understanding of low flow effects, but the approaches and methods used are broadly effective at exploring the effects of other stressors in flowing waters. Ultimately addressing freshwater threats will require not only understanding the mechanisms at play, but also knowledge of how to restore ecosystems based

on natural history. Even perfect knowledge of the environment will come to nothing if zeal and love for nature do not spur action and sacrifice; scientists must continue to share the beauty of the natural world within their unique community spheres.

References

Angert, A. L. 2024. The space-for-time gambit fails a robust test. Proceedings of the National Academy of Sciences 121:e2320424121.

Bowler, D. E., C. Hof, P. Haase, I. Kröncke, O. Schweiger, R. Adrian, L. Baert, H.-G. Bauer, T. Blick, R. W. Brooker, W. Dekoninck, S. Domisch, R. Eckmann, F. Hendrickx, T. Hickler, S. Klotz, A. Kraberg, I. Kühn, S. Matesanz, A. Meschede, H. Neumann, R. O'Hara, D. J. Russell, A. F. Sell, M. Sonnewald, S. Stoll, A. Sundermann, O. Tackenberg, M. Türkay, F. Valladares, K. van Herk, R. van Klink, R. Vermeulen, K. Voigtländer, R. Wagner, E. Welk, M. Wiemers, K. H. Wiltshire, and K. Böhning-Gaese. 2017. Cross-realm assessment of climate change impacts on species' abundance trends. Nature Ecology & Evolution 1:1–7.

Carlisle, D. M., S. M. Nelson, and J. May. 2016. Associations of stream health with altered flow and water temperature in the Sierra Nevada, California. Ecohydrology 9:930–941.

Cayan, D. R., T. Das, D. W. Pierce, T. P. Barnett, M. Tyree, and A. Gershunova. 2010. Future dryness in the Southwest US and the hydrology of the early 21st century drought. Proceedings of the National Academy of Sciences of the United States of America 107:21271–21276.

Dewson, Z. S., A. B. W. James, and R. G. Death. 2007a. Invertebrate responses to short-term water abstraction in small New Zealand streams. Freshwater Biology 52:357–369.

Dewson, Z. S., A. B. W. James, and R. G. Death. 2007b. A review of the consequences of decreased flow for instream habitat and macroinvertebrates. Journal of the North American Benthological Society 26:401–415.

Elliott, J. M. 2000. Pools as refugia for brown trout during two summer droughts: Trout responses to thermal and oxygen stress. Journal of Fish Biology 56:938–948.

Hawkins, C. P., J. N. Hogue, L. M. Decker, and J. W. Feminella. 1997. Channel Morphology, Water Temperature, and Assemblage Structure of Stream Insects. Journal of the North American Benthological Society 16:728–749.

Herbst, D. B., S. D. Cooper, R. B. Medhurst, S. W. Wiseman, and C. T. Hunsaker. 2019. Drought ecohydrology alters the structure and function of benthic invertebrate communities in mountain streams. Freshwater Biology 64:886–902.

Hogg, I. D., and D. D. Williams. 1996. Response of stream invertebrates to a global-warming thermal regime: an ecosystem-level manipulation. Ecology 77:395–407.

Isaak, D. J., M. K. Young, C. H. Luce, S. W. Hostetler, S. J. Wenger, E. E. Peterson, J. M. Ver Hoef, M. C. Groce, D. L. Horan, and D. E. Nagel. 2016. Slow climate velocities of mountain streams portend their role as refugia for cold-water biodiversity. Proceedings of the National Academy of Sciences 113:4374–4379.

Karl, T. R., and K. E. Trenberth. 2003. Modern Global Climate Change. Science 302:1719–1723.

Leach, J. A., and R. D. Moore. 2019. Empirical Stream Thermal Sensitivities May Underestimate Stream Temperature Response to Climate Warming. Water Resources Research 55:5453–5467.

Ledger, M. E., L. E. Brown, F. K. Edwards, L. N. Hudson, A. M. Milner, and G. Woodward. 2013. Extreme Climatic Events Alter Aquatic Food Webs. A Synthesis of Evidence from a Mesocosm Drought Experiment. Advances in Ecological Research 48:343–395.

Levin, S. A. 1992. The problem of pattern and scale in ecology. Ecology 73:1943–1967.

Lisi, P. J., D. E. Schindler, T. J. Cline, M. D. Scheuerell, and P. B. Walsh. 2015. Watershed geomorphology and snowmelt control stream thermal sensitivity to air temperature. Geophysical Research Letters 42:3380–3388.

Lovell, R. S. L., S. Collins, S. H. Martin, A. L. Pigot, and A. B. Phillimore. 2023. Space-for-time substitutions in climate change ecology and evolution. Biological Reviews 98:2243–2270.

Malmqvist, B., and G. Sackmann. 1996. Changing risk of predation for a filter-feeding insect along a current velocity gradient. Oecologia 108:450–458.

Moritz, C., and R. Agudo. 2013. The Future of Species Under Climate Change: Resilience or Decline? Science 341:504–508.

Musselman, K. N., M. P. Clark, C. Liu, K. Ikeda, and R. Rasmussen. 2017. Slower snowmelt in a warmer world. Nature Climate Change 7:214–219.

Palmer, M., and A. Ruhi. 2019. Linkages between flow regime, biota, and ecosystem processes: Implications for river restoration. Science 365.

Pauli, H., and S. R. P. Halloy. 2019. High Mountain Ecosystems Under Climate Change. Page Oxford Research Encyclopedia of Climate Science. Oxford University Press.

Poff, N. L., J. D. Olden, and D. L. Strayer. 2012. Climate Change and Freshwater Fauna Extinction Risk. Pages 309–336 *in* L. Hannah, editor. Saving a Million Species. Island Press/Center for Resource Economics, Washington, DC.

Pyne, M. I., and N. L. R. Poff. 2017. Vulnerability of stream community composition and function to projected thermal warming and hydrologic change across ecoregions in the western United States. Global Change Biology 23:77–93.

Reich, K., N. Berg, D. Walton, M. Schwartz, F. Sun, X. Huang, and A. Hall. 2018. Climate Change in the Sierra Nevada: California's Water Future. UCLA Center for Climate Science.

Rolls, R. J., C. Leigh, and F. Sheldon. 2012. Mechanistic effects of low-flow hydrology on riverine ecosystems: ecological principles and consequences of alteration. Freshwater Science 31:1163–1186.

Rosero-López, D., M. Todd Walter, A. S. Flecker, B. De Bièvre, R. Osorio, D. González-Zeas, S. Cauvy-Fraunié, and O. Dangles. 2022. A whole-ecosystem experiment reveals flow-induced shifts in a stream community. Communications Biology 5:420.

Trimmel, H., P. Weihs, D. Leidinger, H. Formayer, G. Kalny, and A. Melcher. 2018. Can riparian vegetation shade mitigate the expected rise in stream temperatures due to climate change during heat waves in a human-impacted pre-alpine river? Hydrology and Earth System Sciences 22:437–461.

Waddle, T. J., and J. G. Holmquist. 2013. Macroinvertebrate response to flow changes in a subalpine stream: Predictions from two-dimensional hydrodynamic models. River Research and Applications 29:366–379.

Weiskopf, S. R., M. A. Rubenstein, L. G. Crozier, S. Gaichas, R. Griffis, J. E. Halofsky, K. J. W. Hyde, T. L. Morelli, J. T. Morisette, R. C. Muñoz, A. J. Pershing, D. L. Peterson, R. Poudel, M. D. Staudinger, A. E. Sutton-Grier, L. Thompson, J. Vose, J. F. Weltzin, and K. P. Whyte. 2020. Climate change effects on biodiversity, ecosystems, ecosystem services, and natural resource management in the United States. Science of The Total Environment 733:137782.

Woods, T., A. Kaz, and X. Giam. 2021. Phenology in freshwaters: a review and recommendations for future research. Ecography 6:1–14.

Woodward, G., D. M. Perkins, and L. E. Brown. 2010. Climate change and freshwater ecosystems: Impacts across multiple levels of organization. Philosophical Transactions of the Royal Society B: Biological Sciences 365:2093–2106.

Yarnell, S. M., J. H. Viers, and J. F. Mount. 2010. Ecology and Management of the Spring Snowmelt Recession. BioScience 60:114–127.

2

Climate change is poised to alter mountain stream ecosystem processes via organismal phenological shifts

Abstract

Climate change is affecting the phenology of organisms and ecosystem processes across a wide range of environments. However, the links between organismal and ecosystem process change in complex communities remain uncertain. In snow dominated watersheds, snowmelt in the spring and early summer, followed by a long low-flow period, characterizes the natural flow regime of streams and rivers. Here, we examined how earlier snowmelt will alter the phenology of mountain stream organisms and ecosystem processes via an outdoor mesocosm experiment in stream channels in the Eastern Sierra Nevada, California. The low-flow treatment, simulating a three to six week earlier return to summer baseflow conditions projected under climate change scenarios in the region, increased water temperature and reduced biofilm production to respiration ratios by 32%. Additionally, most of the invertebrate species explaining community change (56% and 67% of the benthic and emergent taxa, respectively), changed in phenology as a consequence of the low-flow treatment. Further, emergent flux pulses of the dominant insect group (Chironomidae) almost doubled in magnitude, benefitting a generalist riparian predator. Changes in both invertebrate community structure (composition) and functioning (production) were mostly fine-scale, and response diversity at the community level stabilized seasonally-aggregated responses. Our study illustrates how climate change in vulnerable mountain streams at the rain-to-snow transition is poised to alter the dynamics of stream food webs via fine-scale changes in phenology—leading to novel predator-prey 'matches' or 'mismatches' even when community structure and ecosystem processes appear stable at the annual scale.

Introduction

Recent climate shifts in temperature and precipitation patterns have already altered the phenology of many organisms (1, 2). Climate warming has changed the timing of key life history events such as hatching, migration, mating, blooming, and death in a wide variety of plants and animals (3). These changes may benefit individual species via extended growing seasons and resource pulses; or harm them via stress, habitat contraction, and spatio-temporal mismatches between energy needs and food availability (4, 5). Mounting evidence supports that even phenological shifts of individual species can impact ecosystem processes at large scales. For example, milder winters have delayed mortality of mountain pine beetles (*Dendroctonus ponderosae*), enabling range expansion and causing widespread tree mortality that has transformed forests from being carbon sinks to sources (6). Similarly, warmer springs have advanced ephemeral plant flowering but not pollinator emergence, ultimately reducing production (7). However, many ecosystem processes (e.g., primary production, secondary production, and cross-ecosystem subsidies) often depend on many species. While it is typically assumed that phenological shifts can alter ecosystem processes, few studies have examined this question in complex, multi-trophic systems (8, 9).

Understanding the link between phenological change and ecosystem process change is particularly crucial in streams and rivers because freshwater ecosystems are highly sensitive to environmental change (10). Climate change has disproportionately eroded freshwater species populations (11), and extinction rates for freshwater organisms under future climate change are expected to be an order of magnitude higher than for marine and terrestrial counterparts (10, 12). This high vulnerability is due to the fragmented nature of freshwater habitat, the climate-sensitivity of thermal and hydrologic regimes (10, 12), and the dominance of ectotherms in freshwater food webs (13). Despite the high potential for climate-driven phenological shifts in fresh waters, it is uncertain how whole communities may respond to warming–and whether phenological change may alter the ecosystem processes that these organisms control (14).

Among freshwater ecosystems, small streams in snow-dominated catchments are particularly vulnerable to climate change (15). In mountain ranges where snow is the dominant form of precipitation (e.g., in California's Sierra Nevada), snowmelt in the late spring and early summer constitutes the majority of annual runoff and is often followed by a period of baseflow conditions in late summer and fall (16), in which streams are sustained by groundwater. Here, we use the general term *low flow* in place of *baseflow* to describe low discharge levels during the dry season (17). Climate change is predicted to reduce snowpack and advance snowmelt, which will extend summer low flow duration by up to two months by the end of the century, increasing the overlap between periods of low flow and peak air temperature (18). Climate change has already altered snowmelt in mid-elevation mountain ranges globally, by decreasing snowpack and shifting the rain-to-snow transition zone (19). Some impacts of extended summer low flows on stream biodiversity and ecosystem processes, like fish population declines, often occur rapidly via physiological stress when flow drops below a threshold (20); in contrast, other responses may be cumulative [e.g., the accumulation of cyanobacteria in biofilm (21)] and may thus only be noticeable after a period of time. However, few studies have examined the immediate vs. delayed effects of low flows on stream biodiversity and ecosystem processes using frequent temporal

monitoring. Such an approach is costlier than before-after experimental designs, but may reveal the scales and mechanisms driving ecological change more precisely (20).

One key impact of earlier, extended summer low flow conditions in small streams is that low flows may accelerate climate-driven warming via reduced thermal buffering. Warming can shift community composition and structure by replacing species adapted to cold, well-oxygenated waters (cold stenotherms) with those from warmer environments (eurytherms) (22). Warming also controls key ecosystem processes, and often increases ecosystem-level primary production and respiration rates (23, 24). Because water temperature controls metabolic rates of ectotherms, warming is expected to speed up aquatic insect growth rates and development, potentially advancing the timing of metamorphosis and emergence of adult, flying insects. In turn, changes in the timing and/or magnitude of emerging insects could affect foraging behavior of riparian birds, lizards, and bats, which often rely on emerging aquatic insects as a resource pulse (25). However, we note here that temperature-driven changes in secondary production are not well understood. Theory predicts that warming should not affect secondary production, given the approximately opposed effects that warming should have on community biomass (by shrinking mean body size of species) and turnover rates (by accelerating them) (26, 27). Empirical tests have provided mixed support for this expectation, owing to variation in species thermal preferences (28) and basal resources responding to warming (29). The link between warming-driven community change in a stream food web and changes in ecosystem processes has become a recent focus of research (24), and it could be greatly advanced by experiments with more complex, realistic assemblages.

Here we sought to test how climate-induced, extended summer low flow conditions, simulating an end-of-century hydroclimate of reduced snowpack and earlier snowmelt (18) will alter the phenology of mountain stream organisms—and the ecosystem processes that these organisms control. In contrast to most research on the topic, focused on the effects of flow magnitude (30–33), here we focused on the effects of an earlier snowmelt-driven flow recession associated with a longer summer low flow period (i.e., low-flow timing and duration) to better examine ecological impacts arising from phenological change. We broadly hypothesized that this climate change-induced flow regime change would alter the whole food web—from epilithic biofilm metabolism to stream invertebrate production and emergence, primarily through increases in water temperature (3, 4). However, in agreement with recent findings on thermal response diversity [i.e., different species respond in different directions and/or magnitudes to temperature change (27)], we also expected the community-level responses to be buffered against change, relative to population-level responses.

Specifically, we predicted that extended summer low flow would: (1) increase water temperature and biofilm respiration—altering the rates and balance of biofilm metabolism; (2) advance phenology and secondary production of stream invertebrates, but not change production at the seasonal scale due to stabilizing mechanisms (e.g., response diversity); and (3) advance cross-ecosystem subsidies of emergent stream invertebrates, which could be consequential if overlap shifts between peak resource availability and peak demand by riparian predators. Notably, while some of these changes may be apparent immediately, others may build over time (Figure 1).
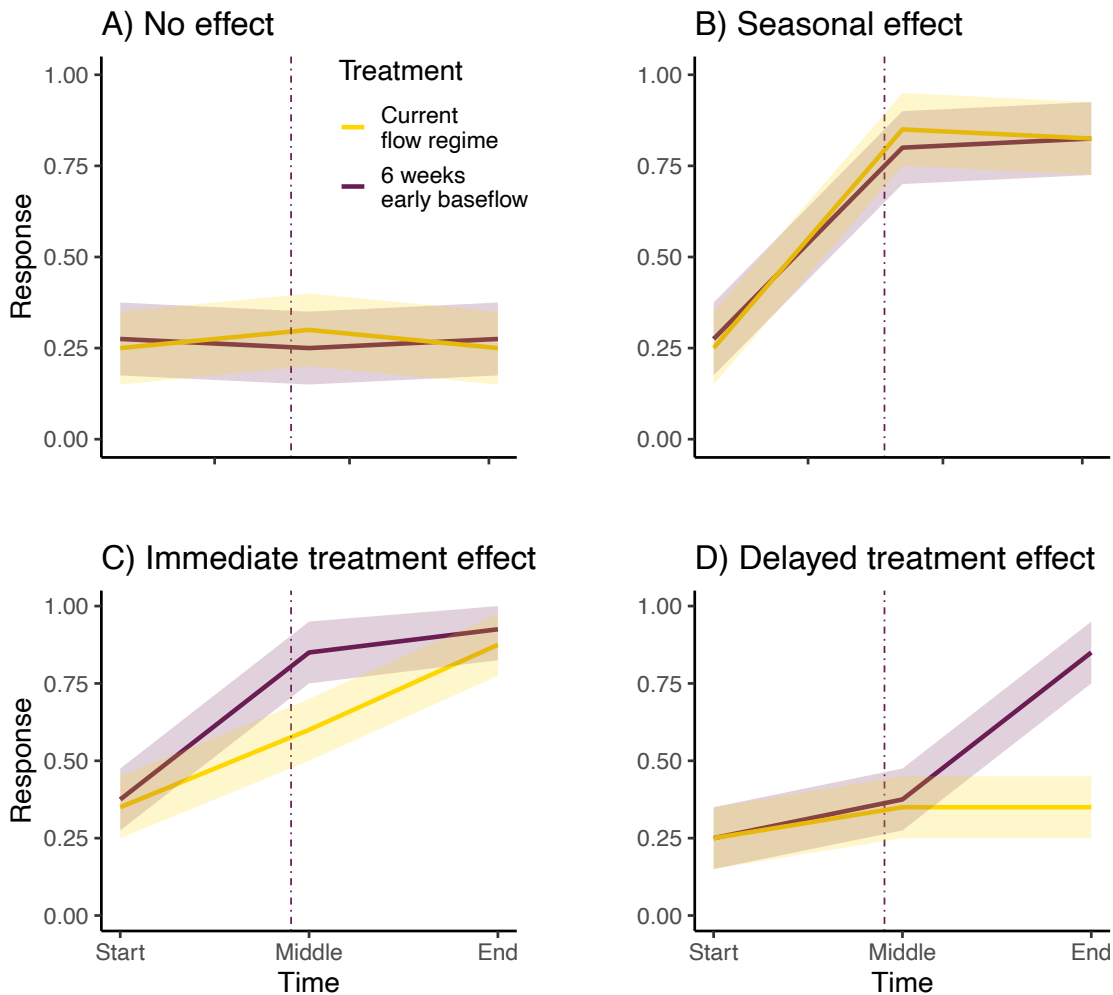
Figure 1. Potential ecological responses to low-flow treatment. Each pair of solid lines represents a potential ecological response to the low-flow treatment, arising from comparing treatment trajectories at the *start*, *middle*, and *end* of the experiment. The vertical dashed line indicates the onset of summer low-flow. (A) No discernible change over the study period would support the absence of seasonal or treatment effects. (B) Seasonal effects would be evidenced by both treatments exhibiting similar shifts over time. (C) An immediate treatment effect would be evidenced by treatments differing significantly at the onset of treatment differences in the *middle* period, but not at the *start*. This difference may be temporary (as shown here), or sustained through the *end* of the experiment. (D) A delayed treatment effect would be evidenced by no shift occurring immediately after treatment onset, but rather at the *end* of the experiment. In our study, we predicted that differences in the timing of the onset and duration of summer low flow would cause immediate or delayed changes in our ecological responses. Onset of summer low flow in the *6-week* treatment marks the transition between the *start* and *middle* periods; while onset of summer low flow for the *Current* treatment marks the transition between the *middle* and *end* periods. See Table S1 for details on how statistical tests provide support for each of the four potential responses.

In order to test our predictions, we subjected nine flow-through outdoor stream mesocosms (*SI Appendix,* Fig. S1) in California's Sierra Nevada to three flow regime treatments: a flow regime based on historic average conditions (*Current* treatment), a mitigated climate change scenario where streamflow returns to summer low flow levels three weeks earlier than currently (*3-week* treatment), and an unmitigated climate change scenario where summer low flow begins six weeks earlier than currently (*6-week* treatment) (18). Over the course of a season, we regularly measured epilithic biofilm production and community composition, production, and emergence of benthic and emergent stream invertebrates. We examined support for seasonal, immediate, and delayed ecological responses to the low-flow treatment (Fig. 1) by quantifying changes in magnitude and phenology for each response variable. Specifically, we combined study *period* (i.e., *start*, *middle*, and *end*) with *treatment* (*Current, 3-week, 6-week)*, creating a variable that captures both timing and treatment effects (i.e., *period-treatment*; Fig. 1). This allows us to examine how low-flow treatments altered phenology. When *period-treatment* had an effect, we ran directed pairwise tests to identify which response type occurred (i.e., a *seasonal* effect, an *immediate* treatment effect, or a *delayed* treatment effect; Table S1). In addition to testing each prediction, we ran a piecewise structural equation model to identify causal pathways connecting extended low flows to our ultimate end point in the food web: aquatic insect benthic production and emergence, a critical cross-ecosystem subsidy connecting streams to riparian ecosystems (34, 35).

Methods

Experimental design

The experiment took place over four months, from May 2019 to August 2019, in nine outdoor, flow-through channels at the Sierra Nevada Aquatic Research Lab (SNARL) located near Mammoth Lakes, California [*SI Appendix,* Fig. S1 (61)]. The channels are 50 m long by 1 m wide, consist of six pools connected by long riffle sections in a meandering fashion, and are fed by the adjacent Convict Creek. Convict Creek also provided natural substrate consisting of cobbles, sand, and silt. This experimental array has been used in past research questions investigating fish growth and stream invertebrate community composition (56, 62). The artificial channels have the advantage of mimicking natural ecosystems better than recirculating field mesocosms or laboratory flumes, while allowing for replication that is difficult to obtain in natural streams. The channels were naturally colonized without alteration for over a year prior to the start of the experiment. We assigned each channel to one of three treatments (with three replicate channels each) in a block design. The three treatments were: (1) current hydrologic conditions based on the historic (long-term) hydrograph at Convict Creek (Fig. S2), with a flow regime that reaches low flow conditions around August 3rd (i.e., *Current* treatment); (2) hydrologic conditions under a mitigated climate change scenario, where the stream would return to low flow conditions three weeks earlier than it currently does (i.e., *3-week* treatment); and (3) hydrologic conditions under unmitigated climate change, where the stream would return to low flow six weeks earlier than it currently does (i.e., *6-week* treatment). These scenarios connect greenhouse gas emission trajectories to the timing and duration of summer low flow (i.e., flow at or near designed low flow), based on a recent report using hybrid downscaling to project end-of-century hydrologic change in the Sierra Nevada (18).

We regulated discharge by controlling sluice gates at the head of each channel. Flows in the channels differed by one order of magnitude between high-flow and low-flow conditions (i.e., 15 L/s and 1.5 L/s, respectively), following a typical Sierra Nevada stream hydrograph for a small stream (*SI Appendix,* Fig. S3) (63). The tenfold magnitude change in discharge, characteristic of Sierra Nevada streams, is due to the strong influence of snowmelt on the flow regime. We removed fish in the channels prior to the experiment, kept screens in place to exclude them (mesh size = 1.25 cm), and conducted electrofishing during the experiment to ensure their absence. These efforts allowed us to avoid confounding top-down effects and increase realism given first-order streams in the region tend to be fishless (unless artificially stocked). Channels were inspected and maintained daily, were heavily instrumented (see next section), and were monitored and sampled for several responses: epilithic biofilm metabolism, secondary production, and benthic and emerging stream invertebrates (composition and abundance). We tested whether each variable was explained by low flow treatment or, for time-varying variables, by *period-treatment* (i.e., the combination of time *period* and low-flow *treatment*). The three *periods* we designated in the study are: *start* (5/11/2019 - 6/10/2019), *middle* (6/11/2019 - 8/2/2019), and *end* (8/3/2019 - 8/21/2019). *Period* timespans were based on treatment timing: *start* and *middle* periods are separated by the onset of summer low flow in the *6-week* treatment, and the *middle* and *end* periods are separated by the onset of summer low flow in the *Current* treatment. The number of sampling events was balanced among periods for biofilm production and benthic macroinvertebrates. However, more samples were taken in the *middle* period for emergent macroinvertebrates compared to the other periods, as a function of the higher frequency at which this ecological response was measured (i.e., every 10 days instead of 21), to account for its pulsated nature (64).

Monitoring of environmental variables

We measured water depth and water temperature every five minutes throughout the experiment (4/21/2019–8/25/2019) with replicated pressure transducers (HOBO U20L-04, Onset). We placed a pressure transducer in the fifth pool downstream in each channel and two emerged sensors on land to correct data for fluctuations in atmospheric pressure, and thus calculate water level (i.e., pool depth). Water level series were subsequently transformed into discharge series via channel-specific rating curves. Rating curves were developed for each channel by estimating discharge manually using channel depth and velocity measurements taken with a Marsh-McBirney Flo-Mate 2000 current meter throughout the summer (17-26 repeated estimates per channel). We measured water temperature using the same HOBO U20L-04 sensors that recorded data every five minutes in pools. We averaged discharge and water temperature to hourly values, which we then used to calculate daily metrics (i.e., daily mean, minimum, maximum, and diel range).

Estimation of epilithic biofilm metabolism

We estimated epilithic biofilm production and respiration using the light/dark bottle method at each channel, once every three weeks [as done previously (65)]. We calculated respiration (ER), net primary production (NPP), and the sum of their absolute values–gross primary production (GPP). We used three representative cobbles from the streambed for each sample and measured their surface area using aluminum foil to correct for differences in surface

area. All epilithic biofilm production measurements were taken during peak sunlight hours between 10 am and 2 pm using two 90-minute incubation periods for light, followed by dark measurements. Benthic stream invertebrates were removed from rocks prior to incubation. We conducted three replicates for each channel at each sampling date ($n = 162$). Daily GPP per channel was estimated by multiplying the channel average hourly rate by the number of sunlight hours at each date ($n = 54$). We estimated daily ER per channel by multiplying the channel average hourly rate by 24 hours at each date ($n = 54$). Daily epilithic biofilm production was then estimated for the interval between each sampling date by averaging the bookend interval values. We multiplied the average interval value by the number of days in the interval and finally summed these values to generate cumulative seasonal channel estimates ($n = 9$). GPP and ER can both be higher during the day when sunlight and temperatures peak, so there is some uncertainty around our extrapolated daily and seasonal estimates. We also collected continuous dissolved oxygen series in all channels and in the feeder channel, but short water residence times in the channels prevented us from using diel variation in dissolved oxygen to model whole-ecosystem metabolism.

Sampling and processing benthic invertebrates

We sampled benthic stream invertebrates using a 500 micron Surber sampler at six visit dates three weeks apart throughout the experiment. Each sample was a composite of three subsamples (two riffle and one pool samples for 0.279 m^2 total) to represent the overall stream community. We took benthic samples for the *Current* and *6-week* treatment channels ($n = 36$) and stored them in 70% ethanol. We then subsampled the composite samples using a rotating-drum splitter in the laboratory to sort and identify at least 500 individuals from each composite sample under a stereomicroscope. All subsamples were completely processed to avoid bias regarding the size of individuals picked and identified. Benthic stream invertebrates were identified to the highest resolution possible, typically genus or species level, and all intact specimens were measured. Benthic stream invertebrate biomass was then estimated using published taxon-specific length-mass relationships (66–70). The subsampled community was multiplied by the inverse of the fraction of the total sample that was identified (e.g., if ¼ of the sample was identified to get a count over 500 individuals, then the abundance of each taxon was multiplied by 4). We assigned length values to these extrapolated individuals (and individuals that could be identified but not measured due to damage) using the length values from randomly selected individuals of the same taxon in the sample.

We sampled emergent stream invertebrates using emergence traps, each deployed for 72 hours every three weeks during the experiment. We sampled emergence four additional times halfway between the three-week intervals for every sample visit after the second one, when flows began to differ between treatments ($n = 90$ overall). We deployed emergence traps at the tail of riffles (to capture the influence of both riffle and pool habitat) next to HOBO sensors. We identified emergent insects to genus or family level (depending on taxa), and measured length of intact specimens. Emergence traps were tent-shaped, covered 0.33 m^2 of the stream, and had 2 mm white mesh (71). We chose to use emergence traps over sticky traps or other alternatives because they do not damage individuals, allowing for fine taxonomic identification that is critical to assess phenology (72). We derived seasonally-aggregated values of benthic and emergent abundance or flux, respectively, as the sum of all samples taken for each channel.

Secondary production

We estimated benthic stream invertebrate secondary production via a combination of three methods. We used the size-frequency method for taxa that were abundant throughout the experiment (i.e., >1% of total abundance) and had known generation times, excluding Chironomidae, Oligochaeta, Turbellaria, and Muscidae (73). For Chironomids, we used the instantaneous growth rate method. Production was calculated using regression equations for non-Tanypodinae chironomids, which incorporate mean temperature into growth estimates for small, medium, and large chironomids (74). Finally, we used the production to biomass ratio method (P/B) for the remaining taxa, including Tanypodinae, by multiplying seasonal biomass by known P/B ratios in literature of the closest related taxa possible (75, 76). Uncertainty in production from P/B ratios is unlikely to affect our results, as taxa in this group comprised <1% of the total assemblage production. We estimated emergent insect biomass using published, taxon-specific length-mass relationships (77). We derived seasonally-aggregated estimates of emergent production by taxon, by multiplying the average biomass between successive samples by the number of days in the interval, and by then summing interval estimates for the season.

Brewer's Blackbird feeding observations

We noticed Brewer's Blackbirds (*Euphagus cyanocephalus*) feeding in the *6-week* treatment channels at the onset of summer low flow (June 22, 2019). Brewer's Blackbirds were nesting nearby and waded in the channels to pick benthic macroinvertebrates as food for their young. We recorded feeding behavior of Brewer's Blackbirds shortly thereafter to examine if they altered the invertebrate community in the channels. We studied Brewer's Blackbird behavior by observing the time duration that any bird occupied the benthos of the channels over a 30-minute period. We measured this behavior with a stopwatch and made observations periodically throughout the remainder of the experiment between noon and 6 pm (78). We switched our target from daily to weekly observations once Brewer's Blackbirds fledged and moved to meadow habitat, far (>5 km) from the channels. Two researchers conducted these observations each time, with one person observing the six upper channels and another person observing the three lower channels. Brewer's Blackbirds were not observed feeding in the channels before summer low flow, as the high water depth prevented them from wading and they were not yet nesting at that point.

Data analysis

For our first prediction that extended summer low flow would shift epilithic biofilm metabolism phenology, we tested GPP:ER, GPP, and ER across *period-treatment* using repeated measures ANOVA and pairwise post-hoc comparisons with the Benjamini-Hochberg correction when appropriate (i.e., when *period-treatment* was significant). We log transformed GPP:ER to improve the normality of residuals. We assessed cumulative season-long GPP:ER across treatments using a 2-way analysis of variance (ANOVA) in order to assess if epilithic biofilm metabolism varied across low flow treatments. GPP and ER were tested similarly. Several ANOVA and repeated measures ANOVA tests throughout our analyses violated the assumption of equal variance (based on a Fligner-Killeen test) but were still the best available method to test

our questions. In such cases, we visually confirmed that statistical patterns were not driven by a single sample with high leverage.

For our second prediction regarding stream invertebrate phenology and production, we first used permutational multivariate analysis of variance (PERMANOVA) tests based on 999 permutations with the function *adonis2* in the *vegan* R package in order to quantify benthic and emergent community change over time and across treatments (79). We also ran pairwise post-hoc comparisons with the Benjamini-Hochberg correction, when appropriate. We estimated community dissimilarity using the Bray-Curtis statistic, and visualized community trajectories via non-metric multidimensional scaling (NMDS). We fit individual taxa using the function *envfit*, also in the *vegan* package, and subsequently filtered the taxa based on which had a highly significant correlation with the NMDS axes ($P \leq 0.002$; *SI Appendix,* Fig. S10, Table S6, and Table S12). Taxa that were significantly correlated with a NMDS axis were further tested for variation in abundance across *period-treatment*.

In order to quantify how *period-treatment* may change benthic stream invertebrate taxa populations and emergent flux in aquatic insects, we used repeated measures ANOVA tests and pairwise post-hoc comparisons with the Benjamini-Hochberg correction when appropriate. We square-root transformed taxa abundance when needed to improve normality of residuals, although some skewed distributions did not strictly pass the homogeneity of variance test. We tested if shifts in scraper abundance (i.e., grazing invertebrates) occurred across *period-treatment* levels to examine the possibility that the experimental treatment altered top-down (herbivory) control. To this end, we assigned taxa to functional feeding groups (using 80), and pooled all scrapers to assess their change over time and treatments.

In order to test if cumulative seasonal benthic stream invertebrate secondary production responded to low flow treatment, we used 95% confidence intervals of bootstrapped data ($n = 1000$) from each channel (73). The 95% confidence intervals of the treatments included the 97.5th and the 2.5th percentiles of all values from the same treatment. We tested if low flow treatments affected cumulative seasonal emergent production for the community and individual emergent taxa using a 2-way ANOVA.

Lastly, we tested response diversity of the 15 most abundant benthic macroinvertebrates using dissimilarity abundance responses to discharge change. We first took the derivative of the relationship between abundance and discharge for each species, then estimated dissimilarity based on pairwise Euclidean distances in derivatives between all pairs of species in the community (following 36). We excluded our first sampling date so that low discharge always corresponded with warmer conditions. We compared the distribution of dissimilarity values in our study with previous values reported in the literature, as benchmarks of low and high response diversity (dissimilarity) levels (36).

For our third prediction, we used piecewise structural equation models with the *psem* function in the *piecewiseSEM* R package in order to mechanistically test the relationships between discharge, water temperature, benthic production, and emergent production (81). Piecewise structural equation models allow more flexibility in model structure (which we needed to run repeated measures linear mixed effect models) than traditional structural equation models.

We focused on emergent Chironomidae, as that was the only taxon that had time-varying benthic production (i.e., the instantaneous growth rate method provided time-varying secondary production, unlike other methods). Calculated growth rates for taxa are rare in the literature and were unavailable for other taxa in the study. We calculated benthic production using the average biomass between sampling dates, so that five sampling midpoints were used for analysis in the model. All other variables were averaged for sample midpoint dates matching benthic production ($n = 30$). We further tested the mechanisms and links between discharge and Chironomidae production with a second model that used benthic and emergent size along with benthic and emergent abundance. All six sampling dates were used in this case ($n = 36$). We log transformed benthic abundance, emergent abundance, and emergent production to give model residuals a normal distribution. Both piecewise structural equation models were supported for inference based on the Fisher's C statistic. Model coefficients were standardized by standard deviation for comparison.

We also used repeated measures ANOVA tests in order to analyze how *period-treatment* affected emergent Chironomidae production. We used pairwise post-hoc comparisons with the Benjamini-Hochberg correction for the ANOVA data. Lastly, we tested Brewer's Blackbird feeding time using the Kruskal-Wallis rank sum test. We specifically tested if the time that Brewer's Blackbirds were observed in the channel was explained by low flow treatment. We also tested if Brewer's Blackbirds altered the macroinvertebrate community following a Before-After-Control-Impact (BACI) design, focusing on the interaction term between treatment and time (i.e., before vs. after blackbird presence). We ran a total of 6 different tests, to explore potential effects of blackbirds on benthic and emergent invertebrate richness and abundance (via repeated measures ANOVA models), and on benthic and emergent composition (via a PERMANOVA, given the multivariate nature of the data). If Brewer's Blackbirds caused an effect, we would expect the interaction term to be significant, reflecting a 'difference in difference' between the *6-week* and *Current* treatment after the blackbirds' arrival.

Results

Effects of earlier, extended low flows on abiotic variables and epilithic biofilm

The early low-flow treatment drove changes in water temperature, including a 4.6-7.5°C increase in maximum water temperature with the onset of summer low flow ($F_{8,14} = 120.3$, $P < 0.001$; *SI Appendix,* Fig. S2, Fig. S3, Fig. S4, and Table S2). We also observed a 2.6°C increase in the diel range of water temperature in the *6-week* treatment with the onset of summer low flow, as maximum temperatures were higher and minimum temperatures were lower (*SI Appendix,* Fig. S5). Dissolved oxygen declined seasonally ($F_{8,13} = 14.18$, $P < 0.001$), but channels remained well oxygenated throughout the experiment (Fig. S6 and Table S3).

Low-flow timing affected the estimated production and respiration rates of epilithic biofilm—the base of production of our stream food web, which lacked macrophytes or plankton. Cumulative seasonal epilithic biofilm gross production to respiration ratios (GPP:ER) did not differ significantly by treatment, but there was an immediate decline in GPP:ER ratios with low-flow treatment (Fig. 2). The GPP:ER ratio responded to *period-treatment* ($F_{8,41} = 3.307$, $P = 0.005$) and was 32.2% lower for the *6-week* treatment in the *middle* of the experiment compared

to the *Current* treatment, partially supporting our prediction (*SI Appendix,* Table S4). ER increased immediately for the *6-week* treatment in the *middle* period ($F_{8,41} = 3.707$, $P = 0.002$), showing 77.4% higher ER levels than the *Current* treatment (*SI Appendix,* Fig. S7 and Table S5). GPP also responded to treatment over time ($F_{8,41} = 2.3$, $P = 0.039$), but there was no support for any of the potential response types. Overall, the low-flow treatment shifted the phenology of epilithic biofilm metabolism as expected, tipping the balance between production (GPP) and respiration (ER) towards the latter.
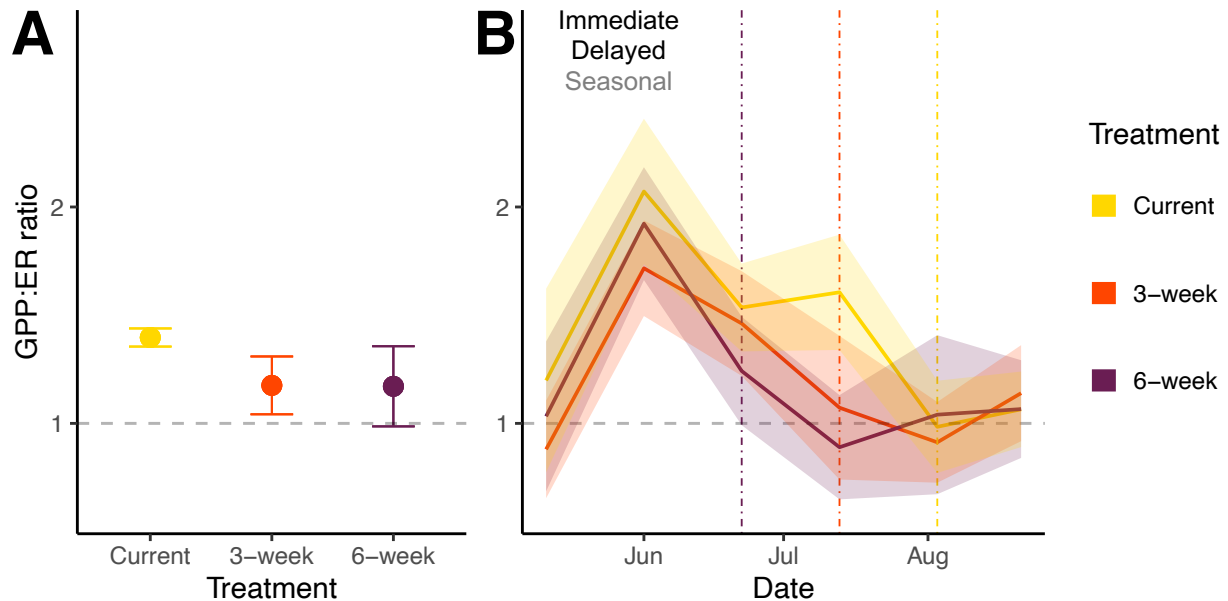
Figure 2. Earlier, extended low flows altered epilithic biofilm metabolism. (A) Mean epilithic biofilm GPP:ER ratio (± standard error) for the cumulative seasonal GPP and ER. The horizontal dashed gray line represents an equilibrium between GPP and ER ($N = 9$). (B) Mean GPP:ER ratio (± standard error) at each sampling date. The *6-week* treatment GPP:ER in the *middle* of the experiment was significantly lower than that of the *Current* treatment ($t_{45} = -3.22$, $P = 0.011$). The *Current* treatment was the only treatment in which ratios significantly declined between the *middle* and *end* periods, constituting a *delayed* effect ($t_{45} = 3.43$, $P = 0.011$). Vertical dashed lines represent the onset of summer low flow, colored by treatment. The three potential response types (*immediate* treatment effect*, delayed* treatment effect*, seasonal* effect) are listed, and are colored black when supported (see conceptual framework in Fig. 1, and Table S1 for how statistical tests connect with each response type). Breakpoints in the time series plot denote each sampling event.

Effects of earlier, extended low flows on invertebrate communities

 The benthic stream invertebrate community exhibited fine-scale responses to low-flow timing. Cumulative (seasonally-aggregated) benthic stream invertebrate abundance did not differ by treatment (Fig. 3A). However, the *6-week* treatment had a delayed effect on the community due to several taxa responding to summer low flow, either by increasing or by decreasing in abundance (pseudo-$F_{5,30} = 2.571$, $P < 0.001$; Fig. 3B-C; *SI Appendix,* Fig. S8 and Tables S6-S10). Among the taxa that significantly explained community dissimilarity, 38% of them

increased and 25% decreased in abundance under low-flow treatment. Taxa with the greatest responses included Chironomini ($F_{5,26} = 5.267$, $P = 0.002$; Fig. 3B), *Hydroptila* ($F_{5,26} = 15.77$, $P < 0.001$), and *Micrasema* ($F_{5,26} = 7.017$, $P < 0.001$). Notably, Chironomini abundance for the *6-week* treatment at the *end* of the experiment was 173% higher than that in the *middle* of the experiment. Highly-resolved taxonomy for a subset of Chironomini and Pseudochironomini support that abundance increases were driven by *Apedilum*, *Polypedilum aviceps*, and *Pseudochironomus*–taxa that tolerate warm conditions. Chironomini and *Micrasema* also experienced magnitude responses in abundance, increasing and decreasing respectively under the low-flow treatment. The subset of flow-sensitive taxa caused a delayed response at the community level (*SI Appendix,* Table S11), leading to a novel assemblage at the *end* of the season. However, we note here that the abundance of scrapers (i.e., biofilm-grazing invertebrates) did not respond to low-flow treatment ($F_{5,28} = 1.512$, $P > 0.05$).
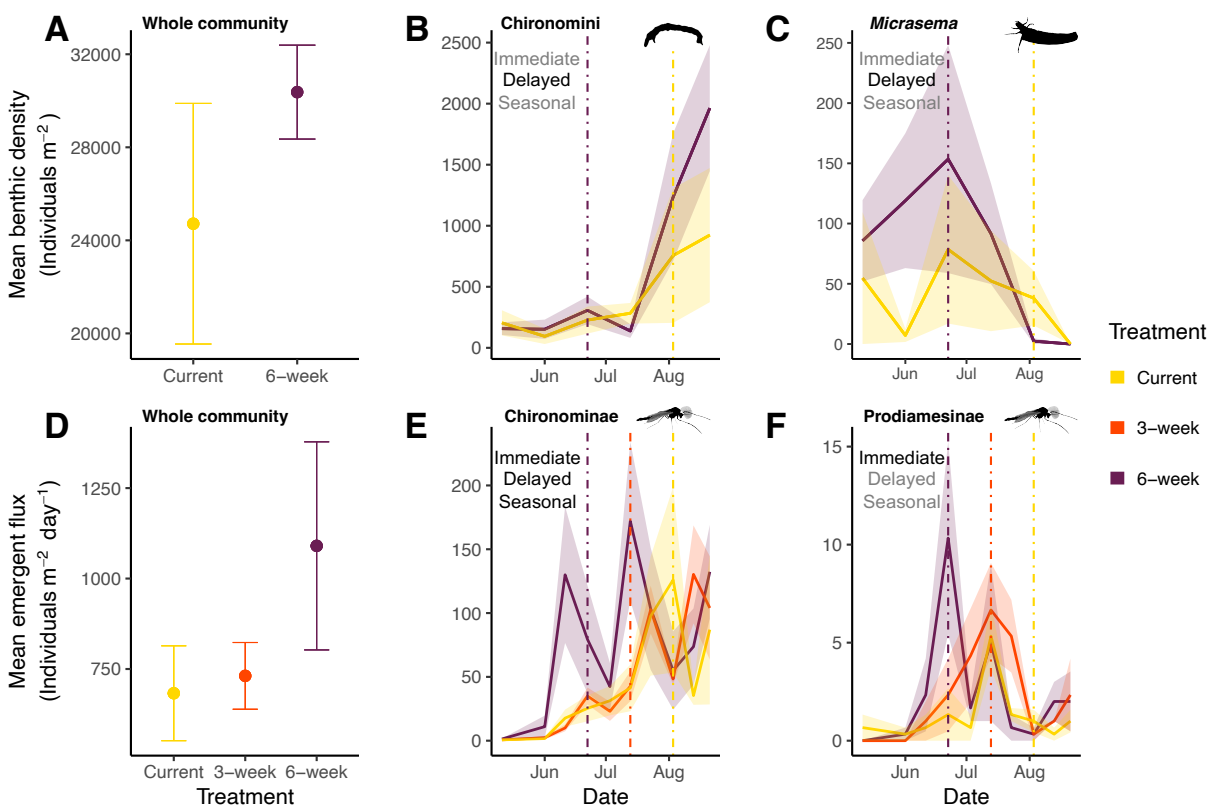
Figure 3. Earlier, extended low flows did not alter aggregate seasonal density or emergence, but phenological shifts occurred in several taxa. In each panel, the mean density/flux of stream invertebrates (± standard error; shaded area) is represented across treatments or time. Panels A and D display average values across channels under each treatment, after aggregating all samples from the experiment within each channel. In all shown taxa, density or flux values were significantly explained by *period-treatment* ($P < 0.05$). The three potential response types (*immediate* treatment effect, *delayed* treatment effect, and *seasonal* effect) are listed, and colored black when supported (see conceptual framework in Fig. 1, and Table S1 for how statistical tests connect with each response type). Vertical dashed lines represent the onset of summer low flow, colored by treatment. (A) We did not observe any significant community-level response when looking at seasonally-aggregated data ($N = 6$), but (B-C) Chironomini ($F_{5,26} = 5.267$, $P = 0.002$)

and *Micrasema* ($F_{5,26}$ = 7.017, P < 0.001) had delayed increases and declines in abundance, respectively, under the low-flow treatment (N = 36). (D) We also did not observe any significant emergent community-level response when looking at seasonally-aggregated data (N = 9), but (E-F) Chironominae (t_{81} = 2.97, P = 0.008) and Prodiamesinae (t_{81} = 4.89, P = 0.027) experienced an immediate increase in emergent flux in the *middle* period (N = 90). Chironominae in the *3-week* treatment exhibited a *delayed* increase (t_{81} = -2.40, P = 0.0299). Breakpoints in the time series plots denote each sampling event.

Emergent stream invertebrates responded to the low-flow treatments, but, in contrast to the benthic community, they did so immediately and exhibited strong phenological change (pseudo-$F_{8,81}$ = 5.728, P < 0.001; *SI Appendix,* Fig. S8). Among the taxa that significantly explained emergent community dissimilarity, 67% of them increased in abundance under low-flow treatment (*SI Appendix,* Table S12). Chironominae was important again in driving the shift, with its abundance increasing immediately by 147% in the *middle* period ($F_{8,77}$ = 3.79, P < 0.001; Fig. 3E; *SI Appendix,* Table S13). Post-hoc analysis supported an immediate shift in emergent community composition, based on the *6-week* community being different from the *Current* community (*SI Appendix,* Table S14). This composition shift reflected a phenological shift, as the *6-week* community in the *middle* period anticipated the assemblage at the *end* of the experiment in the other treatments.

In turn, low-flow treatment did not significantly alter cumulative invertebrate secondary production (i.e., production integrated across the experiment) for either the benthic or the emergent portion of the community (Fig. 4A & D). However, we did observe a wide diversity of responses across taxa, both in how their secondary production responded to low-flow treatment and in their contribution to community-wide secondary production (Fig. 4C & F). We tested if the lack of seasonal aggregate response in our community could be due to response diversity. We found that response diversity to change in discharge, measured as response dissimilarity, was high in our community compared to published benchmarks for response-diverse communities (36), with a median value of 2.5 (*SI Appendix,* Fig. S9). Overall, these results partially support our prediction that extended low flow conditions will shift stream invertebrate phenology. However, changes in both structure (composition) and functioning (production) were mostly fine-scale, and seasonally-aggregated responses were stabilized by high community response diversity.
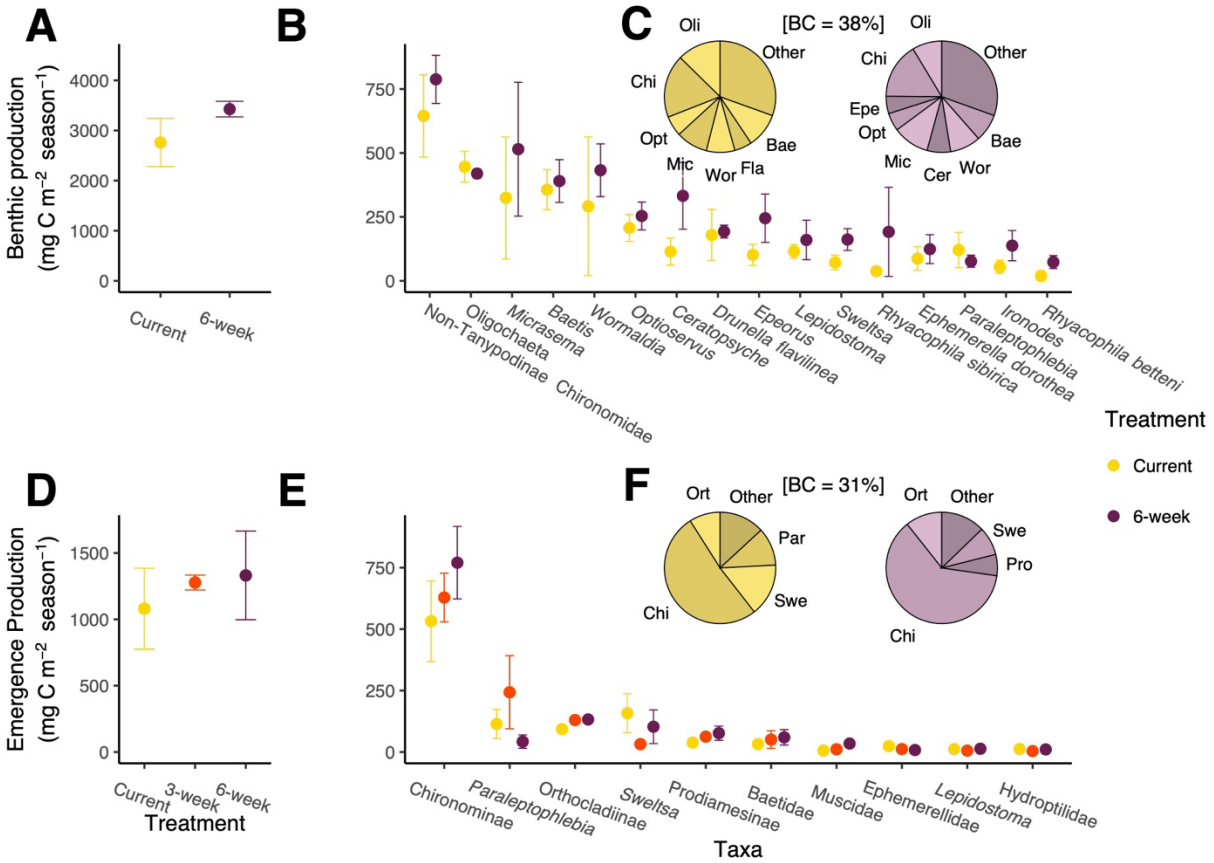
Figure 4. Seasonal secondary production did not differ across treatments. Mean cumulative secondary production over the study period (± standard error) for: (A) the entire benthic community ($N = 6$); (B) the 16 most productive benthic taxa ($N = 96$); (D) the entire emergent community ($N = 9$); and (E) the 10 most productive emergent taxa ($N = 90$). Orthocladiinae emergence production was significantly explained by *treatment* ($F_{2,4} = 12.17$, $P = 0.020$). (C, F) Pie plots displaying the relative proportion of production for taxa with more than 5% of the total community production. Taxon names are abbreviated to the first three letters, and pie plots are separated by *treatment* for the *Current* and *6-week* treatments. Average Bray-Curtis dissimilarity between treatments is listed in brackets between the pie plots.

Causal pathways connecting low flows to cross-ecosystem resource pulses

Using a set of structural equation models (SEM), we examined the mechanisms connecting environmental drivers to the secondary production and subsequent emergence of the dominant aquatic insect group, Chironomidae midges (Fig. 5). This group accounted for 70% of the emergent production and 93% of the emergent abundance, thus controlling both in-stream processes and cross-ecosystem (i.e., stream-to-land) subsidies. Despite the apparent stability of Chironomidae production at the seasonal scale (see previous section), low-flow driven warming drove subseasonal variation in Chironomidae benthic and emergent production (Fig. 5A). This influence was realized via dual, opposing effects of temperature on Chironomidae abundance and body size (Fig. 5B). Specifically, warming decreased mean Chironomidae body size, but

also increased their numerical abundance, with the positive effect on abundance outweighing the negative effect on body size by a factor of three (Fig. 5B).
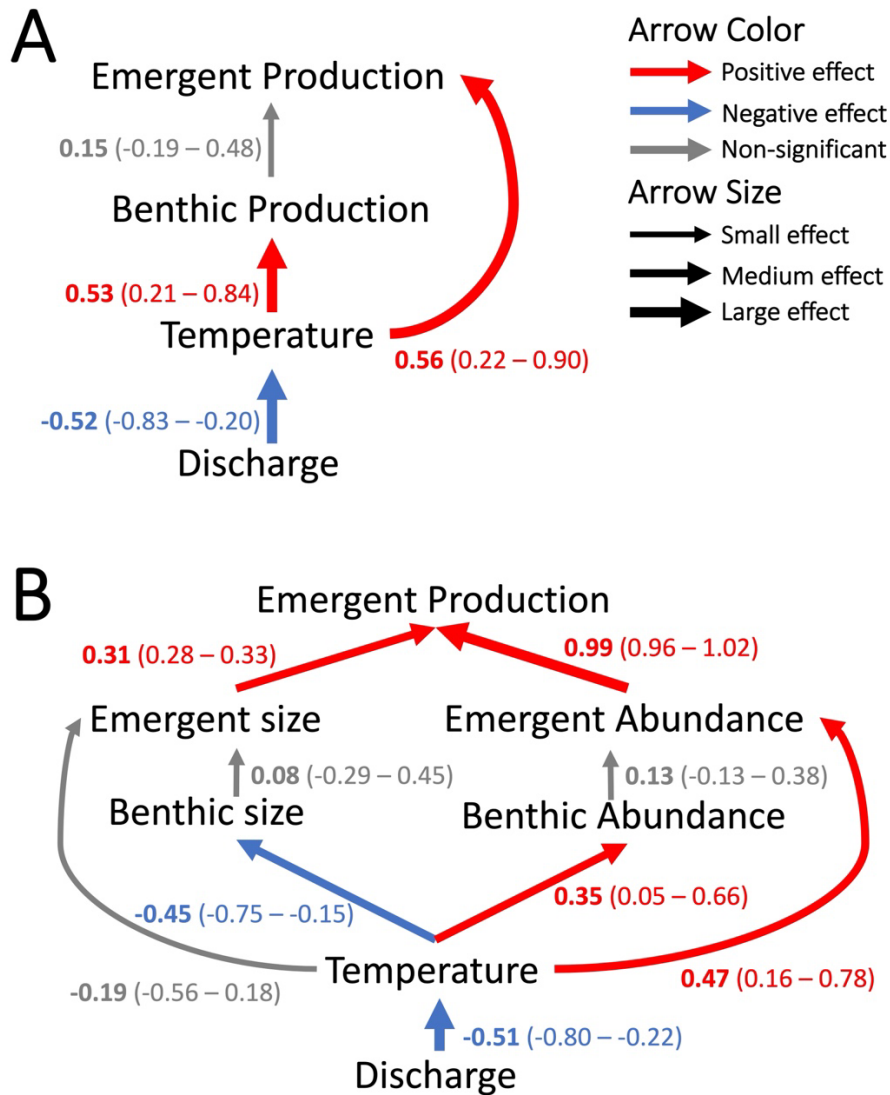
Figure 5. Low-flow induced warming increased Chironomidae production and emergence via increased abundance of individuals, despite reductions in body size. (A) Piecewise structural equation model of the relationship between discharge and emergent Chironomidae production with temperature and benthic production linking them. Discharge has a negative relationship with water temperature (low-flow induced warming). Water temperature has positive relationships with both benthic and emergent production. (B) Piecewise structural equation model of the relationship between discharge and emergent Chironomidae production with mechanistic drivers linking them. Discharge has a negative effect on water temperature. Water temperature increases both benthic and emergent Chironomidae abundance but has a negative effect on benthic Chironomidae size. Emergent Chironomidae size and abundance both have positive effects on emergent Chironomidae production. Comparison of models (A) and (B) suggests that low-flow induced warming increases the emergent flux of Chironomidae midges

(model A); this increase is realized via an increase in numerical abundance that overcompensates for their smaller body sizes, both in the benthic and emergent stages (model B). Both models are supported for inference based on the Fisher's C statistic (Model A: $C_4 = 1.108$, $P > 0.05$; Model B: $C_{24} = 30.296$, $P > 0.05$). Standardized estimates and associated 95% confidence intervals are shown next to linking arrows.

Lastly, we recorded riparian bird feeding behavior to assess how low-flow treatment may have altered the behavior of a generalist predator we noticed visiting and nesting in the area, the Brewer's Blackbirds (*Euphagus cyanocephalus*), once the experiment was underway (Fig. 6). Brewer's Blackbirds fed on benthic macroinvertebrates in the *6-week* channels when discharge dropped to summer low-flow conditions. We began to record their behavior afterwards to account for possible effects on the macroinvertebrate community. We found that emergent Chironomidae production increased in the *middle* period during Brewer's Blackbirds nesting ($F_{8,68} = 5.663$, $P < 0.001$; Fig. 6). The time that Brewer's Blackbirds spent feeding on benthic stream invertebrates in each channel was also associated with treatment ($x^2_2 = 13.836$, $P = 0.001$): they spent the most time in channels undergoing the *6-week* treatment (*6-week* vs. *Current*: $P = 0.018$; *6-week* vs. *3-week*: $P = 0.01$). Brewer's Blackbirds departed from the study site upon fledging, resulting in few observations after early July. Brewer's Blackbirds did not have a measurable influence on the benthic or emergent macroinvertebrate community, measured either as abundance, species richness, or composition (*SI Appendix,* Table S15). Overall, these results support our prediction that our low-flow treatment will alter the phenology of aquatic-terrestrial subsidies–with changes that can be influential even if they take place at short timescales.
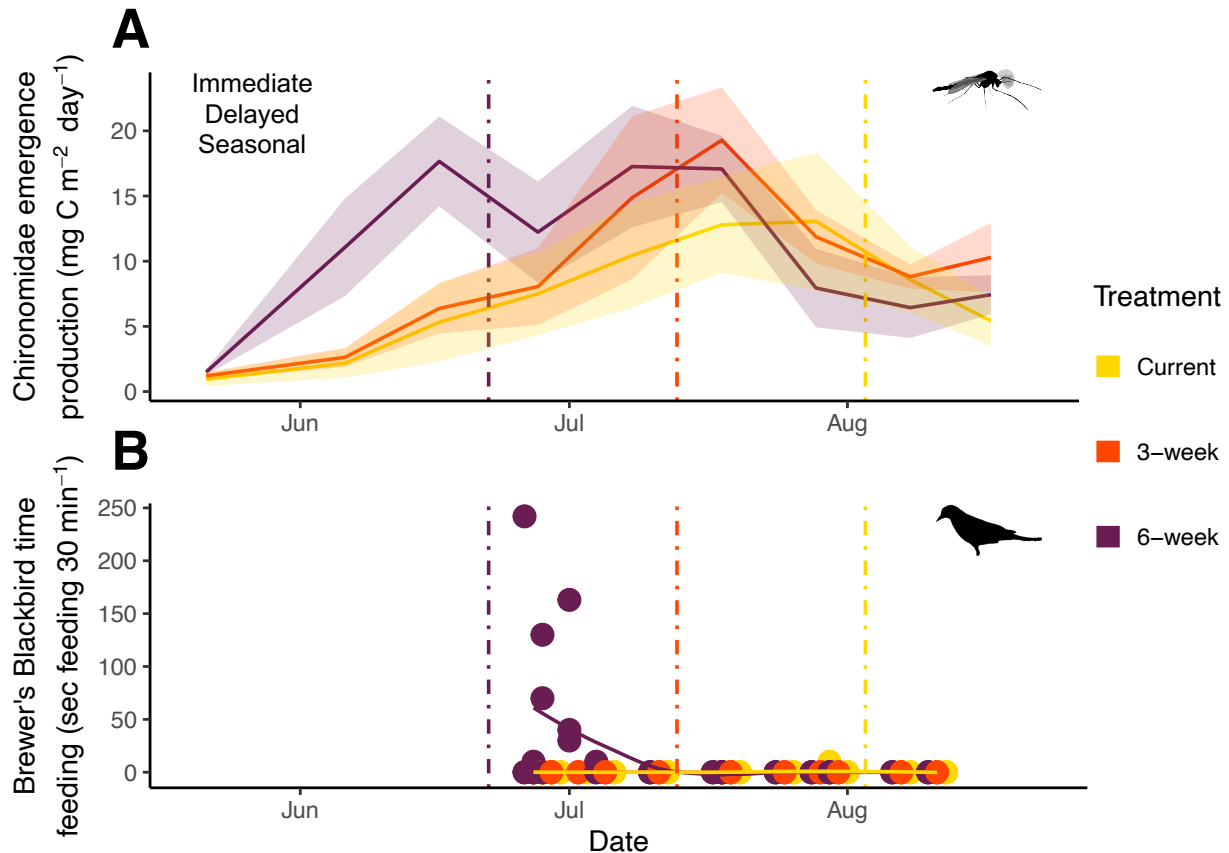
Figure 6. Earlier, extended low flows increased cross-ecosystem pulses. (A) Mean daily Chironomidae emergent production (± standard error) over time ($N = 81$). The three potential response types (*immediate* treatment effect, *delayed* treatment effect, *seasonal* effect) are listed, and colored in black as they were all supported (see conceptual framework in Fig. 1, and Table S1 for how statistical tests connect with each response type). Chironomidae production in the *6-week* treatment was immediately higher than in the other treatments in the *middle* period ($t_{72} = 3.56$, $P = 0.004$ vs. *Current*; $t_{72} = 2.36$, $P = 0.039$ vs. *3-week*) although all treatments showed a seasonal increase. Chironomidae production in the *6-week* treatment also showed a *delayed* decline in production from the *middle* to *end* periods ($t_{72} = 2.92$, $P = 0.014$). Vertical dashed lines represent the onset of summer low flow, colored by treatment. (B) Time in seconds that Brewer's Blackbirds were observed in the artificial channels, over 30-minute periods ($N = 117$). Brewer's Blackbirds were present significantly more in the *6-week* treatment compared to the *Current* ($P = 0.018$) and *3-week* treatments ($P = 0.01$). The solid lines are smoothed conditional means using LOESS (locally estimated scatterplot smoothing) for each treatment, to assist in visualizing temporal trends.

Discussion

Numerous studies suggest that climate-driven phenological shifts will alter ecosystem processes (8, 9). However, few studies to date have empirically examined this link in complex, multi-trophic communities (8, 9). Here we used an outdoor, artificial stream system in California's Sierra Nevada to simulate future hydroclimatic conditions in mountain streams. We

measured how extended summer low flows are likely to affect organism phenology, ecosystem processes, and the link between the two. We found that earlier, extended low-flow conditions will likely: (1) raise water temperature, increase epilithic biofilm respiration (ER), and consequently tip the balance between epilithic biofilm production and respiration (GPP:ER); (2) advance phenology of the stream invertebrate community, even if compensatory mechanisms buffer change in production at longer, seasonal scales; and (3) alter cross-ecosystem resource fluxes by advancing emergence of key insect groups (such as Chironomidae) and by creating novel feeding opportunities for generalist riparian predators. Our findings add mechanism to the link between climate-driven phenological shifts and ecosystem process shifts (8, 24). Further, we advance the notion that ecological processes that appear insensitive to climate change at long scales can respond at finer scales—with far-reaching implications for food-web matches and mismatches (2, 37).

Our study highlights that different species responding in diverse ways to climate change stressors can stabilize community-level properties at seasonal scales. This property, often referred to as response diversity, played out at two different levels: at the population level (i.e., diverse demographic changes in size and phenology) and at the community level (i.e., dissimilar responses in species abundance across species). Notably, we found response diversity values in our complex community to be greater than those in communities previously used to illustrate a 'high' response diversity level (36). Our results are consistent with observations from long-term field studies showing that even if animals have generally advanced their phenology 2.9 days per decade, substantial variation among taxa may buffer aggregate community shifts (1). While small ectotherms are generally more responsive to warming, limits to phenologic plasticity exist (1). For example, nonlinear responses to climate change can occur as a result of crossing physiological limits (e.g., critical thermal maxima), along with the local abiotic and biotic contexts interacting with each other (38). In a mesocosm study in southern England, increased temperatures altered community composition and resulting decomposition rates differently depending on the time of year (39). Additionally, temporary ecosystem process shifts due to changing phenology can cancel each other out over seasonal or yearly timescales, like we observed in the ecosystem processes we studied (e.g., secondary production). This characteristic pattern of 'stability despite change' may be akin to that of 'climatic debt' in climate velocity research, where a lack of community composition response can hide impending biodiversity collapse (40).

Our study suggests that streamflow, via its effects on temperature, may be the mechanism whereby climate change in mountain streams is most likely to affect organism phenology and ecosystem processes (41). Many of the low-flow effects we observed resulted from water temperature rising during low flow conditions. The GPP:ER decline we found with increasing water temperature was similar to that reported from a warming mesocosm experiment in the UK (42). In both cases, reduced GPP:ER was likely due to respiration increasing at a faster rate than GPP, based on their respective activation energies. However, low flows and high water temperatures may increase biofilm production and reduce water quality if the stream is not nutrient limited, as in our oligotrophic system (43, 44). Our methods captured biofilm production and respiration, which is only a portion of ecosystem metabolism (45). Because the light-dark bottle method excludes hyporheic metabolism and respiration from invertebrate heterotrophs, we cannot use estimates from the light-dark bottle to scale up to whole stream ecosystem

24

metabolism. These exclusions likely underestimated ecosystem-level ER, thus preventing us from upscaling biofilm GPP:ER ratios to ecosystem-level GPP:ER ratios. Additionally, both low flows and increased water temperature have also been shown to favor small, flow-sensitive taxa like Chironomidae, which can alter overall community composition, in agreement with our results (15). We did not, however, notice a general decline in sensitive Ephemeroptera, Plecoptera, and Trichoptera taxa due to early low flows, as observed elsewhere (46). This discrepancy is likely explained by many of these taxa emerging in spring and early summer in high mountain streams. The lack of a cumulative secondary production response we observed differs from the conventional belief that low flows reduce production (20), as is often the case if flow intermittency occurs (31). However, some studies have reported that low flows may not impair, or may even slightly increase, stream invertebrate secondary production, given overcompensating increases in Chironomidae production (47). Likewise, we found that extended summer low flow is poised to increase Chironomidae production by increasing their abundance more than reducing their body size—showing that changes in ecosystem processes driven by organisms (and their phenology) may depend on a fragile balance of life-history mechanisms.

Given the dynamic nature of most responses observed, our study illustrates the need to record time-varying rather than 'time-averaged' ecosystem responses to climate change. In our case, tracking responses over time allowed us to parse out *immediate* shifts (e.g., water temperature, biofilm production, emergence, and riparian predator feeding) from *delayed* or time-lagged shifts (e.g., benthic stream invertebrate community composition). These changes may connect different trophic levels—leading to novel, climate-driven 'matches' or 'mismatches' between resource availability and demand. While climate change leading to predator-prey mismatches is unsurprising (48), we found a novel match between peak Chironomidae emergence and Brewer's Blackbirds nesting. Understanding when and where these new food-web links could replace current connections is important for conservation (49). However, novel matches can also be ecologically harmful. For example, advanced hatching in the moth *Agriopis aurantiaria* is increasingly coinciding with sub-Arctic birch budburst, causing widespread tree die-off (50). Notably, interspecific variation in phenological responses may preserve ecosystem processes when species are not tightly linked, or when voltinism is plastic (51). The study of predator-prey mismatch remains challenging (52), and requires tracking how climate change is affecting organismal phenology at a high taxonomic and temporal resolution.

Our experiment is one of the few assessing phenological change at the community level in a realistic, outdoor mesocosm system (2); however, our approach has limitations. First, a multi-year experiment may have found greater declines in sensitive taxa abundance that are caused by inter-generational effects. High temperatures can reduce egg survival and adult fecundity via reduced body size, which may not be noticeable over a single season (27). Second, unmeasured abiotic variables beyond flow and temperature may have partly driven biotic responses. For example, reduced flow can increase retention of allochthonous particulate organic matter, which could influence biofilm metabolism (23); similarly, reduced water velocity may have influenced fluctuations in dissolved oxygen, even if biologically harmful hypoxia was not reached in our case [*SI Appendix,* Fig. S6 (53, 54)]. Reduced flow can also increase the concentration of nutrients with higher residence time, even if this is unlikely in our oligotrophic system (44, 55). Overall, disentangling abiotic change driven by vs. covarying with flow alteration requires further research. Third, we did not measure immigration or drift of

individuals. While immigration from nearby Convict Creek during the experiment could have reduced treatment differences, drift into the channels was negligible in a past study (56). However, emigrant drift may have differed among our treatments, as described by studies that found short-term increases in drift under reduced flow conditions followed by drift declines (20). Some of our results could also be driven by a reduced period of high flow rather than by an earlier, longer summer low flow period, if organisms require prolonged high flow conditions for dispersal, filter-feeding, or some other life history. Lastly, the artificial channels are not connected to groundwater, which can cool down low-order stream habitats experiencing summer low flow conditions (57). These factors suggest that care should be applied when transferring our results to other climatic and geologic contexts.

The temporal shifts in phenology and ecosystem processes we observed are meaningful given ongoing climate change trends in mountain ranges globally (19), and particularly in the rain-to-snow transition zone. In addition to climate change leading to advanced and extended summer low flow conditions, warmer air temperatures will increasingly overlap with periods of reduced thermal buffering from low flows (20, 58), increasing stream water temperatures even further (58). Warmer air temperatures will also increase the likelihood of precipitation falling as rain and rain-on-snow events, raising the frequency and magnitude of flooding (59). These changes in snow-dominated mountain streams are expected to cause widespread ecological change, as is already seen when comparing communities from unusually wet to dry years (15). Our study shows that response diversity may help maintain stability in key ecosystem processes, similarly to how biodiversity stabilizes ecosystem processes in warming terrestrial ecosystems [e.g., as seen with bee diversity and plant pollination (60)]. However, stabilizing mechanisms may be further eroded if environmental change continues to extirpate species locally (11). Studying community phenology at fine temporal scales is vital to capture the vulnerability of taxa facing climate change and to understand impending effects of climate change on ecosystem processes.

Acknowledgements

References

1. J. M. Cohen, M. J. Lajeunesse, J. R. Rohr, A global synthesis of animal phenological responses to climate change. *Nat. Clim. Change* 8, 224–228 (2018).

2. D. W. Inouye, Climate change and phenology. *WIREs Clim. Change* 13 (2022).

3. T. L. Root, *et al.*, Fingerprints of global warming on wild animals and plants. *Nature* 421, 57–60 (2003).

4. C. Both, M. Van Asch, R. G. Bijlsma, A. B. Van Den Burg, M. E. Visser, Climate change and unequal phenological changes across four trophic levels: Constraints or adaptations? *J. Anim. Ecol.* 78, 73–83 (2009).

5. A. Ozgul, *et al.*, Coupled dynamics of body mass and population growth in response to environmental change. *Nature* 466, 482–485 (2010).

6. W. A. Kurz, *et al.*, Mountain pine beetle and forest carbon feedback to climate change. *Nature* 452, 987–990 (2008).

7. G. Kudo, T. Y. Ida, Early onset of spring increases the phenological mismatch between plants and pollinators. *Ecology* 94, 2311–2320 (2013).

8. K. H. Beard, K. C. Kelsey, A. J. Leffler, J. M. Welker, The Missing Angle: Ecosystem Consequences of Phenological Mismatch. *Trends Ecol. Evol.* 34, 885–888 (2019).

9. M. Edwards, A. J. Richardson, Impact of climate change on marine pelagic phenology and trophic mismatch. *Nature* 430, 881–884 (2004).

10. N. L. Poff, J. D. Olden, D. L. Strayer, "Climate Change and Freshwater Fauna Extinction Risk" in *Saving a Million Species*, L. Hannah, Ed. (Island Press/Center for Resource Economics, 2012), pp. 309–336.

11. D. E. Bowler, *et al.*, Cross-realm assessment of climate change impacts on species' abundance trends. *Nat. Ecol. Evol.* 1, 1–7 (2017).

12. D. L. Ficklin, J. T. Abatzoglou, S. M. Robeson, S. E. Null, J. H. Knouft, Natural andmanaged watersheds show similar responses to recent climate change. *Proc. Natl. Acad. Sci.* 115, 8553–8557 (2018).

13. S. J. Thackeray, *et al.*, Trophic level asynchrony in rates of phenological change for marine, freshwater and terrestrial environments. *Glob. Change Biol.* 16, 3304–3313 (2010).

14. T. Woods, A. Kaz, X. Giam, Phenology in freshwaters: a review and recommendations for future research. *Ecography* 6, 1–14 (2021).

15. D. B. Herbst, S. D. Cooper, R. B. Medhurst, S. W. Wiseman, C. T. Hunsaker, Drought ecohydrology alters the structure and function of benthic invertebrate communities in mountain streams. *Freshw. Biol.* 64, 886–902 (2019).

16. S. M. Yarnell, J. H. Viers, J. F. Mount, Ecology and Management of the Spring Snowmelt Recession. *BioScience* 60, 114–127 (2010).

17. V. U. Smakhtin, Low flow hydrology. *J. Hydrol.* 240, 147–186 (2001).

18. K. Reich, *et al.*, Climate Change in the Sierra Nevada: California's Water Future. *UCLA Cent. Clim. Sci.* (2018).

19. I. T. Stewart, Changes in snowpack and snowmelt runoff for key mountain regions. *Hydrol. Process.* 23, 78–94 (2009).

20. R. J. Rolls, C. Leigh, F. Sheldon, Mechanistic effects of low-flow hydrology on riverine ecosystems: ecological principles and consequences of alteration. *Freshw. Sci.* 31, 1163–1186 (2012).

21. D. Rosero-López, *et al.*, A whole-ecosystem experiment reveals flow-induced shifts in a stream community. *Commun. Biol.* 5, 420 (2022).

22. S. Domisch, S. C. Jähnig, P. Haase, Climate-change winners and losers: stream macroinvertebrates of a submontane region in Central Europe. *Freshw. Biol.* 56, 2009–2020 (2011).

23. A. Harjung, *et al.*, Experimental evidence reveals impact of drought periods on dissolved organic matter quality and ecosystem metabolism in subalpine streams. *Limnol. Oceanogr.* 64, 46–60 (2019).

24. M. A. Palmer, Ruhi, Albert, Linkages between flow regime, biota, and ecosystem processes: Implications for river restoration. *Science* 365 (2019).

25. H. E. Anderson, L. K. Albertson, D. M. Walters, Water temperature drives variability in salmonfly abundance, emergence timing, and body size. *River Res. Appl.* 35, 1013–1022 (2019).

26. J. A. Sheridan, D. Bickford, Shrinking body size as an ecological response to climate change. *Nat. Clim. Change* 1, 401–406 (2011).

27. L. Bonacina, F. Fasano, V. Mezzanotte, R. Fornaroli, Effects of water temperature on freshwater macroinvertebrates: a systematic review. *Biol. Rev.* 98, 191–221 (2023).

28. D. Nelson, *et al.*, Experimental whole-stream warming alters community size structure. *Glob. Change Biol.* 23, 2618–2628 (2017).

29. C. J. Patrick, *et al.*, Precipitation and temperature drive continental-scale patterns in stream invertebrate production. *Sci. Adv.* 5, 1–10 (2019).

30. N. L. Poff, J. K. H. Zimmerman, Ecological responses to altered flow regimes: a literature review to inform the science and management of environmental flows. *Freshw. Biol.* 55, 194–205 (2010).

31. M. E. Ledger, F. K. Edwards, L. E. Brown, A. M. Milner, G. Woodward, Impact of simulated drought on ecosystem biomass production: An experimental test in stream mesocosms. *Glob. Change Biol.* 17, 2288–2297 (2011).

32. Z. S. Dewson, A. B. W. James, R. G. Death, Invertebrate responses to short-term water abstraction in small New Zealand streams. *Freshw. Biol.* 52, 357–369 (2007).

33. A. W. Walters, D. M. Post, An experimental disturbance alters fish size structure but not food chain length in streams. *Ecology* 89, 3261–3267 (2008).

34. S. Nakano, M. Murakami, Reciprocal subsidies: Dynamic interdependence between terrestrial and aquatic food webs. *Proc. Natl. Acad. Sci.* 98, 166–170 (2001).

35. C. V. Baxter, K. D. Fausch, W. Carl Saunders, Tangled webs: reciprocal flows of invertebrate prey link streams and riparian zones. *Freshw. Biol.* 50, 201–220 (2005).

36. S. R. P. -J. Ross, O. L. Petchey, T. Sasaki, D. W. Armitage, How to measure response diversity. *Methods Ecol. Evol.* 14, 1150–1167 (2023).

37. C. Both, S. Bouwhuis, C. M. Lessells, M. E. Visser, Climate change and population declines in a long-distance migratory bird. *Nature* 441, 81–83 (2006).

38. N. Chr. Stenseth, A. Mysterud, Climate, changing phenology, and other life history traits: Nonlinearity and match–mismatch to the environment. *Proc. Natl. Acad. Sci.* 99, 13379–13381 (2002).

39. M. Dossena, *et al.*, Warming alters community size structure and ecosystem functioning. *Proc. R. Soc. B Biol. Sci.* 279, 3011–3019 (2012).

40. V. Devictor, *et al.*, Differences in the climatic debts of birds and butterflies at a continental scale. *Nat. Clim. Change* 2, 121–124 (2012).

41. N. L. Poff, *et al.*, The Natural Flow Regime: A Paradigm for River Conservation and Restoration. *BioScience* 47, 769–784 (1997).

42. G. Yvon-Durocher, J. I. Jones, M. Trimmer, G. Woodward, J. M. Montoya, Warming alters the metabolic balance of ecosystems. *Philos. Trans. R. Soc. B Biol. Sci.* 365, 2117–2126 (2010).

43. A. M. Suren, B. J. F. Biggs, C. Kilroy, L. Bergey, Benthic community dynamics during summer low-flows in two rivers of contrasting enrichment 1. Periphyton. *N. Z. J. Mar. Freshw. Res.* 37, 53–70 (2003).

44. H. V. Leland, J. L. Carter, Effects of copper on production of periphyton, nitrogen fixation and processing of leaf litter in a Sierra Nevada, California, stream. *Freshw. Biol.* 15, 155–173 (1985).

45. R. O. Hall, E. R. Hotchkiss, "Stream Metabolism" in *Methods in Stream Ecology*, (Elsevier, 2017), pp. 219–233.

46. H. Leland, S. Fend, J. Carter, A. Mahood, Composition and abundance of periphyton and aquatic insects in a Sierra Nevada, California, stream. *Gt. Basin Nat.* 46, 595–611 (1986).

47. E. A. Scholl, H. M. Rantala, M. R. Whiles, G. V. Wilkerson, Influence of Flow on Community Structure and Production of Snag-Dwelling Macroinvertebrates in an Impaired Low-Gradient River. *River Res. Appl.* 32, 677–688 (2016).

48. X. Chevillot, *et al.*, Toward a phenological mismatch in estuarine pelagic food web? *PLOS ONE* 12, e0173752 (2017).

49. M. Schleuning, *et al.*, Trait-Based Assessments of Climate-Change Impacts on Interacting Species. *Trends Ecol. Evol.* 35, 319–328 (2020).

50. J. U. Jepsen, *et al.*, Rapid northwards expansion of a forest insect pest attributed to spring phenology matching with sub-Arctic birch. *Glob. Change Biol.* 17, 2071–2083 (2011).

51. R. J. Knell, S. J. Thackeray, Voltinism and resilience to climate-induced phenological mismatch. *Clim. Change* 137, 525–539 (2016).

52. H. M. Kharouba, E. M. Wolkovich, Disconnects between ecological theory and data in phenological mismatch research. *Nat. Clim. Change* 10, 406–415 (2020).

53. J. R. Blaszczak, *et al.*, Extent, patterns, and drivers of hypoxia in the world's streams and rivers. *Limnol. Oceanogr. Lett.* 8, 453–463 (2023).

54. A. V. Nebeker, Effect of Low Oxygen Concentration on Survival and Emergence of Aquatic Insects. *Trans. Am. Fish. Soc.* 101, 675–679 (1972).

55. P. S. Lake, Ecological effects of perturbation by drought in flowing waters. *Freshw. Biol.* 48, 1161–1172 (2003).

56. P. Saffarinia, K. E. Anderson, D. B. Herbst, Effects of experimental multi-season drought on abundance, richness, and beta diversity patterns in perennially flowing stream insect communities. *Hydrobiologia* 849, 879–897 (2022).

57. A. S. Ward, M. N. Gooseff, P. A. Johnson, How can subsurface modifications to hydraulic conductivity be designed as stream restoration structures? Analysis of Vaux's conceptual models to enhance hyporheic exchange. *Water Resour. Res.* 47 (2011).

58. K. Leathers, D. Herbst, M. Safeeq, A. Ruhi, Dynamic, downstream-propagating thermal vulnerability in a mountain stream network: Implications for biodiversity in the face of climate change. *Limnol. Oceanogr.* 68, S101–S114 (2022).

59. T. Das, M. D. Dettinger, D. R. Cayan, H. G. Hidalgo, Potential increase in floods in California's Sierra Nevada under future climate projections. *Clim. Change* 109, 71–94 (2011).

60. I. Bartomeus, *et al.*, Biodiversity ensures plant-pollinator phenological synchrony against climate change. *Ecol. Lett.* 16, 1331–1338 (2013).

61. K. Leathers, D. B. Herbst, G. de Mendoza, G. Doerschlag, A. Ruhi, Data for: Climate change is poised to alter mountain stream ecosystem processes via organismal phenological shifts (2024) https:/doi.org/10.6078/D10712.

62. T. M. Jenkins, S. Diehl, K. W. Kratz, S. D. Cooper, Effects of population density on individual growth of brown trout in streams. *Ecology* 80, 941–956 (1999).

63. C. T. Hunsaker, T. W. Whitaker, R. C. Bales, Snowmelt Runoff and Water Yield Along Elevation and Temperature Gradients in California's Southern Sierra Nevada. *J. Am. Water Resour. Assoc.* 48, 667–678 (2012).

64. H. E. Anderson, L. K. Albertson, D. M. Walters, Thermal variability drives synchronicity of an aquatic insect resource pulse. *Ecosphere* 10, e02852 (2019).

65. C. McNeely, M. E. Power, Spatial variation in caddisfly grazing regimes within a northern California watershed. *Ecology* 88, 2609–19 (2007).

66. A. C. Benke, A. D. Huryn, L. A. Smock, J. B. Wallace, Length-Mass Relationships for Freshwater Macroinvertebrates in North America with Particular Reference to the Southeastern United States. *J. North Am. Benthol. Soc.* 18, 308–343 (1999).

67. T. A. Johnston, R. A. Cunjak, Dry mass-length relationships for benthic insects: A review with new data from Catamaran Brook, New Brunswick, Canada. *Freshw. Biol.* 41, 653–674 (1999).

68. M. Mährlein, M. Pätzig, M. Brauns, A. M. Dolman, Length–mass relationships for lake macroinvertebrates corrected for back-transformation and preservation effects. *Hydrobiologia* 768, 37–50 (2016).

69. R. O. Hall, M. F. Dybdahl, M. C. VanderLoop, Extremely High Secondary Production Of Introduced Snails In Rivers. *Ecol. Appl.* 16, 1121–1131 (2006).

70. M. L. Miserendino, Length-mass relationships for macroinvertebrates in freshwater environments of Patagonia (Argentina). *Ecol. Austral* 11, 3–8 (2001).

71. R. L. Malison, J. R. Benjamin, C. V. Baxter, Measuring adult insect emergence from streams: the influence of trap placement and a comparison with benthic sampling. *J. North Am. Benthol. Soc.* 29, 647–656 (2010).

72. C. V. Baxter, T. A. Kennedy, S. W. Miller, J. D. Muehlbauer, L. A. Smock, "Macroinvertebrate Drift, Adult Insect Emergence and Oviposition" in *Methods in Stream Ecology, Volume 1*, (Elsevier, 2017), pp. 435–456.

73. A. C. Benke, A. D. Huryn, "Secondary Production of Macroinvertebrates" in *Methods in Stream Ecology*, (Elsevier, 2007), pp. 691–710.

74. D. A. Walther, M. R. Whiles, M. B. Flinn, D. W. Butler, Assemblage-level estimation of nontanypodine chironomid growth and production in a southern Illinois stream. *J. North Am. Benthol. Soc.* 25, 444–452 (2006).

75. C. C. Krueger, T. F. Waters, Annual Production of Macroinvertebrates in Three Streams of Different Water Quality. *Ecology* 64, 840–850 (1983).

76. D. M. Stagliano, M. R. Whiles, Macroinvertebrate Production and Trophic Structure in a Tallgrass Prairie Headwater Stream. *J. North Am. Benthol. Soc.* 21, 97–113 (2002).

77. J. L. Sabo, J. L. Bastow, M. E. Power, Length–mass relationships for adult aquatic and terrestrial invertebrates in a California watershed. *J. North Am. Benthol. Soc.* 21, 336–343 (2002).

78. M. Griesser, P. Halvarsson, S. M. Drobniak, C. Vilà, Fine-scale kin recognition in the absence of social familiarity in the Siberian jay, a monogamous bird species. *Mol. Ecol.* 24, 5726–5738 (2015).

79. J Oksanen, GL Simpson, FG Blanchet, R Kindt, vegan: Community Ecology Package (2022) (November 1, 2022).

80. N. K. M. Vieira, *et al.*, A Database of Lotic Invertebrate Traits for North America. *US Geol. Surv. Data Ser.* 187, 1–15 (2006).

81. J. S. Lefcheck, PIECEWISESEM: Piecewise structural equation modelling in R for ecology, evolution, and systematics. *Methods Ecol. Evol.* 7, 573–579 (2016).

Supplementary Materials
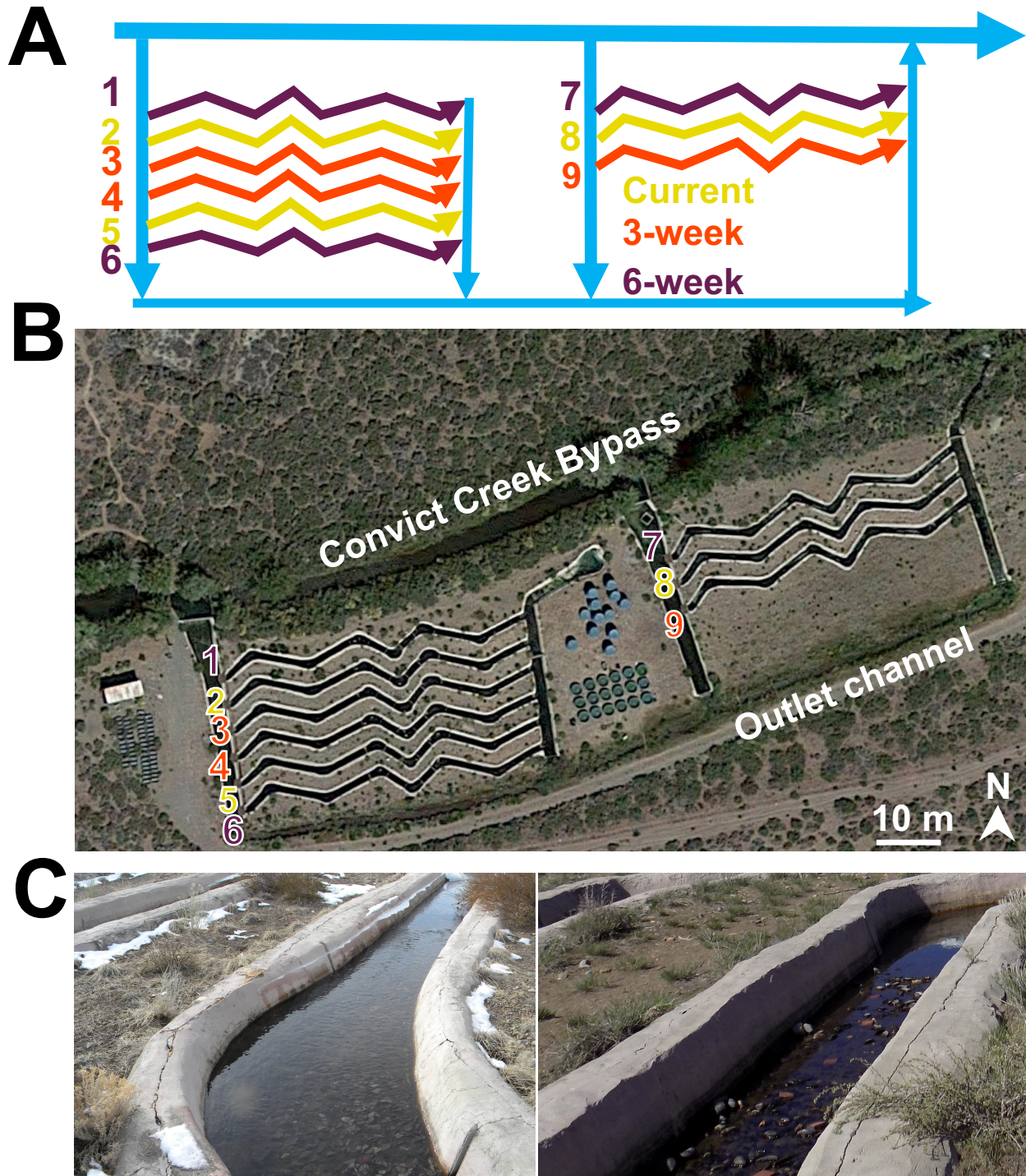
Figure S1. Diagram and photos of the outdoor channel array at the Sierra Nevada Aquatic Research Laboratory (SNARL) in Mammoth Lakes, California, USA. (A) Channels were assigned to one of three treatments with three replicate channels each in a block design. Channel number is shown to the left of the channel inlet and colored according to treatment. The treatments were: (1) current hydrologic conditions based on the historic (long-term) hydrograph

at Convict Creek with a flow regime that reaches baseflow conditions around August 3rd (i.e., *Current* treatment); (2) hydrologic conditions under a mitigated climate change scenario, where the stream would return to baseflow conditions three weeks earlier than it currently does (i.e., *3-week* treatment); and (3) hydrologic conditions under unmitigated climate change, where the stream would return to baseflow six weeks earlier than it currently does (i.e., *6-week* treatment). (B) Aerial photo of the artificial channels, courtesy of Google Maps. (C) Photos of high flow (left; ~15 L/s) and low flow (i.e., baseflow) conditions (right; ~1.5 L/s). Photo credits: Carol Blanchette (B), Guillermo de Mendoza (C1), and Ludmila Sromek (C2).
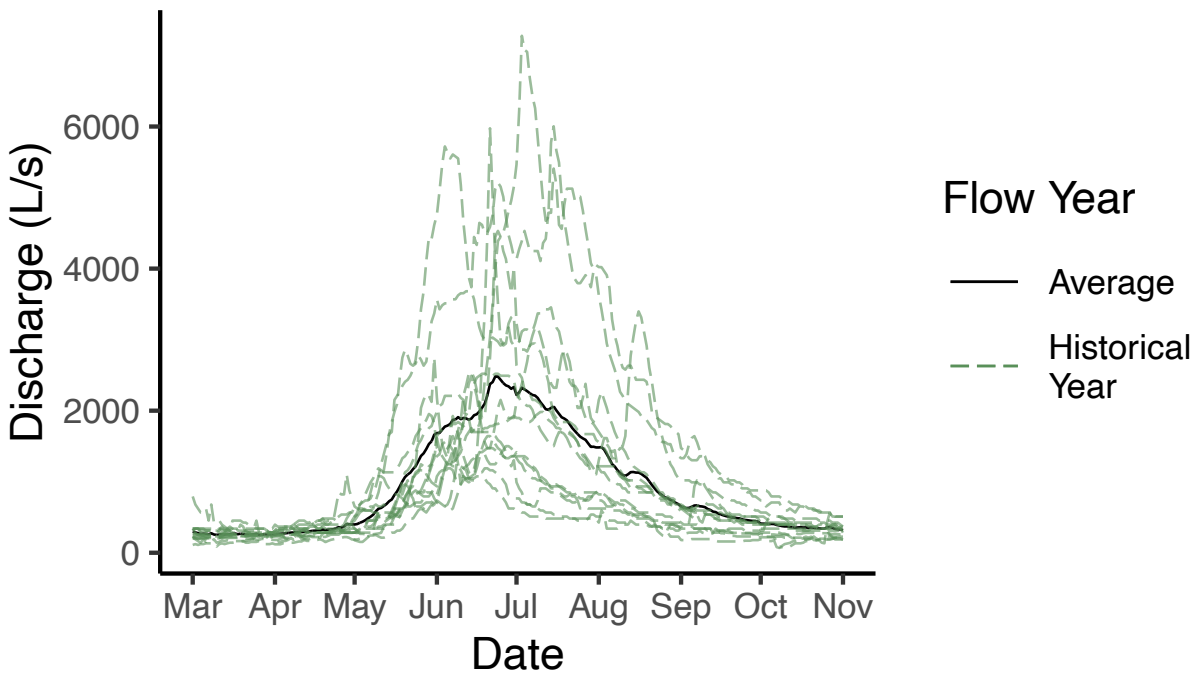
Figure S2. Historical flow regime of Convict Creek. Long-term seasonal trends in mean daily discharge in Convict Creek from March to November each year from 1960 to 1974 (in dashed green lines), as measured by the available data from U.S. Geological Survey streamgage 10265200. We averaged the 15 years of streamflow data to create a daily mean discharge value (black line). We then used this average flow regime as the basis for the "*Current*" flow regime and advanced the start of summer low flows for the *3-week* and *6-week* treatments from this baseline, in agreement with downscaled climate change projections from Reich et al. 2018 (1; Figure S3). The first-order streams that our experimental channels are simulating are smaller than Convict Creek and located at a higher altitude. They thus experience faster return to summer baseflow conditions.
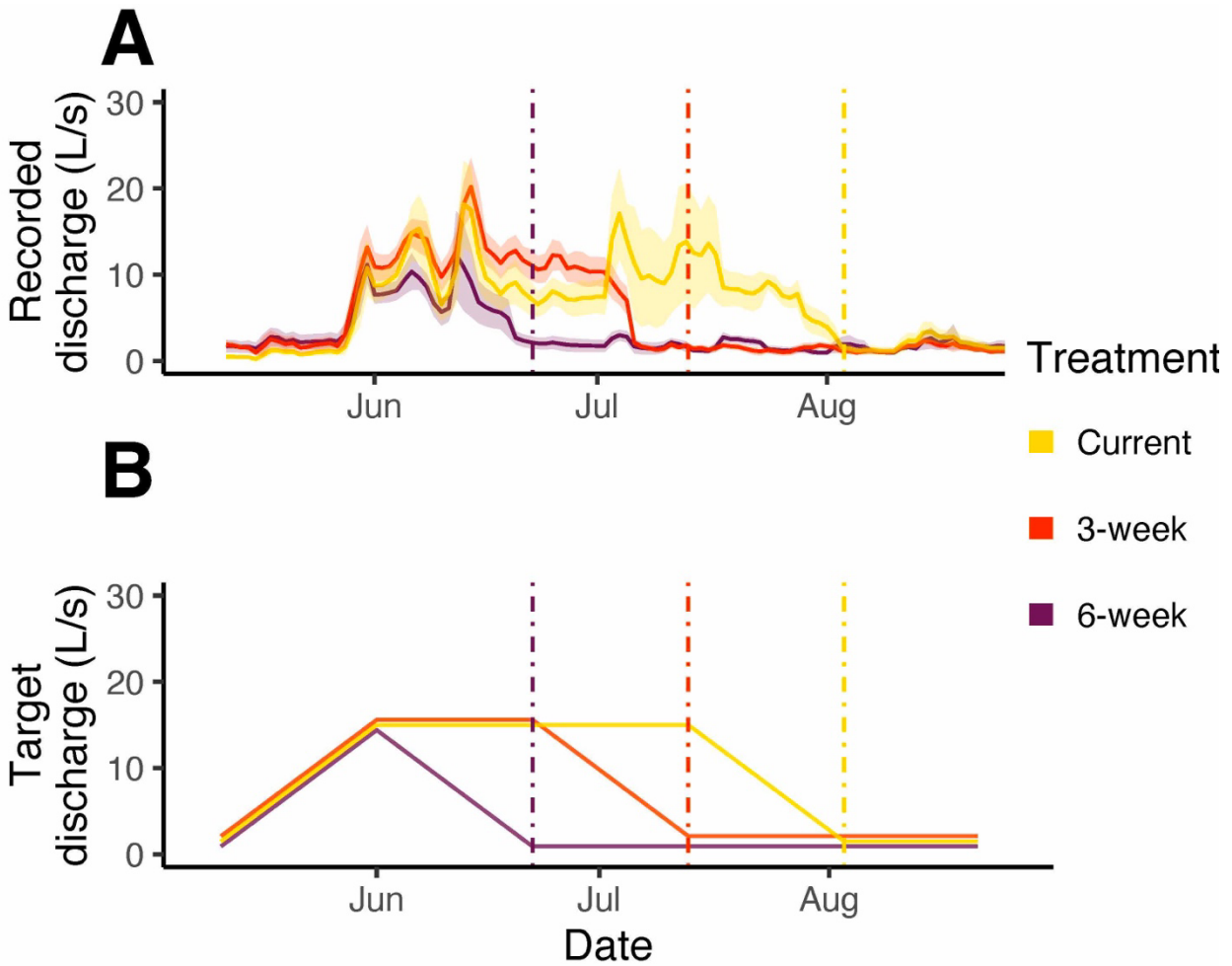
Figure S3. Average recorded and targeted daily discharge for each treatment throughout the experiment. (A) The recorded discharge was calculated using high frequency water depth sensors and rating curves in each channel. Discharge was manually controlled by opening or closing the sluice gate at the inlet of each channel to match the target flow regime. (B) Target discharge in the *Current* treatment follows the historic average flow regime timing of snowmelt recession in the water source, Convict Creek (see Fig. S3). The other two treatments were designed to experience summer low flow three and six weeks earlier in the year, respectively, following downscaled climate change projections (see methods for details). The designed onset of summer low-flow conditions is indicated for each treatment by a dashed vertical line colored by treatment. The shaded area represents ±1 standard error.
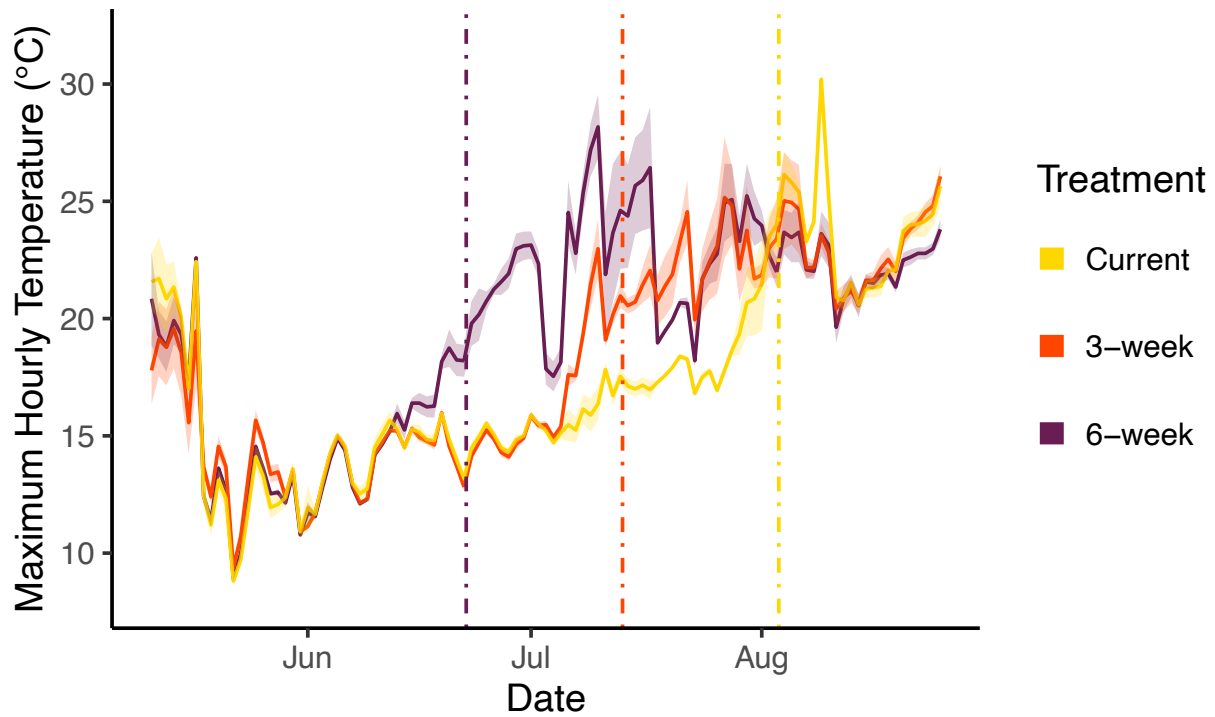
Figure S4. Maximum daily water temperature for each treatment, throughout the experiment. Maximum water temperature increased with advanced low flow treatments. The targeted onset of summer low-flow conditions is indicated for each treatment by a dashed vertical line, colored by treatment. Average treatment maximum water temperature (± standard error) is shown. See Figure S3 for targeted and observed hydrographs.
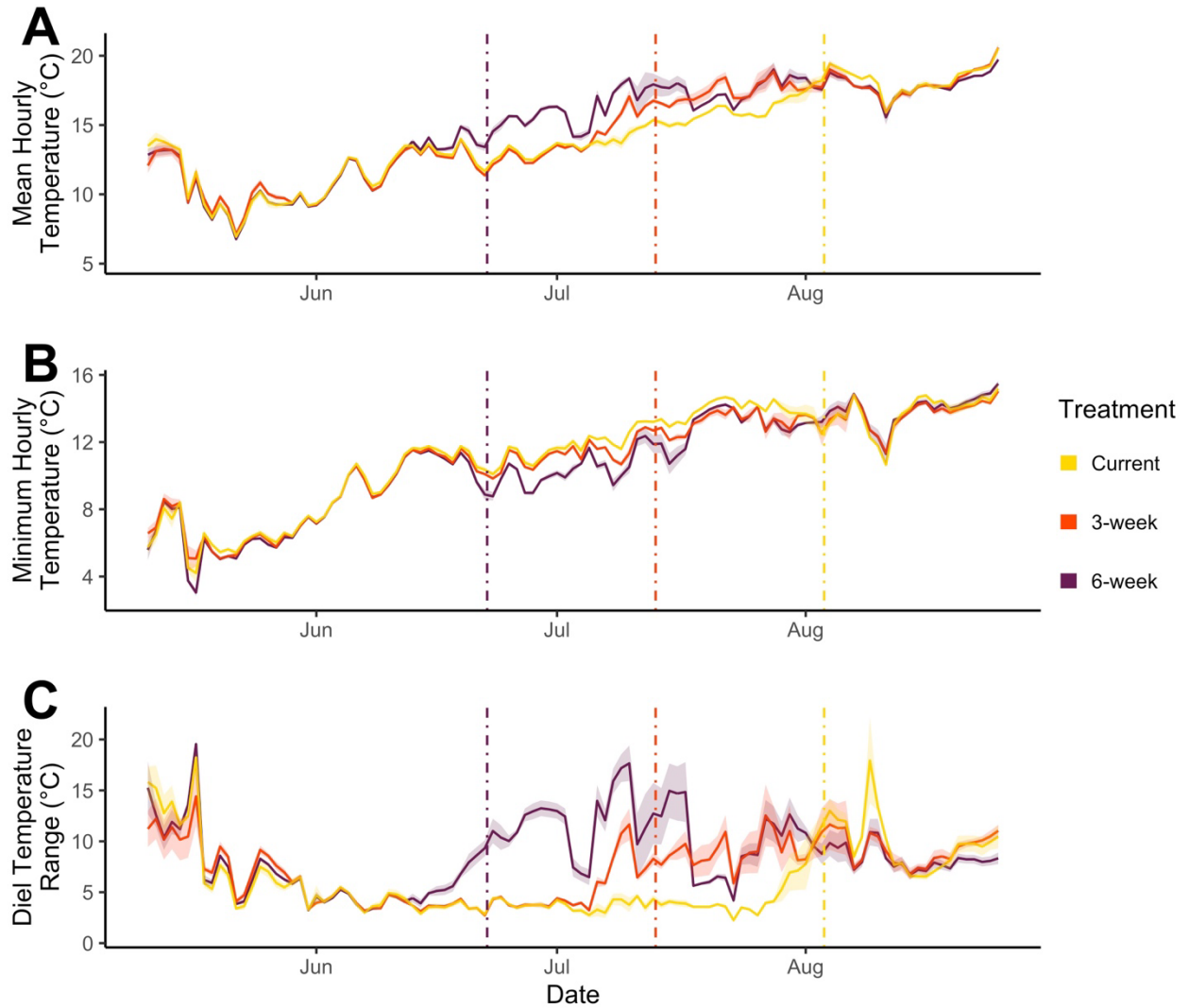
Figure S5. Mean, minimum, and diel range of water temperature for each treatment throughout the experiment. Advanced low flow treatments affected all water temperature metrics immediately. The designed onset of summer low-flow conditions is indicated for each treatment by a dashed vertical line colored by treatment. The means of each water temperature metric (± standard error) are shown by treatment.
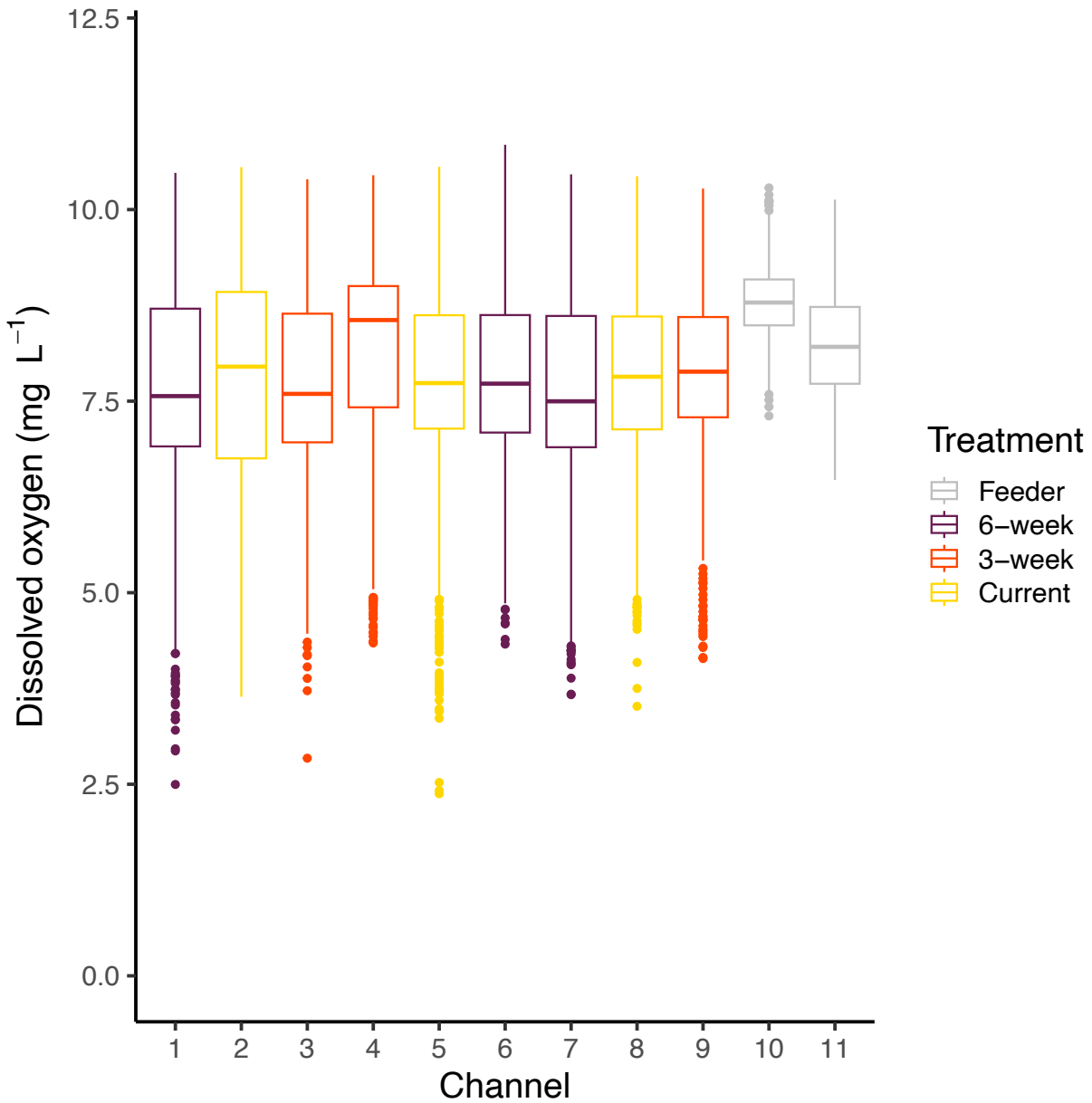
Figure S6. Distribution of dissolved oxygen hourly concentrations in each channel, pooled across the duration of the experiment. The boxplots display channel-specific medians (bold lines), interquartile ranges (boxes), and interquartile range*1.5 extents (whiskers). Hypoxia, defined as dissolved oxygen concentrations dropping below 2 mg/L (2), was never detected in the experiment, and almost all readings (99.6% of them) were over 5 mg/L, a threshold often used to assess long-term performance of sensitive, coldwater mayflies and stoneflies (3 and references therein). The "Feeder" label refers to measurements taken at the two inlets connecting Convict Creek to the experimental channels.
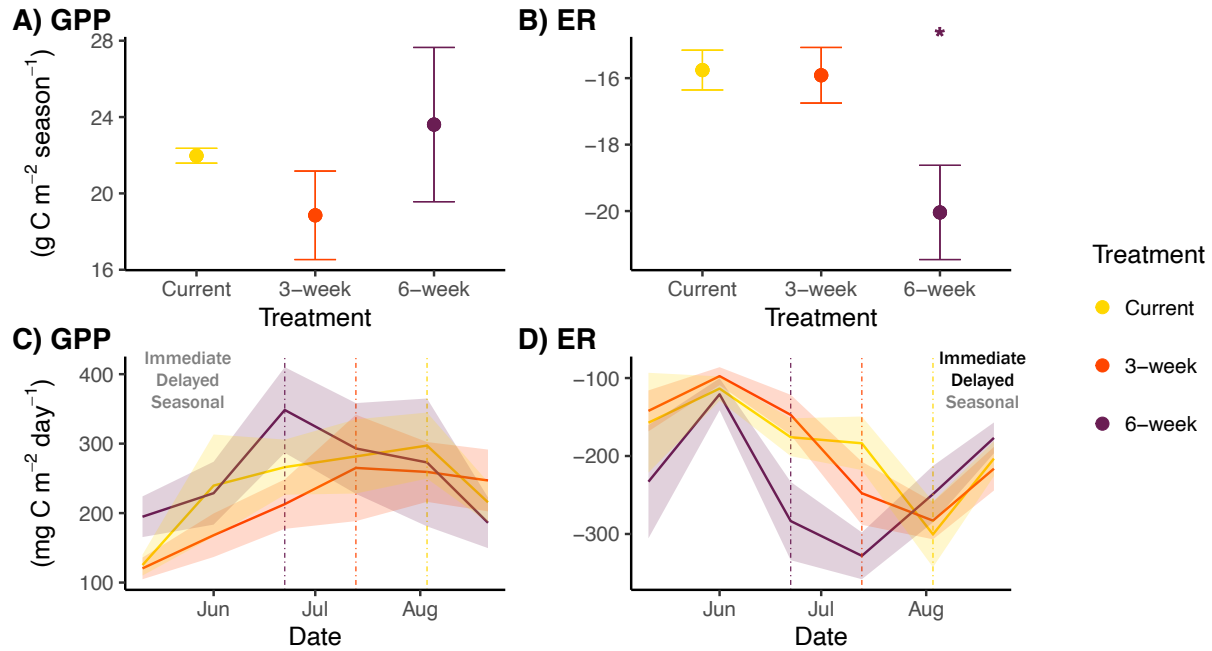
Figure S7. Seasonal and time-varying estimates of epilithic biofilm production (GPP) and respiration (ER). (A) No differences were observed between treatments for cumulative seasonal GPP. (B) Cumulative seasonal ER was significantly higher in magnitude for the *6-week* treatment relative to the other two treatments (indicated by *). (C) No predicted responses were observed for GPP. (D) An immediate increase in the magnitude of ER occurred in the *6-week* treatment based on comparisons between the *middle* and *start* of the experiment. Shaded error ribbons and error bars represent ±1 standard error. Each breakpoint in the time series plots denotes a sampling event. The three potential response types (*immediate* treatment effect, *delayed* treatment effect, and *seasonal* effect) are listed, and colored in black when supported (see conceptual framework in Fig. 1, and Table S1 for how statistical tests connect with each response type).
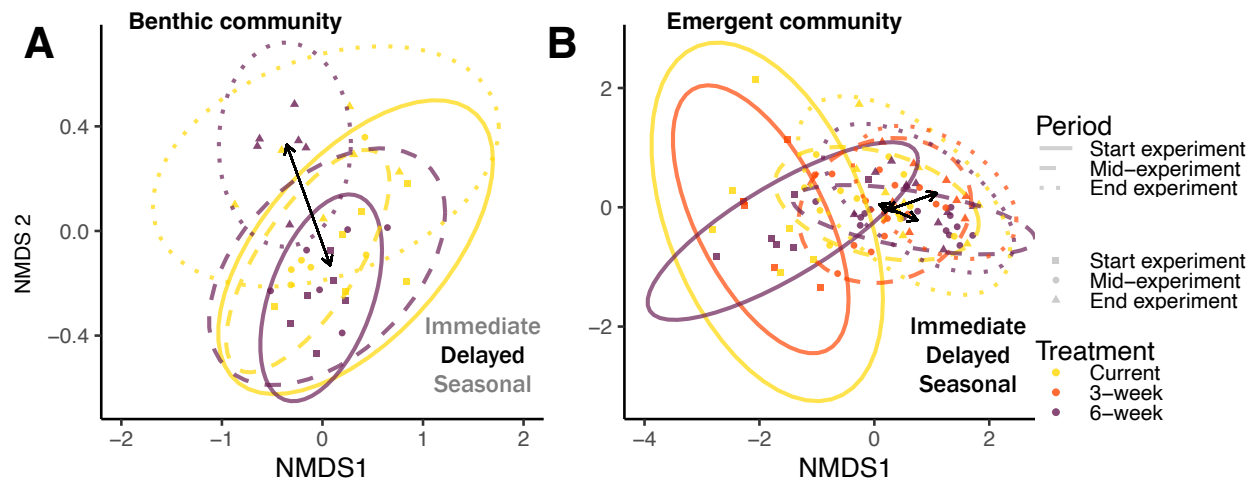
Figure S8. Low-flow treatment effects on stream invertebrate community structure. Earlier, extended low flows had a delayed effect on benthic stream invertebrate community composition and an immediate effect on emergent insect community composition. Black arrows represent significant post-hoc differences due to predicted responses, where arrow end points indicate ellipse centroids. (A) The benthic stream invertebrate community experienced a *delayed* response, based on differences between the *6-week* treatment at the *end* and the *middle* of the experiment. (B) The community composition of emergent stream invertebrates changed immediately in the *middle* period between the *6-week* treatment and the *Current* treatment. There was a *delayed* change in the community in the *3-week* treatment. The *middle* period in this study begins ten days preceding the onset of summer low flow for the *6-week* treatment, to reflect that falling discharge can cause effects before minimum summer low flow is reached. The three potential response types (*immediate* treatment effect, *delayed* treatment effect, *seasonal* effect) are listed, and colored black when supported (see conceptual framework in Fig. 1, and Table S1 for how statistical tests connect with each response type).
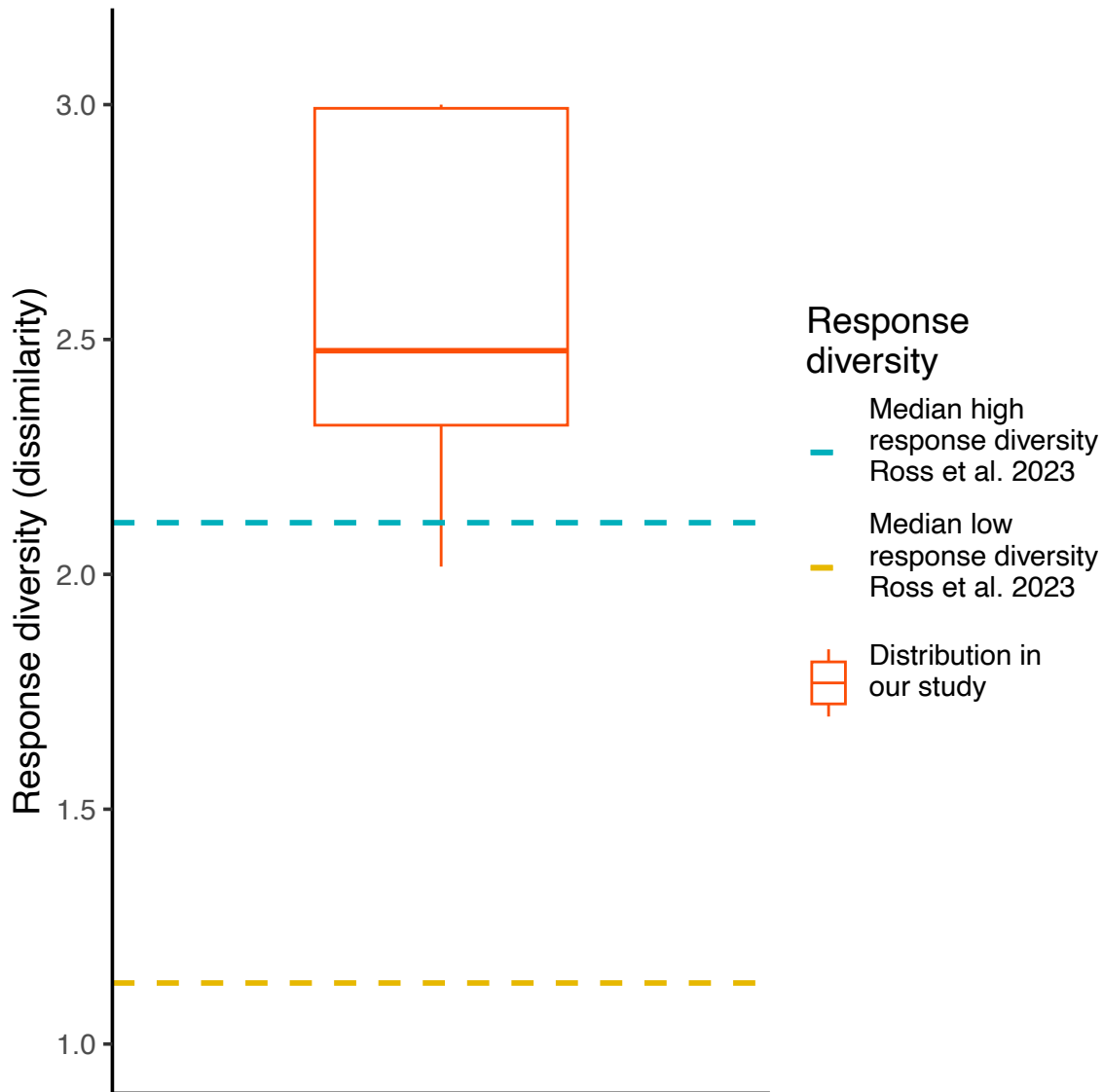
Figure S9. Response diversity in our study relative to values in the literature. We measured response diversity using dissimilarity in how species abundance responded to change in discharge, via the method described in Ross et al. 2023 (4). We note dissimilarity has a minimum value of 1, and higher values indicate higher response diversity. The 15 most abundant benthic taxa were included in our analyses, and response diversity was calculated for each channel independently. The boxplot displays the median (bold red line), interquartile range (box), and interquartile range*1.5 (whiskers) of all channel response diversity values. Samples from the first sampling date were excluded for this analysis to focus on the experimental response. The dashed horizontal lines are median dissimilarity values used as benchmarks, reported to have low and high dissimilarity in Ross et al. 2023.
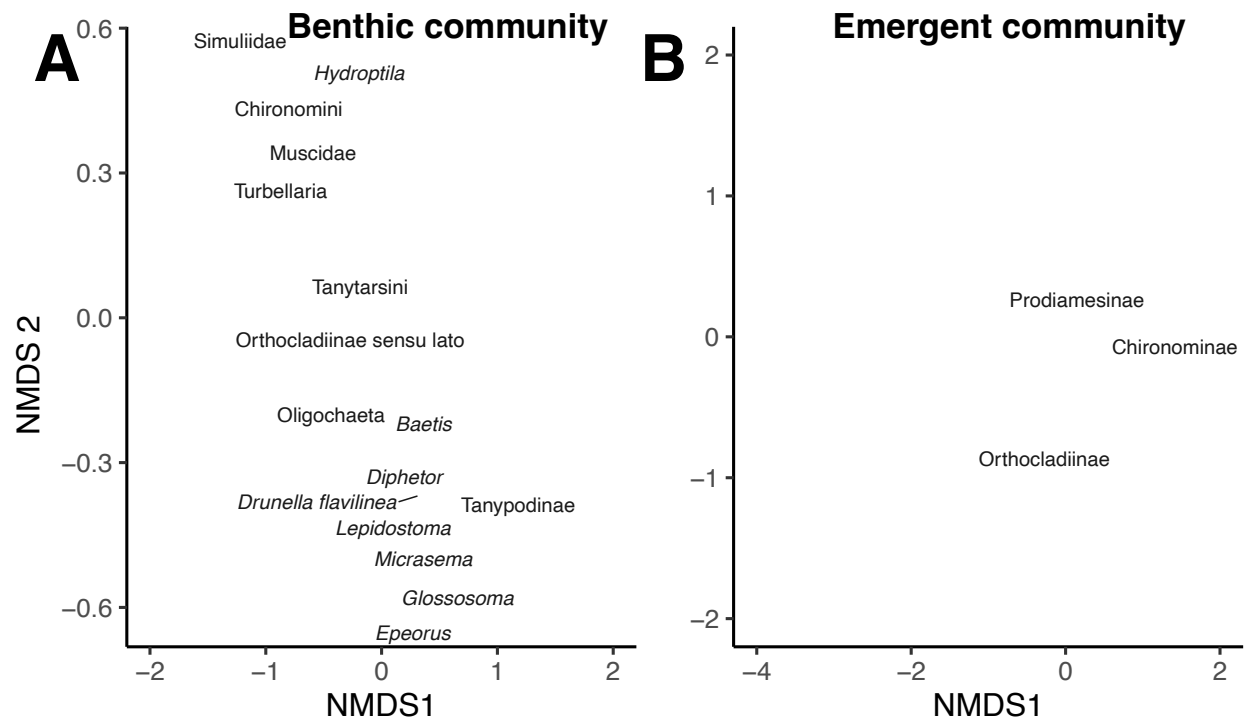
Figure S10. Taxa driving community dissimilarity in Figure S8. The NMDS space is the same here as that in Figure S8. (A) Benthic taxa that significantly explained community dissimilarity among samples are shown ($P \leq 0.002$). The position of the taxa label indicates where the taxa is in the NMDS space. The label position for *Drunella flavilinea* is moved to prevent overlap and the line connected to it indicates the actual space it corresponds to in the NMDS. (B) Emergent taxa that significantly ($P \leq 0.002$) explained community dissimilarity among samples.

Table S1. Description of how statistical tests support evidence for each of the potential ecological responses described in Figure 1 (*no* effect, *seasonal* effect, *immediate* treatment effect, *delayed* treatment effect). Responses reflect a change in magnitude or phenology of the response variable. A *seasonal* effect is inferred when an advanced low flow treatment and the *Current* conditions treatment exhibit a shift in the same direction and magnitude over time. An example of a *seasonal* effect is Chironominae emergence (Figure 3; Table S13), where all three treatments increase in emergence in the *middle* period compared to the *start* period. An *immediate* effect occurs when there is a difference in how treatments change from the *start* to the *middle* period, or when a difference occurs between treatments within the *middle* period (i.e., at the onset of treatment differences). An *immediate* effect is seen in Chironominae, where emergence under the *6-week* treatment is significantly different from emergence under the *Current* treatment (*middle* period). Lastly, a *delayed* effect occurs when there is a difference in how treatments change from the *middle* to *end* period, or between treatments within the *end* period. An example of a *delayed* effect occurred in benthic Chironomini (Figure 3), where abundance increased significantly between the *middle* and *end* periods for the *6-week* treatment, but not for the *Current* treatment. Immediate and delayed effects could theoretically occur sequentially in the same response variable, but we did not expect it a priori, and it did not occur in our study.

Response type	Relevant comparisons	Rationale
Seasonal effect	Middle 6-week *vs.* Start 6-week Middle Current *vs.* Start Current Middle 3-week *vs.* Start 3-week End 6-week *vs.* Middle 6-week End Current *vs.* Middle Current End 3-week *vs.* Middle 3-week	If the C*urrent* treatment and either the *6-week* or *3-week* treatment exhibit the same significant response over time, then we describe a seasonal effect.
Immediate effect	Middle 6-week *vs.* Start 6-week Middle Current *vs.* Start Current Middle 3-week *vs.* Start 3-week Middle 6-week *vs.* Middle Current Middle 3-week *vs.* Middle Current	An immediate effect may be evidenced by a significant difference between the C*urrent* and *6-week* or *3-week* treatments in the *middle* period. An immediate effect can also take place if the C*urrent* and *6-week* or *3-week* treatments differ in how they change between the *start* and *middle* periods.

Delayed effect	End 6-week *vs.* Middle 6-week End Current *vs.* Middle Current End 3-week *vs.* Middle 3-week End 6-week *vs.* End Current End 3-week *vs.* End Current	A delayed effect may be evidenced by a significant difference between the *Current* and *6-week* or *3-week* treatments in the *end* period. A delayed effect can also take place if the *Current* and *6-week* or *3-week* treatments differ in how they change between the *middle* and *end* periods.

Table S2. Pairwise comparisons of maximum water temperature among *period-treatment* groups. We examined maximum daily temperature via post-hoc pairwise comparisons (*P*-values) corrected by the Benjamini–Hochberg method. A bolded *P*-value indicates that the pairwise comparison was significant for that response type. If the *Current* and *3-week* or *6-week* treatments are significant for the same comparison across periods (e.g., *start* vs. *middle*) then *P*-values are bolded for *seasonal* effects but not for *immediate* or *delayed* treatment effects, as that would indicate similar change over time regardless of treatment. See conceptual framework on response types in Fig. 1, and Table S1 for how statistical tests connect with each response type.

Response type	Relevant comparisons	*P*-value
Seasonal effect	Middle 6-week *vs.* Start 6-week	1.07E-12
	Middle Current *vs.* Start Current	5.49E-06
	Middle 3-week *vs.* Start 3-week	1.81E-09
	End 6-week *vs.* Middle 6-week	0.0231
	End Current *vs.* Middle Current	3.93E-12
	End 3-week *vs.* Middle 3-week	2.02E-09
Immediate treatment effect	Middle 6-week *vs.* Start 6-week	1.07E-12
	Middle Current *vs.* Start Current	5.49E-06
	Middle 3-week *vs.* Start 3-week	1.81E-09
	Middle 6-week *vs.* Middle Current	1.35E-09
	Middle 3-week *vs.* Middle Current	1.85E-04
Delayed treatment effect	End 6-week *vs.* Middle 6-week	0.0231
	End Current *vs.* Middle Current	3.93E-12
	End 3-week *vs.* Middle 3-week	2.02E-09
	End 6-week *vs.* End Current	0.017
	End 3-week *vs.* End Current	0.425

Table S3. Pairwise comparisons of dissolved oxygen among *period-treatment* groups. We examined dissolved oxygen over time via post-hoc pairwise comparisons (*P*-values) corrected by the Benjamini–Hochberg method. A bolded *P*-value indicates that the pairwise comparison was significant for that response type. If the *Current* and *3-week* or *6-week* treatments are significant for the same comparison across periods (e.g., *start* vs. *middle*) then *P*-values are bolded for *seasonal* effects but not for *immediate* or *delayed* treatment effects, as that would indicate similar change over time regardless of treatment. See conceptual framework on response types in Fig. 1, and Table S1 for how statistical tests connect with each response type.

Response type	Relevant comparisons	*P*-value
Seasonal effect	Middle 6-week *vs.* Start 6-week	1.78E-06
	Middle Current *vs.* Start Current	2.16E-05
	Middle 3-week *vs.* Start 3-week	9.83E-06
	End 6-week *vs.* Middle 6-week	0.918
	End Current *vs.* Middle Current	6.12E-03
	End 3-week *vs.* Middle 3-week	9.99E-02
Immediate treatment effect	Middle 6-week *vs.* Start 6-week	1.78E-06
	Middle Current *vs.* Start Current	2.16E-05
	Middle 3-week *vs.* Start 3-week	9.83E-06
	Middle 6-week *vs.* Middle Current	4.33E-01
	Middle 3-week *vs.* Middle Current	8.93E-01
Delayed treatment effect	End 6-week *vs.* Middle 6-week	0.918
	End Current *vs.* Middle Current	6.12E-03
	End 3-week *vs.* Middle 3-week	9.99E-02
	End 6-week *vs.* End Current	0.042
	End 3-week *vs.* End Current	0.133

Table S4. Pairwise comparisons of epilithic biofilm GPP:ER ratios among *period-treatment* groups. We examined GPP:ER ratios over time via post-hoc pairwise comparisons (*P*-values) corrected by the Benjamini–Hochberg method. A bolded *P*-value indicates the pairwise comparison was significant for that response type. If the *Current* and *3-week* or *6-week* treatments are significant for the same comparison across periods (e.g., *start* vs. *middle*), then *P*-values are bolded for *seasonal* effects but not for *immediate* or *delayed* treatment effects, as that would indicate similar change over time regardless of treatment. See conceptual framework on response types in Fig. 1, and Table S1 for how statistical tests connect with each response type.

Response type	Relevant comparisons	*P*-value
Seasonal effect	Middle 6-week *vs.* Start 6-week	7.21E-02
	Middle Current *vs.* Start Current	9.89E-01
	Middle 3-week *vs.* Start 3-week	9.63E-01
	End 6-week *vs.* Middle 6-week	0.989
	End Current *vs.* Middle Current	1.12E-02
	End 3-week *vs.* Middle 3-week	2.26E-01
Immediate treatment effect	Middle 6-week *vs.* Start 6-week	7.21E-02
	Middle Current *vs.* Start Current	9.89E-01
	Middle 3-week *vs.* Start 3-week	9.63E-01
	Middle 6-week *vs.* Middle Current	1.12E-02
	Middle 3-week *vs.* Middle Current	1.71E-01
Delayed treatment effect	End 6-week *vs.* Middle 6-week	0.989
	End Current *vs.* Middle Current	1.12E-02
	End 3-week *vs.* Middle 3-week	2.26E-01
	End 6-week *vs.* End Current	0.937
	End 3-week *vs.* End Current	0.989

Table S5. Pairwise comparisons of biofilm respiration among *period-treatment* groups. We examined biofilm respiration over time via post-hoc pairwise comparisons (*P*-values) corrected by the Benjamini–Hochberg method. A bolded *P*-value indicates the pairwise comparison was significant for that response type. If the *Current* and *3-week* or *6-week* treatments are significant for the same comparison across periods (e.g., *start* vs. *middle*) then *P*-values are bolded for *seasonal* effects but not for *immediate* or *delayed* treatment effects, as that would indicate similar change over time regardless of treatment. See conceptual framework on response types in Fig. 1, and Table S1 for how statistical tests connect with each response type.

Response type	Relevant comparisons	*P*-value
Seasonal effect	Middle 6-week *vs.* Start 6-week	3.55E-04
	Middle Current *vs.* Start Current	1.51E-01
	Middle 3-week *vs.* Start 3-week	3.07E-02
	End 6-week *vs.* Middle 6-week	0.0242
	End Current *vs.* Middle Current	4.86E-02
	End 3-week *vs.* Middle 3-week	1.78E-01
Immediate treatment effect	Middle 6-week *vs.* Start 6-week	3.55E-04
	Middle Current *vs.* Start Current	1.51E-01
	Middle 3-week *vs.* Start 3-week	3.07E-02
	Middle 6-week *vs.* Middle Current	1.52E-03
	Middle 3-week *vs.* Middle Current	6.02E-01
Delayed treatment effect	End 6-week *vs.* Middle 6-week	0.0242
	End Current *vs.* Middle Current	4.86E-02
	End 3-week *vs.* Middle 3-week	1.78E-01
	End 6-week *vs.* End Current	0.298
	End 3-week *vs.* End Current	0.845

Table S6. Effects of *period-treatment* on the abundance of benthic taxa that significantly explained community dissimilarity in Figure S8. Significant responses are assigned to seasonal and to treatment effects (*immediate* or *delayed*). Asterisks indicate $P < 0.05$ for *period-treatment*. Short horizontal dashes (~) indicate $P < 0.10$. A positive sign (+) or negative sign (-) indicates if advanced low flow treatment had a positive or negative effect, respectively, on taxa abundance, provided that treatment differences explained post-hoc differences. A combination of positive and negative signs (±) indicates that low flow treatment had positive and negative effects at different times. See conceptual framework on response types in Fig. 1, and Table S1 for how statistical tests connect with each response type.

Taxa	ANOVA response		
	Period-Treatment	Treatment effect (Immediate/Delayed/Absent)	Seasonal effect (Present/Absent)
Chironomini	*	Delayed (+)	Absent
Epeorus	~	Immediate (-)	Absent
Glossosoma			
Hydroptila	*	Delayed (+)	Present
Muscidae	*	Absent	Absent
Oligochaeta			
Orthocladiinae sensu lato			
Simuliidae	*	Delayed (+)	Present
Tanytarsini			
Turbellaria	~	Delayed (+)	Absent
Baetis	*	Immediate & Delayed (±)	Absent
Tanypodinae sensu lato			
Diphetor			
Lepidostoma	*	Delayed (+)	Present
Micrasema	*	Delayed (-)	Absent

Drunella flavilnea	*	Immediate (-)	Present

Table S7. Pairwise comparisons of benthic Chironomini abundance among *period-treatment* groups. We examined benthic Chironomini abundance via post-hoc pairwise comparisons (*P*-values) corrected by the Benjamini–Hochberg method. A bolded *P*-value indicates the pairwise comparison was significant for that response type. If the *Current* and *3-week* or *6-week* treatments are significant for the same comparison across periods (e.g., *start* vs. *middle*) then *P*-values are bolded for *seasonal* effects but not for *immediate* or *delayed* treatment effects, as that would indicate similar change over time regardless of treatment. See conceptual framework on response types in Fig. 1, and Table S1 for how statistical tests connect with each response type.

Response type	Relevant comparisons	*P*-value
Seasonal effect	Middle 6-week *vs.* Start 6-week	0.672
	Middle Current *vs.* Start Current	0.545
	End 6-week *vs.* Middle 6-week	0.000519
	End Current *vs.* Middle Current	0.113
Immediate treatment effect	Middle 6-week *vs.* Start 6-week	0.672
	Middle Current *vs.* Start Current	0.545
	Middle 6-week *vs.* Middle Current	0.862
Delayed treatment effect	End 6-week *vs.* Middle 6-week	0.000519
	End Current *vs.* Middle Current	0.113
	End 6-week *vs.* End Current	0.0506

Table S8. Pairwise comparisons of benthic Hydroptila abundance among *period-treatment* groups. Benthic *Hydroptila* abundance post-hoc pairwise comparisons (*P*-values) corrected by the Benjamini–Hochberg method. A bolded *P*-value indicates the pairwise comparison was significant for that response type. If the *Current* and *3-week* or *6-week* treatments are significant for the same comparison across periods (e.g., *start* vs. *middle*) then *P*-values are bolded for *seasonal* effects but not for *immediate* or *delayed* treatment effects, as that would indicate similar change over time regardless of treatment. See conceptual framework on response types in Fig. 1, and Table S1 for how statistical tests connect with each response type.

Response type	Relevant comparisons	*P*-value
Seasonal effect	Middle 6-week *vs.* Start 6-week	0.238
	Middle Current *vs.* Start Current	0.985
	End 6-week *vs.* Middle 6-week	1.54E-09
	End Current *vs.* Middle Current	0.00459
Immediate treatment effect	Middle 6-week *vs.* Start 6-week	0.238
	Middle Current *vs.* Start Current	0.985
	Middle 6-week *vs.* Middle Current	0.238
Delayed treatment effect	End 6-week *vs.* Middle 6-week	1.54E-09
	End Current *vs.* Middle Current	0.00459
	End 6-week *vs.* End Current	0.0000721

Table S9. Pairwise comparisons of benthic Simuliidae abundance among *period-treatment* groups. Benthic Simuliidae abundance post-hoc pairwise comparisons (*P*-values) corrected by the Benjamini–Hochberg method. A bolded *P*-value indicates the pairwise comparison was significant for that response type. If the *Current* and *3-week* or *6-week* treatments are significant for the same comparison across periods (e.g., *start* vs. *middle*) then *P*-values are bolded for *seasonal* effects but not for *immediate* or *delayed* treatment effects, as that would indicate similar change over time regardless of treatment. See conceptual framework on response types in Fig. 1, and Table S1 for how statistical tests connect with each response type.

Response type	Relevant comparisons	*P*-value
Seasonal effect	Middle 6-week *vs.* Start 6-week	0.8
	Middle Current *vs.* Start Current	0.9
	End 6-week *vs.* Middle 6-week	0.0000146
	End Current *vs.* Middle Current	0.0197
Immediate treatment effect	Middle 6-week *vs.* Start 6-week	0.8
	Middle Current *vs.* Start Current	0.9
	Middle 6-week *vs.* Middle Current	0.8
Delayed treatment effect	End 6-week *vs.* Middle 6-week	0.0000146
	End Current *vs.* Middle Current	0.0197
	End 6-week *vs.* End Current	0.0152

Table S10. Pairwise comparisons of benthic *Micrasema* abundance among *period-treatment* groups. Benthic *Micrasema* abundance post-hoc pairwise comparisons (*P*-values) corrected by the Benjamini–Hochberg method. A bolded *P*-value indicates the pairwise comparison was significant for that response type. If the *Current* and *3-week* or *6-week* treatments are significant for the same comparison across periods (e.g., *start* vs. *middle*) then *P*-values are bolded for *seasonal* effects but not for *immediate* or *delayed* treatment effects, as that would indicate similar change over time regardless of treatment. See conceptual framework on response types in Fig. 1, and Table S1 for how statistical tests connect with each response type.

Response type	Relevant comparisons	*P*-value
Seasonal effect	Middle 6-week *vs.* Start 6-week	0.837
	Middle Current *vs.* Start Current	0.347
	End 6-week *vs.* Middle 6-week	0.0169
	End Current *vs.* Middle Current	0.28
Immediate treatment effect	Middle 6-week *vs.* Start 6-week	0.837
	Middle Current *vs.* Start Current	0.347
	Middle 6-week *vs.* Middle Current	0.341
Delayed treatment effect	End 6-week *vs.* Middle 6-week	0.0169
	End Current *vs.* Middle Current	0.28
	End 6-week *vs.* End Current	0.516

Table S11. Pairwise comparisons of benthic stream invertebrate NMDS community composition among *period-treatment* groups. A PERMANOVA test was first conducted with *period-treatment* as a fixed effect and it was found to significantly explain benthic community composition (pseudo-$F_{5,35}$ = 2.571, P < 0.001). Benthic stream invertebrate NMDS community post-hoc pairwise comparisons (P-values) corrected by the Benjamini–Hochberg method. A bolded P-value indicates the pairwise comparison was significant for that response type. If the *Current* and *3-week* or *6-week* treatments are significant for the same comparison across periods (e.g., *start* vs. *middle*) then P-values are bolded for *seasonal* effects but not for *immediate* or *delayed* treatment effects, as that would indicate similar change over time regardless of treatment. See conceptual framework on response types in Fig. 1, and Table S1 for how statistical tests connect with each response type.

Response type	Relevant comparisons	P-value
Seasonal effect	Middle 6-week *vs.* Start 6-week	0.105
	Middle Current *vs.* Start Current	0.171
	End 6-week *vs.* Middle 6-week	0.0188
	End Current *vs.* Middle Current	0.209
Immediate treatment effect	Middle 6-week *vs.* Start 6-week	0.105
	Middle Current *vs.* Start Current	0.171
	Middle 6-week *vs.* Middle Current	0.464
Delayed treatment effect	End 6-week *vs.* Middle 6-week	0.0188
	End Current *vs.* Middle Current	0.209
	End 6-week *vs.* End Current	0.171

Table S12. The effects of *period-treatment* on the abundance of emergent taxa that significantly explain community dissimilarity ($P \leq 0.002$) in Figure S8. Significant responses are determined to be due to seasonal or treatment effects. Asterisks indicate $P < 0.05$ for *period-treatment*. A positive sign (+) indicates that low flow treatment had a positive effect on taxa abundance, provided that treatment differences explained post-hoc differences. See conceptual framework on response types in Fig. 1, and Table S1 for how statistical tests connect with each response type.

Taxa	ANOVA response		
	Period-Treatment	Treatment effect (Immediate/Delayed/Absent)	Seasonal effect (Present/Absent)
Chironominae	*	Immediate & Delayed (+)	Present
Prodiamesinae	*	Immediate (+)	Absent
Orthocladiinae	*	Absent	Absent

Table S13. Pairwise comparisons of emergent Chironominae abundance among *period-treatment* groups. Emergent Chironominae abundance post-hoc pairwise comparisons (*P*-values) corrected by the Benjamini–Hochberg method. A bolded *P*-value indicates the pairwise comparison was significant for that response type. If the *Current* and *3-week* or *6-week* treatments are significant for the same comparison across periods (e.g., *start* vs. *middle*), then *P*-values are bolded for *seasonal* effects but not for *immediate* or *delayed* treatment effects, as that would indicate similar change over time regardless of treatment. See conceptual framework on response types in Fig. 1, and Table S1 for how statistical tests connect with each response type.

Response type	Relevant comparisons	*P*-value
Seasonal effect	Middle 6-week *vs.* Start 6-week	3.75E-05
	Middle Current *vs.* Start Current	4.07E-03
	Middle 3-week *vs.* Start 3-week	4.39E-03
	End 6-week *vs.* Middle 6-week	0.755
	End Current *vs.* Middle Current	1.48E-01
	End 3-week *vs.* Middle 3-week	2.99E-02
Immediate treatment effect	Middle 6-week *vs.* Start 6-week	3.75E-05
	Middle Current *vs.* Start Current	4.07E-03
	Middle 3-week *vs.* Start 3-week	4.39E-03
	Middle 6-week *vs.* Middle Current	8.18E-03
	Middle 3-week *vs.* Middle Current	9.32E-01
Delayed treatment effect	End 6-week *vs.* Middle 6-week	0.755
	End Current *vs.* Middle Current	1.48E-01
	End 3-week *vs.* Middle 3-week	2.99E-02
	End 6-week *vs.* End Current	0.755
	End 3-week *vs.* End Current	0.584

Table S14. Pairwise comparisons of emergent stream invertebrate NMDS community composition among *period-treatment* groups. A PERMANOVA test was first conducted with *period-treatment* as a fixed effect and it was found to significantly explain emergent community composition (pseudo-$F_{8,89}$ = 5.7277, P < 0.001). Emergent stream invertebrate NMDS community post-hoc pairwise comparisons (*P*-values) corrected by the Benjamini–Hochberg method. A bolded *P*-value indicates the pairwise comparison was significant for that response type. If the *Current* and *3-week* or *6-week* treatments are significant for the same comparison across periods (e.g., *start* vs. *middle*) then *P*-values are bolded for *seasonal* effects but not for *immediate* or *delayed* treatment effects, as that would indicate similar change over time regardless of treatment. See conceptual framework on response types in Fig. 1, and Table S1 for how statistical tests connect with each response type.

Response type	Relevant comparisons	*P*-value
Seasonal effect	Middle 6-week *vs.* Start 6-week	0.00257
	Middle Current *vs.* Start Current	0.00257
	Middle 3-week *vs.* Start 3-week	0.00257
	End 6-week *vs.* Middle 6-week	0.38
	End Current *vs.* Middle Current	0.197
	End 3-week *vs.* Middle 3-week	0.0208
Immediate treatment effect	Middle 6-week *vs.* Start 6-week	0.00257
	Middle Current *vs.* Start Current	0.00257
	Middle 3-week *vs.* Start 3-week	0.00257
	Middle 6-week *vs.* Middle Current	0.0394
	Middle 3-week *vs.* Middle Current	0.883
Delayed treatment effect	End 6-week *vs.* Middle 6-week	0.38
	End Current *vs.* Middle Current	0.197
	End 3-week *vs.* Middle 3-week	0.0208
	End 6-week *vs.* End Current	0.883
	End 3-week *vs.* End Current	0.532

Table S15. Assessment of potential Brewer's Blackbird effects on benthic and emergent macroinvertebrate communities, using a Before-After-Control-Impact (BACI) design. We tested if benthic community composition and structure changed immediately after blackbird arrival in channels that were visited relative to channels that were not visited. The interaction term of treatment*time (time being binary: pre vs post-bird presence) was not statistically significant when examining either benthic or emergent invertebrate abundance, richness, or composition, denoting no significant bird effects. Degrees of freedom (df) lists the df for the treatment*time interaction first, then the df of residuals.

Response variable	df	F statistic	*P*-value for treatment*time
Benthic abundance	1, 30	0.238	0.629
Benthic species richness	1, 30	1.649	0.209
Benthic community composition	1, 32	0.957	0.438
Emergent abundance	2, 82	0.269	0.765
Emergent species richness	2, 82	0.62	0.540
Emergent community composition	2, 84	0.716	0.693

SI References

1. K. Reich, *et al.*, Climate Change in the Sierra Nevada: California's Water Future. *UCLA Cent. Clim. Sci.* (2018).

2. J. R. Blaszczak, *et al.*, Extent, patterns, and drivers of hypoxia in the world's streams and rivers. *Limnol. Oceanogr. Lett.* 8, 453–463 (2023).

3. A. V. Nebeker, Effect of Low Oxygen Concentration on Survival and Emergence of Aquatic Insects. *Trans. Am. Fish. Soc.* 101, 675–679 (1972).

4. S. R. P. -J. Ross, O. L. Petchey, T. Sasaki, D. W. Armitage, How to measure response diversity. *Methods Ecol. Evol.* 14, 1150–1167 (2023).

Transition from Chapters 2 to 3

The artificial stream experiment in Chapter 2 showed a strong causal relationship between reduced flow and stream water warming – even over short distances. Warm water temperatures during low-flow conditions can be particularly consequential to stream ecosystems, shifting both species phenologies and ecosystem processes. However, it is uncertain to what extent climate change is poised to alter real thermal regimes in Sierra Nevada streams via a combination of air and water warming, and reduced flow. Although thermal buffering declines with low flow, increased groundwater contributions can cool streams, and other local factors could mediate thermal sensitivity to warming, complicating predictions. Existing models predicting future stream water temperatures may fall short due to assumptions that the relationship between water and air temperature is static, along with uncertainty regarding how thermal regimes vary across spatial scales (Lisi et al. 2015, Leach and Moore 2019). Addressing these knowledge gaps, and accounting for how water temperature propagates downstream, can enable watershed-wide projections of thermal conditions, now and in a warmer future. Chapter 3 was motivated by a desire to learn how, when, and where Sierra Nevada streams may be the most sensitive and vulnerable to climate change.

References

Leach, J. A., and R. D. Moore. 2019. Empirical Stream Thermal Sensitivities May Underestimate Stream Temperature Response to Climate Warming. Water Resources Research 55:5453–5467.

Lisi, P. J., D. E. Schindler, T. J. Cline, M. D. Scheuerell, and P. B. Walsh. 2015. Watershed geomorphology and snowmelt control stream thermal sensitivity to air temperature. Geophysical Research Letters 42:3380–3388.

3

Dynamic, downstream-propagating thermal vulnerability in a mountain stream network: Implications for biodiversity in the face of climate change

Abstract

As climate change continues to increase air temperature in high-altitude ecosystems, it has become critical to understand the controls and scales of aquatic habitat vulnerability to warming. Here we used a nested array of high-frequency sensors, and advances in time-series models, to examine spatiotemporal variation in thermal vulnerability in a model Sierra Nevada watershed. Stream thermal sensitivity to atmospheric warming fluctuated strongly over the year and peaked in spring and summer—when hot days threaten invertebrate communities most. The reach scale (~50 m) best captured variation in summer thermal regimes. Elevation, discharge, and conductivity were important correlates of summer water temperature across reaches, but upstream water temperature was the paramount driver—supporting that cascading warming occurs downstream in the network. Finally, we used our estimated summer thermal sensitivity and downscaled projections of summer air temperature to forecast end-of-the-century stream warming, when extreme drought years like 2020-2021 become the norm. We found that 25.5% of cold-water habitat may be lost under high-emissions scenario RCP 8.5 (or 7.9% under mitigated RCP 4.5). This estimated reduction suggests that 27.2% of stream macroinvertebrate biodiversity (11.9% under the mitigated scenario) will be stressed or threatened in what was previously cold-water habitat. Our quantitative approach is transferrable to other watersheds with spatially-replicated time series and illustrates the importance of considering variation in the vulnerability of mountain streams to warming over both space and time. This approach may inform watershed conservation efforts by helping identify, and potentially mitigate, sites and time windows of peak vulnerability.

Introduction

Ongoing climate change threatens to drastically increase stream water temperature means and extremes—particularly in ecosystems located in high altitudes or latitudes (Pepin et al. 2015). Throughout much of California's Sierra Nevada, air temperature is predicted to increase between 3°C and 6°C by 2080 relative to historical averages (Null et al. 2010; Reich et al. 2018). This warming is poised to advance snowmelt and thus the onset of baseflow up to 50 days, reducing thermal buffering and potentially subjecting stream communities to stressful temperatures (Reich et al. 2018). Similar patterns have been projected, or even observed during supra-seasonal droughts, in other mountain ranges globally (Larson et al. 2011; Vlach et al. 2020). Mountain streams sustain unique ecosystems and are important sources of drinking water, culture, and recreation, all of which may be affected by warming (Isaak et al. 2015; Siirila-Woodburn et al. 2021). Thus, determining the extent of climate change impacts is paramount. A critical step to that end is understanding how thermal vulnerability (i.e. the combination of a species' sensitivity to temperature and its exposure to temperature) varies within stream networks (Clusella-Trullas et al. 2021).

Although increased air temperature alone may marginally increase montane stream water temperature, warming-induced low flows and stream fragmentation (i.e. flow intermittency) can drastically increase average water temperature by reducing thermal buffering (Mayer 2012; Rolls et al. 2012). For example, Elliott (2000) observed water temperature increasing up to 10°C in a high-gradient, small stream during a drought year relative to an average year. Earlier snowmelt as a result of climate change will likely limit thermal buffering capacity further due to increases in overlap between the timing of peak summer temperature and baseflow (Arismendi et al. 2013). This summer window is particularly stressful to organisms, as they can reach their physiological limits due to thermal stress and/or insufficient dissolved oxygen (Trimmel et al. 2018). Warming also alters individual growth rate, behavior, and fecundity in aquatic insects and fish (Hogg and Williams 1996; Woodward et al. 2010; Ledger et al. 2013) with effects potentially scaling up to whole-ecosystem functioning (e.g. changes in decomposition rates and cross ecosystem subsidies; Dewson et al. 2007; Pyne and Poff 2017; Sardina et al. 2017). While climate warming is a prominent stressor in stream ecosystems of major mountain ranges globally (including the Sierra Nevada), uncertainty exists around when and how warmer air may threaten stream thermal regimes, i.e. the characteristic patterns of variation in temperature over time (Caissie 2006; Steel et al. 2017).

Stream and air temperature typically have a positive correlation, but its strength can vary over time, especially at high elevations (Stefan and Preud'homme 1993). We define the correlation between air temperature and water temperature as thermal sensitivity (Δ°C water/ Δ°C air; Leach and Moore 2019). Air and water temperature are correlated with each other because both are heated through solar radiation, in addition to air temperature affecting water temperature directly via long wave radiation and via sensible heat transfer (Lisi et al. 2015). Thermal sensitivity is typically measured using the slope coefficient in a linear or non-linear model that relates water to air temperature (Mohseni et al. 1998). Most studies have assumed a fixed value of thermal sensitivity for long time periods via linear regression, and a few analyses have used more sophisticated time-series methods (e.g. autoregressive state-space models) focusing on a particular season (e.g. Lisi et al. 2015). Approaches based on Dynamic Linear

Models (DLM) could help refine inferences by estimating thermal sensitivity at shorter timescales (e.g. daily) and in a time-varying way, as shown in other ecological applications (e.g. Scheuerell and Williams 2005).

Ninety years of data showed that thermal sensitivity and air temperature may peak in July-August in low elevation, medium-sized streams (Webb and Nobilis 1997). However, patterns of thermal sensitivity could differ in montane regions, where increases in air temperature can cool down stream water in spring due to increased relative contributions of snowmelt (Brown and Hannah 2007). Further complicating these patterns, snowmelt entering the stream as subsurface flow may warm stream water via heat transfer from the soil (e.g. warming by 1.5°C to 3°C in a study in a low elevation, small stream; Kobayashi et al. 1999). Examining how warmer air may affect stream habitats within and across seasons could help quantify stream network vulnerability to future air warming—with major implications for stream biodiversity conservation.

Calls have also been made to understand how thermal regimes in montane regions vary across spatial scales (Leach and Moore 2019). Identifying the appropriate extent and grain to study water temperature is important, as scale-dependencies may exist (i.e. patterns that are only apparent at a particular scale; Levin 1992). However, studies of stream temperature spanning a range of spatial scales remain scarce (Imholt et al. 2013). Microhabitats, reaches, and watersheds are three relevant scales of biotic and abiotic variation in streams, and they encompass a wide range of thermal drivers (Poff 1997). Variation in thermal regimes within a stream reach (~50 - 100 m) is often driven by factors at the microhabitat scale (i.e. a sediment patch within a reach, ~0.02 – 5 m^2), such as differences in canopy cover or variation in water velocity and depth between riffles and pools (Hawkins et al. 1997). In turn, variation among reaches within a watershed (~10 – 100 km^2) is often driven by a combination of groundwater influence, network topology, aspect, and elevation. Lastly, large-scale changes across watersheds (~>100 km^2) are often controlled by geology and climate (Imholt et al. 2013). Without an explicit focus on scale, regional models may overlook thermal refugia (i.e. a subset of the landscape where organisms can survive stressful thermal conditions) provided by small-scale habitat heterogeneity. Alternatively, studies focusing on small-scale variation may miss drivers that create regional gradients (Steel et al. 2016; Selwood and Zimmer 2020). Determining the spatial scale that best captures variation in thermal regimes requires abundant data but could increase cost-effectiveness of monitoring and conservation of thermal refugia.

Here we sought to examine spatiotemporal variation in thermal vulnerability in a pristine stream network in the Sierra Nevada, using high-frequency air and water temperature data at multiple (nested) spatial scales over an extreme drought year (2020-2021). We contend that determining how thermal sensitivity and thermal regimes vary across spatiotemporal scales is crucial to accurately assess current and future vulnerability to warming (Figure 1). In particular, we asked the following questions: (Q1) How does thermal sensitivity change within and over seasons across a mountain watershed? (Q2) At what spatial scale do thermal regimes vary? (Q3) What is the relative effect of 'local' conditions vs. upstream water temperature in driving spatial variation in maximum water temperature? Lastly, (Q4) how will current thermal stress worsen under future climate change and threaten sensitive invertebrate taxa?
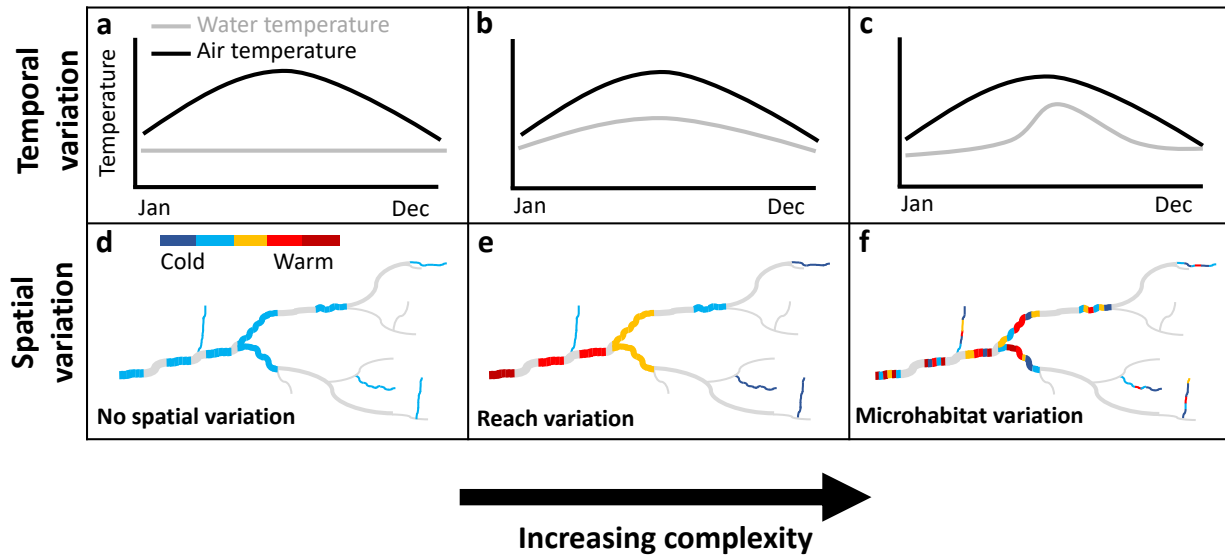
Figure 1. Diagram illustrating different hypothesized levels of thermal complexity over time and space. Water temperature may not respond to variation in air temperature (a), may respond in an approximately static way (b), or may be time-varying, with windows of high sensitivity (c). In turn, variation in water temperature may be homogenous throughout the watershed (d), may be homogenous within reaches but vary across reaches (e), or may vary strongly at small microhabitat-level scales (f). The black and gray lines in A-C represent air and water temperature respectively. Colored segments in the watershed represent the ten reaches examined in this study.

We hypothesized that if analyzed with adequate data and techniques, thermal vulnerability would prove dynamic across time and space. In particular, we predicted that (Q1) thermal sensitivity would be time-varying and peak simultaneously with air temperature in July and August (as suggested from Stefan and Preud'homme 1993; Webb and Nobilis 1997) due to reduced thermal buffering during low flows and peak longwave radiation and sensible heat transfer (Letcher et al. 2016). We also expected that (Q2) the reach scale would best explain spatial variation in thermal regimes as a result of differences in groundwater influence and channel morphology: groundwater inputs can decouple air and water temperature via advection; in turn, reaches with a higher proportion of shallow pool habitat may decrease thermal buffering (Hawkins et al. 1997; Imholt et al. 2013; Hare et al. 2021). In addition to air temperature, we predicted that (Q3) elevation, canopy cover, water depth, and upstream water temperature would all influence local maximum water temperature. Higher elevations reduce air temperature (lapse rate) and shift precipitation from rain to snow (Isaak and Hubert 2001; Ficklin et al. 2013), canopies dampen solar radiation, and deep pools increase thermal buffering through lower surface area to volume ratios (Hawkins et al. 1997; Simmons et al. 2015). Finally, (Q4) we predicted that current invertebrate communities would be vulnerable to projected future warming. Summer air temperature is expected to warm in the future, and we predict that thermal sensitivity peaks in the summer—the combination of these two occurrences would reduce the proportion of cold-water habitat in the stream network when refugia matter the most (Trimmel et al. 2018).

Methods

Study site

This study took place in the southern Sierra Nevada, California, during the severe drought period of 2020-2021, when snowpack amounted to only 45% of long-term average levels—a situation that foreshadows the norm by 2080 if climate change goes unmitigated (Roos 2004; Reich et al. 2018). We focused on the Bull Creek stream network, a watershed in the Kings River Experimental Watersheds (KREW). Habitats within Bull Creek range from meadow-dominated headwaters to Sierra mixed-conifer forest bordered mainstems, and the watershed geology consists of Cagwin soils, derived from granite (Hunsaker et al. 2012). While 75% to 90% of precipitation typically falls as snow (Hunsaker et al. 2012), climate change is poised to increase the relative importance of rainfall at middle elevations (1500-2500 m) where Bull Creek resides (Null et al. 2013). The watershed has been instrumented with four long-term water temperature sensors that enabled contextualizing our 2020-2021 records to long-term data (2007-2019).

Data collection

We deployed a total of 120 Onset MX2202 light-temperature sensors (Onset Computer Corporation, Pocasset, Massachusetts) throughout the Bull Creek watershed in July 2020, for 12 months (7/11/2020 to 6/22/2021) at 15-minute intervals. We targeted ten ~50 m reaches, each receiving six water temperature sensors deployed in three adjacent pool-riffle pairs (Figure 2). This design allowed us to examine variation in thermal regimes across nested scales: from microhabitat to reach to the whole watershed. For each water temperature sensor, we deployed an additional sensor on a secure terrestrial feature to measure air temperature next to the stream channel. Sensors were housed in PVC cases to prevent direct sunlight biasing temperature readings (Isaak et al. 2013).
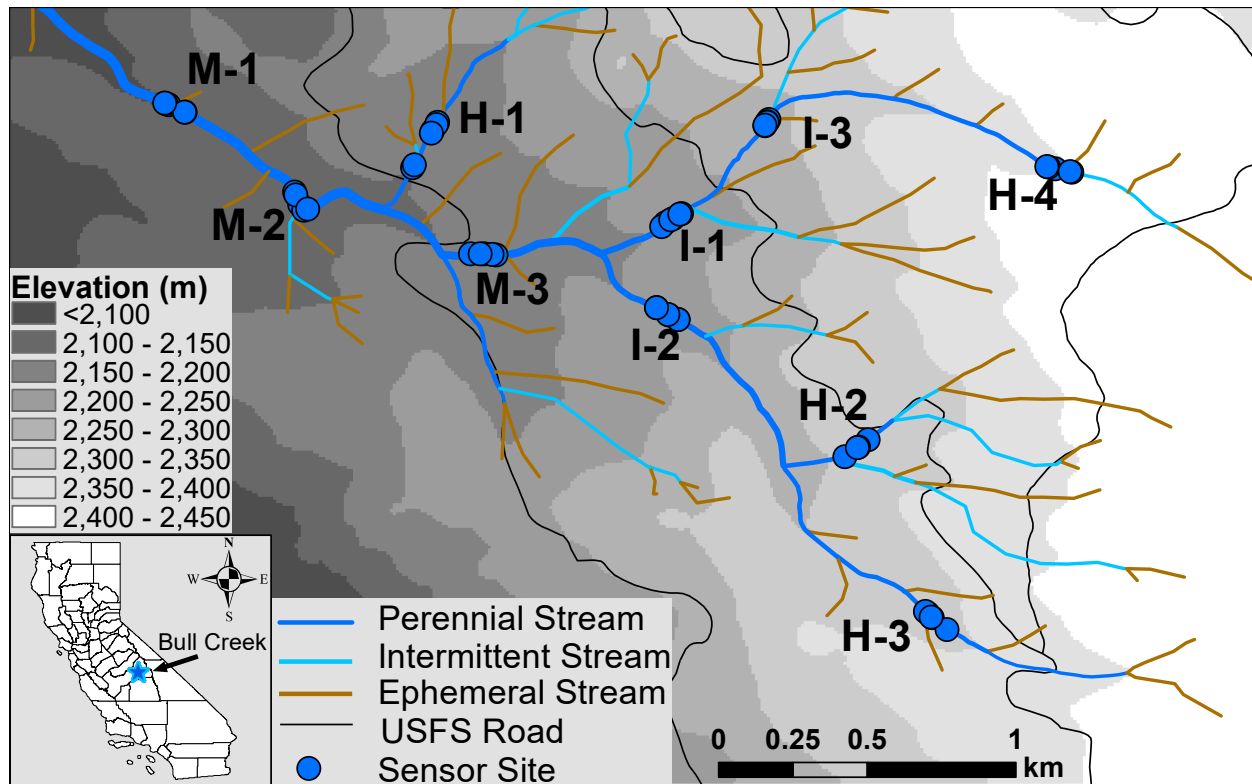
Figure 2. Map of study sites in Bull Creek watershed, California, following a nested spatial design. Each of the 10 reaches had three pairs of pool-riffle sites (often overlapping in the representation due to mapping exact GPS coordinates). Perennial, intermittent, and ephemeral flow regimes are represented, based on the National Hydrography Dataset Plus v.2, except for reaches I-3 and H-4, which were observed as perennial rather than intermittent even during the drought conditions recorded over the study period. Site names reflect the position of each reach within the stream network (*H* = headwater reaches, *I* = intermediate reaches, *M* = Mainstem reaches).

We recovered all 120 sensors. We collected environmental data for each sensor site during low flows in August of 2020, including canopy cover, conductivity, elevation, stream width, depth, velocity, and channel morphology (i.e. pool or riffle). To measure canopy cover, we used a 17-point spherical convex densiometer in four directions over each microhabitat (Ode et al. 2016). We measured conductivity, water velocity, stream depth, and channel width at each microhabitat and discharge at each reach. Site elevation was obtained from a Digital Elevation Model (U.S. Geological Survey 2017).

Time-varying water temperature sensitivity

To answer question 1 on time-varying thermal sensitivity (i.e. water temperature sensitivity to air temperature), we used multivariate Dynamic Linear Models (DLM) on paired water-air temperature data. After inspection of all the time series, eight sensors were removed from analyses because they experienced dry conditions (e.g. due to intermittency or sensor dislodgment by high flows), rendering 15% or more of their daily data unusable. Fifty-two

submerged sensors and their 52 terrestrial pairs were kept for analysis. We averaged 15-minute temperature readings to the daily scale, as we sought to examine variation in thermal sensitivity across days and seasons rather than at subdaily timescales. We averaged air temperature records within each reach to smooth small-scale variation in shading and snow accumulation.

Here we refined past approaches examining thermal sensitivity as a fixed value for long periods of time by estimating it as a time-varying parameter, via DLM. Unlike most current methods, DLM does not incorporate future temperatures in its estimates of thermal sensitivity. We used the *MARSS* package in R (R Core Team 2020) to fit the DLM (Scheuerell and Williams 2005; Holmes et al. 2012). A DLM captures relationships between a predictor and a response variable in a time-varying fashion by fitting a random walk for each parameter of the regression (i.e. one for the slope and another one for the intercept), updating parameters at daily timesteps. We modeled the 52 air-water temperature sensor pairs simultaneously via a multivariate DLM structure—the first multivariate use to our knowledge in any similar context. In the matrix form, the multivariate DLM equations take the following form:

$$x_t = x_{t-1} + w_t, \qquad \text{where } w_t \sim \text{MVN}(0,Q) \qquad (Eq.\ 1)$$
$$y_t = Z_t x_t + v_t, \qquad \text{where } v_t \sim \text{MVN}(0,R) \qquad (Eq.\ 2)$$

The multivariate temperature data (water and air) at day t entered the model in *Eq.2*, as y_t (water temperature, the response variable in each of the 52 sites) and in Z_t, an array that contains the matching paired time series of air temperature (i.e. the covariate data at each site). Water temperature at each site was modeled as a function of air temperature via time-varying regression parameters (x_t), and observation errors (v_t). The time-varying regression parameters (x_t), namely the intercept and slope between air and water temperature, were modeled as random walks for each site (*Eq. 1*), each with its own process error (w_t). Thus, in our study the time-varying slopes (in x_t) are states that capture fluctuations over time in sensitivity of water temperature to variation in air temperature. Process errors (w_t) and observation error (v_t) were modeled as a multivariate normal distribution with a mean of 0 and covariance matrix Q and R respectively. See Supplementary Table 1 for more information on matrix structures and parameters.

Spatial scales of summer water temperature variation

To answer question 2, we focused on the period of peak annual air and water temperature, i.e. the summer period of 7/11/2020 to 8/20/2020. For these 40 days, we calculated sensor-specific daily mean, minimum, and maximum temperature, as well as diel range. We then fit a set of Multivariate Autoregressive models to identify which spatial scale best explained the diversity of thermal regimes (i.e. patterns of stream temperature variation over time) observed across the watershed. The Multivariate Autoregressive model equation in the matrix form is similar to *Eq.1*:

$$x_t = x_{t-1} + Cc_t + w_t, \qquad \text{where } w_t \sim \text{MVN}(0,Q) \qquad (Eq.\ 3)$$

Here x_t is water temperature (unlike in the DLM) at time t, c_t is mean daily air temperature (our covariate), and C is a matrix of covariate effects that captures the effects of air temperature on water temperature. In turn, w_t is process error, assumed to be drawn from a multivariate normal

distribution of mean 0 and variance-covariance matrix Q. Covariate effects (in C) reflect variation in water temperature controlled by air temperature, while process error variance (in Q) captures stochastic (or 'unexplained') fluctuations in water temperature.

While the dimensions of our models remained constant across scales (52 states, one per sensor), we tested hypotheses on the number of thermal regimes present in the watershed by simultaneously constraining the C and Q matrices. We fit models that represented: the watershed scale (1 thermal regime across the whole watershed), pool vs. riffle scale (2 thermal regimes), reach scale (10 thermal regimes), pool-riffle within reach scale (20 thermal regimes), and microhabitat scale (52 sensor-specific thermal regimes; see Supplementary Figure 1). Individual site water temperature was always used, but air temperature was averaged according to spatial scale tested (i.e. c_t varied from a single time series average across all sensors to test the watershed scale, to 52 site-specific time series to test the microhabitat scale). All models converged and were bootstrapped to obtain 95% confidence intervals for coefficients. See Supplementary Table 2 for more details on matrix structures.

Potential drivers of spatial variation in summer water temperature

To answer question 3 and quantify the relative importance of local conditions vs. upstream temperature in driving spatial patterns of summer water temperature, we used Spatial Stream Network (SSN) models on the same sites and summer timeframe (like in the previous section). SSN models use environmental covariates as well as watercourse distances to explain variation in variables along stream networks. This feature is an advantage relative to 'network-agnostic' models when modeling variables like water temperature, as spatial autocorrelation is highly driven by directional flows over short distances (Isaak et al. 2017). Here we selected a range of covariates found to influence stream temperature in previous research, namely mean summer air temperature, stream width, water depth, velocity, pool-riffle morphology, discharge, canopy cover, conductivity, and elevation (Hawkins et al. 1997; Isaak and Hubert 2001; Ficklin et al. 2013; Simmons et al. 2015). Environmental covariates were initially selected using the *bestglm* R package (McManus et al. 2020). After assessing multicollinearity, we used the Gram-Schmidt orthogonalization process on discharge vs. elevation, to 'decouple' these two potential covariates and the discharge residual was used afterwards. Different SSN models were created for maximum, mean, minimum, and diel range in water temperature. Using ArcGIS (ESRI, Redlands, CA), we created the SSN object containing all sites, site conditions, whether sites were flow connected, and their environmental distances from one another. We then used the *SSN* package in R to compare support across model structures. We chose upstream distance as the spatial distance predictor, as downstream temperature should be influenced by upstream temperature (but not *vice versa*). All semivariogram covariance structures that could explain how covariance changes with distance (i.e. none, spherical, exponential, mariah, and linear sill) were tested for model selection using the lowest root mean square prediction error (RMSPE) produced by leave-one-out cross-validation (Ver Hoef et al. 2014). We used the best SSN model for maximum water temperature and universal kriging to estimate maximum water temperature throughout the watershed. We tested estimated temperature accuracy by regressing observed onto modeled temperature values.

Current and future invertebrate habitat suitability

Finally, we sought to determine current and future thermal suitability for the macroinvertebrate community during the summer period, when thermal stress peaks. To this end, we examined current suitability by combining the best-supported SSN model for maximum water temperature over the summer (from question 3), the best-supported spatial scale (from question 2), and extensive data on macroinvertebrate thermal tolerances (see below). We also calculated likely end-of-century stream temperatures in the watershed based on our estimated thermal sensitivity (from question 1) and downscaled maximum air temperature obtained from Multivariate Adaptive Constructed Analogs *(Abatzoglou and Brown 2012)*. Using these results, we compared current to future habitat suitability of Bull Creek for cold-water invertebrates.

Multivariate Adaptive Constructed Analogs (MACA) is a statistical method used for downscaling global climate model outputs, such as temperature and precipitation, to higher spatial resolutions suitable for local analysis (i.e. 1/16th degree). Historical MACA predictions for air temperature in Bull Creek watershed matched historical observations. MACA provided end-of-century estimates of air temperature under Representative Concentration Pathways (RCP) 4.5 and 8.5, representing mitigated *vs.* high-emissions scenario scenarios. We used the difference in maximum air temperature between end-of-century scenarios (i.e. average July and August maximum air temperatures over 2090-2099) and our 2020 average maximum air temperature over July and August to predict end-of-century air warming. Historical data showed that the observed average maximum air temperature in 2020 was similar (within ±1 S.E.) to that of the past two decades. We then forecasted future water temperature increases in Bull Creek by multiplying projected increases in summer air temperature by our estimated thermal sensitivity for July-August.

We assessed the potential ecological impacts of future air-driven stream warming by examining the distribution of thermal preferences of a large subset of representative invertebrate taxa (143 out of 288) observed over more than a decade (2002-2015) within Bull Creek (Herbst et al. 2018). We examined the entire community as well as a subset of orders commonly considered sensitive (Ephemeroptera, Plecoptera, and Trichoptera) and used taxa-specific CD75 values (i.e. the temperature below which 75% of observations of the taxa are found) as a proxy for thermal stress, based on 663 sites across the western US (Yuan 2006). We then calculated the potential loss of cold-water habitat and associated threats to cold-cool eurythermal species (i.e. those occurring below 15°C, based on Vieira et al. 2006). Data used in analyses is available online (Leathers 2022)

Results

Time-varying water temperature sensitivity

As expected, both mean air and water temperatures peaked in late July and August, with peak daily means of 21.2°C for air and 16.8°C for stream temperature (Figure 3). Mean water temperatures varied strongly across headwaters during this time, with some headwater reaches being the warmest (14.2°C in H-1) or the coldest (9.4°C in H-2) across the watershed over the summer. In contrast, mean air temperatures varied little between reaches. Microhabitat-level variation was important in some cases (e.g. a 5.4°C range in mean summer water temperature

across sensors within H-1). As expected, the weeks spanning July-August were the hottest of the year, likely making them the most thermally stressful for aquatic insects present at this time.
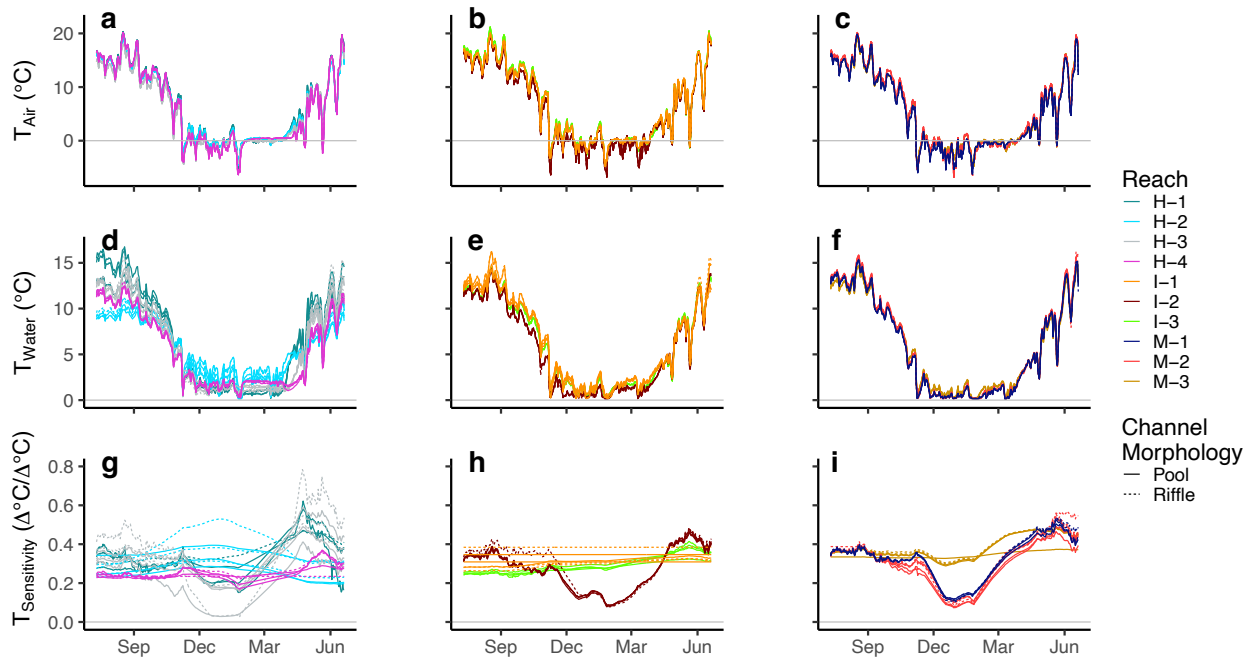

Figure 3. Patterns of mean daily air temperature (a – c), mean water temperature (d – f), and time-varying thermal sensitivity (g – i) at the microhabitat scale (i.e. each individual sensor) across the Bull Creek watershed over the study year (July 2020 – June 2021). In the thermal sensitivity plots, the magnitude of the y axis reflects the increase in water temperature given a 1°C increase in air temperature. Pool microhabitats are displayed as solid lines and riffles are displayed as dashed lines. Site names reflect the position of each reach within the stream network (*H* = headwater reaches, *I* = intermediate reaches, *M* = Mainstem reaches).

The Dynamic Linear Model (DLM) supported that mean air temperature was positively correlated with mean water temperature throughout the year. However, reaches varied in thermal sensitivity and in how sensitivity fluctuated over time at the daily scale (Figure 3). Sensitivity had a clear seasonal trend in some reaches (e.g. H-1, H-3, I-2, M-1, and M-2), being lowest from December to March when snow cover was highest (Supplementary Figure 2). Reaches H-1 and H-3 may have been covered by snow based on the lack of daily variation in air and water temperature observed from February to April. Thermal sensitivity peaked shortly afterwards in May and June immediately following snowmelt. For the entire study period, thermal sensitivity was overwhelmingly positive and statistically significant, with 95% confidence intervals never crossing zero except for one pool-riffle pair in H-3 during winter. Headwater reaches varied widely in their sensitivities, and values from winter vs. summer were often decoupled—for instance, H-3 had the lowest sensitivity among all reaches in the winter (0.16°C/°C) but the highest one in the summer (0.37°C/°C). In contrast, intermediate reaches like I-1 and I-3 showed little seasonal variation in thermal sensitivity. Within-reach variation in sensitivity generally declined as stream size increased from headwater to mainstem habitats. These results partially support our prediction that stream thermal sensitivity would peak simultaneously with air

temperature over the summer period, although in some cases sensitivity peaked in early summer or late spring.

Spatial scales of water temperature variation in summer

In agreement with our hypothesis for question 2, the comparison of Multivariate Autoregressive models supported that summer thermal regimes varied at the reach scale (i.e. a total of 10 regimes) for all temperature metrics (Table 1; see other supported models in Supplementary Table 2). Stream temperature metrics varied substantially throughout the watershed during July and August, with average daily maximum water temperature over the summer ranging from 10.1°C to 23.25°C across sensors (mean across all sensors: 15.7°C). Average pool (15.7°C) and riffle (15.7°C) maximum water temperatures were identical. Notably, a wildfire smoke plume produced a synchronous, short-lived decline in water temperature on August 13 (Supplementary Figure 3).

Table 1. Multivariate Autoregressive model comparison examining the optimal number of thermal regimes across the watershed in the summer. All models had 52 states (one per sensor), but the matrices for process error variance-covariance (Q) and covariate effects (C) reflected the number of thermal regimes (ranging from a single, watershed-wide regime to 52 regimes—one per sensor). Differences in AICc relative to the best model (ΔAICc) are shown for each temperature metric (mean, minimum, maximum, diel range), where ΔAICc = 0 identifies the model that received strongest support.

Spatial scale (number of thermal regimes)	Model type	Mean	Min	Max	Diel
Watershed (1 regime)	Without Air Temp	85.63	150.40	78.09	73.00
	With Air Temp	30.83	55.29	72.57	73.76
Pool-Riffle (2 regimes)	Without Air Temp	87.74	152.49	76.07	72.70
	With Air Temp	35.05	59.49	72.65	75.38
Reach (10 regimes)	Without Air Temp	39.27	81.78	0.00	0.00
	With Air Temp	0.00	0.00	12.07	18.34
Pool-Riffle within Reach (20 regimes)	Without Air Temp	59.63	102.02	15.97	20.37
	With Air Temp	42.35	42.10	49.95	60.36
Microhabitat (52 regimes)	Without Air Temp	119.19	163.51	46.83	76.51
	With Air Temp	176.75	178.22	155.56	190.24

Potential drivers of spatial variation in summer water temperature

We assessed the potential drivers of water temperature in the critical summer period using SSN models and confirmed that temperature propagating downstream was highly influential. Maximum water temperature was largely explained by upstream distance (capturing spatial autocorrelation with upstream water temperature; 72.6% of variation explained) rather than local abiotic conditions (27.4% of variation explained; Supplementary Figure 4). This pattern was true for all temperature metrics (72.6%-91.2% variation explained by downstream propagation alone). The *bestglm* package selected elevation as a covariate for all temperature metrics, conductivity as a covariate for mean and minimum temperature, and discharge as a covariate for maximum and minimum temperature (Table 2; Supplementary Figures 5-7). Elevation and discharge had a negative effect on water temperature, while conductivity had a positive relationship with water temperature. These results partially support our hypothesis that upstream distance, elevation, air temperature, canopy cover, and water depth would best explain variation in water temperature (see reach-level information in Supplementary Table 3). Modeled maximum temperature at the reach (50 m) scale matched observed values (r^2 =0.77, RMSE = 1.08°C; Figure 4A) with prediction skill comparable to previous efforts to model stream temperature in the Western U.S. (e.g. Isaak et al. 2015; FitzGerald et al. 2021).

Table 2. Summary of Spatial Stream Network (SSN) models examining summer stream water temperature variation as a function of local and upstream conditions. Covariate effect sizes from the final SSN model and associated statistical significance (* = $p < 0.05$) are shown. Variance explained is the proportion of variation in water temperature explained by covariates, upstream temperature, and the nugget (i.e. residual variation that is unexplained or occurs on scales smaller than the two closest sensors in this study). See Supplementary Table 4 for details on autocovariance, range, and parsill values.

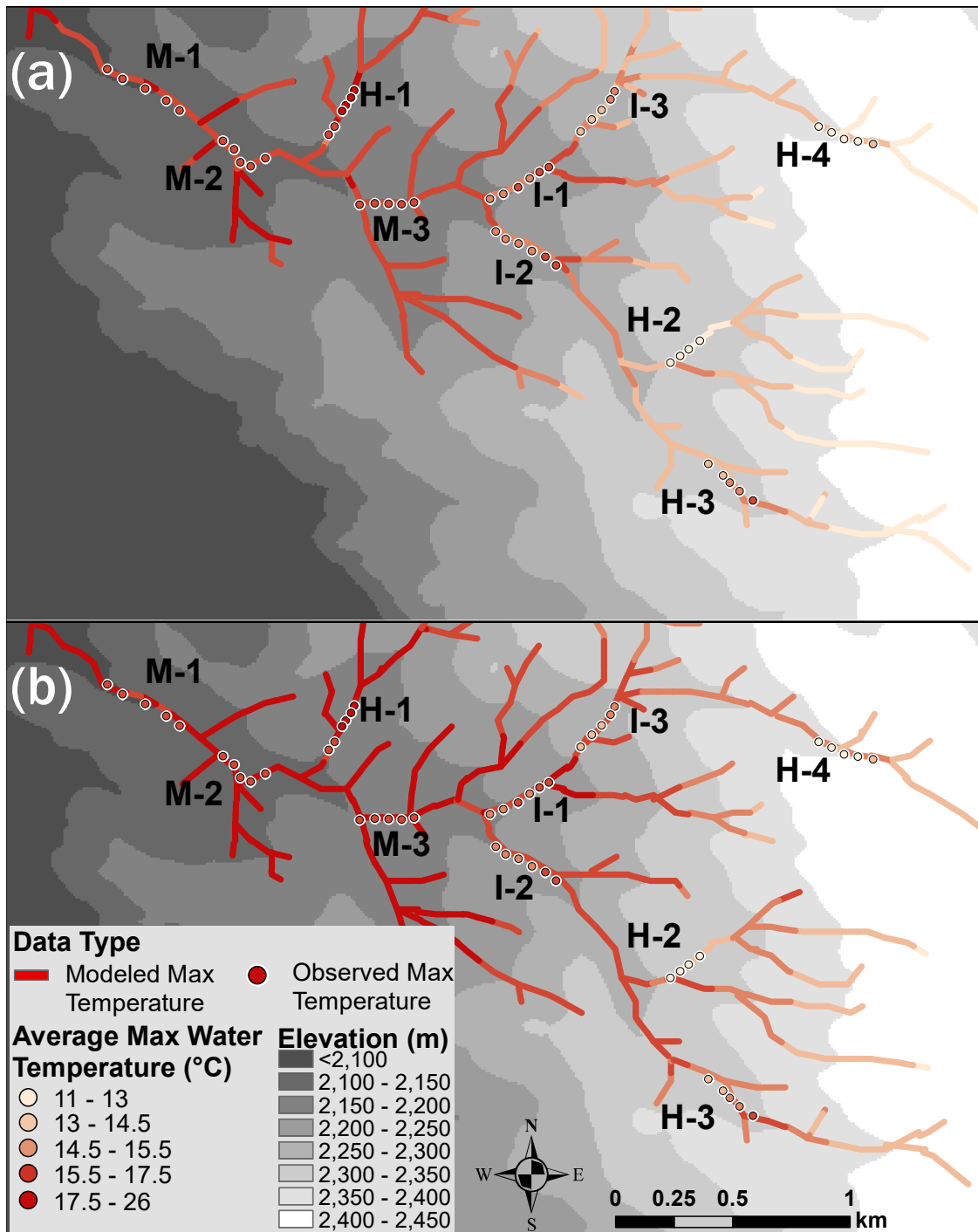|	Parameter	Mean	Minimum	Maximum	Diel
Covariate effect size	*Conductivity*	0.016*	0.008	-	-
	Elevation	-0.011	-0.006	-0.017*	-0.013*
	Q residual	-	-0.050	-0.14	-
Variance explained	*Covariates*	0.159	0.087	0.274	0.156
	Upstream	0.840	0.912	0.726	0.844
	Nugget	<0.001	0.001	<0.001	<0.001
RMSPE		0.158	0.113	0.335	0.271

Figure 4. Maps showing summer maximum water temperatures currently (observed and predicted by the SSN model) and forecasted by the end of the century. (a) The Spatial Stream Network (SSN) map shows observed maximum water temperature in July and August of 2020 and the predicted maximum water temperature using the best model for Bull Creek watershed. The best model had discharge and elevation as selected covariates. (b) The SSN map shows forecasted maximum water temperature by the end of the century under warming predicted for

the high-emissions scenario RCP 8.5 along with 2020 sensor observed maximum water temperature. Maximum water temperature throughout the watershed at the end of the century is predicted to be 1.5°C warmer under projected air warming levels and estimated mean summer thermal sensitivity of 0.32 °C/°C. Maximum water temperatures are displayed using color. Sensor locations were jittered from their actual locations (shown in Figure 2) for better visualization.

Current and future invertebrate habitat suitability

The current distribution of cold-water habitat matched the current distribution of macroinvertebrate thermal thresholds well, both for the overall community and for the sensitive Ephemeroptera, Plecoptera, and Trichoptera subset (Figure 5). For example, 34.3% of modeled taxa in Bull Creek had a CD75 value lower than 15°C (59.9% for Ephemeroptera, Plecoptera, and Trichoptera), meaning they are likely stressed above 15°C, while 52.7% of the watershed stream length had maximum temperatures lower than 15°C (Figure 5). However, by the end of the century maximum air temperature in July and August is expected to increase by 1.6°C under RCP 4.5 (4.9°C under RCP 8.5), which based on the 0.32°C/°C average thermal sensitivity we observed for the summer would increase water temperature in Bull Creek by 0.5°C under RCP 4.5 (or by 1.5°C under RCP 8.5; Figure 4B; Supplementary Figure 8). As a result, the percentage of cold-water habitat in the watershed would decline by 7.9% under RCP 4.5 (from 12.8 km to 10.8 km), and by 25.5% under RCP 8.5 (from 12.8 km to 6.6 km).
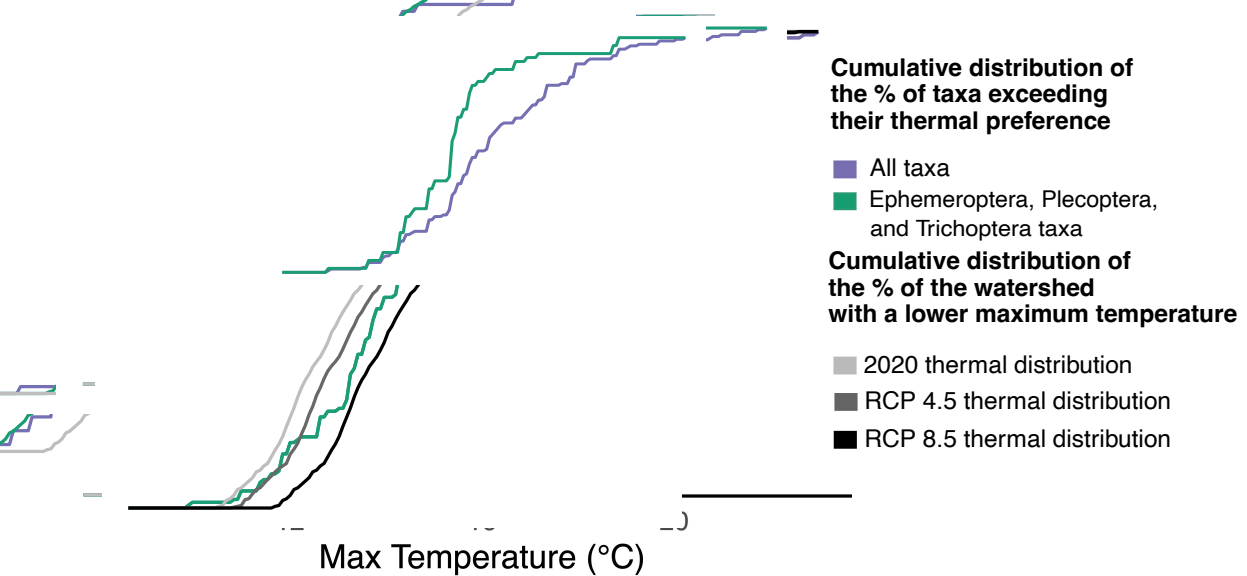

Cumulative distribution of the % of taxa exceeding their thermal preference

- All taxa
- Ephemeroptera, Plecoptera, and Trichoptera taxa

Cumulative distribution of the % of the watershed with a lower maximum temperature

- 2020 thermal distribution
- RCP 4.5 thermal distribution
- RCP 8.5 thermal distribution

Max Temperature (°C)

Figure 5. Cumulative thermal preference distribution of native invertebrate taxa and cumulative distribution of thermal habitat under current vs. future climate change scenarios (RCP 4.5 and RCP 8.5) by the end of the century. Invertebrate taxa were characterized using their individual thermal threshold (CD75 value). This is the temperature above which only 25% of taxa occurrences have been found. The thermal threshold distribution of taxa shows the cumulative percentage of the community that exceed their thermal threshold at a particular maximum temperature (X axis). In turn, the Bull Creek watershed thermal distribution of habitat shows the

cumulative percentage of the stream network that has a lower maximum temperature based on stream length. If the distribution curve of thermal habitat is higher than the taxa thermal threshold distribution, it indicates that there is a disproportionately high amount of suitable habitat relative to the percentage of taxa that prefer that thermal habitat. See Methods for details on warming scenarios.

These warming scenarios threaten cold-water habitat macroinvertebrates, i.e. those occurring mostly under 15°C. The percentage of taxa in the whole community that are potentially stressed (i.e. above their CD75 values) would increase from 34.3% to 46.2% under RCP 4.5 (or up to 61.5% under RCP 8.5) in what is currently cold-water habitat (i.e. 15°C or lower maximum water temperature). For Ephemeroptera, Plecoptera, and Trichoptera taxa alone, such percentages would be even higher, from 59.9% to 76.3% under RCP 4.5 (or up to 86.4% under RCP 8.5). Overall, our projection shows that an additional 11.9% to 27.2% of macroinvertebrate species (and 16.4% to 26.5% of Ephemeroptera, Plecoptera, and Trichoptera) in current cold-water habitat may be threatened by climate-induced air warming at the end of the century.

Discussion

Climate change threatens stream habitats and communities via increases in temperature and altered precipitation patterns (e.g. decreased snowpack) that extend low flows—increasing water temperature indirectly (Yarnell et al. 2010; Reich et al. 2018). Our work adds to a growing body of research on stream thermal vulnerability (e.g. Mayer 2012; Li et al. 2014; Lisi et al. 2015) by showing that sensitivity to air warming varies strongly over time at fine scales— peaking during snowmelt but remaining high from late spring to early fall. We also examined the scales of thermal regimes and found that a medium spatial resolution (~50 m reaches) explained spatial variation best. Spatial variation in water temperature metrics was driven by upstream temperatures propagating downstream throughout the network more than local reach conditions. Finally, we found that stream invertebrates in our watershed are vulnerable to future warming, as suitable habitat will decline for cold-adapted taxa with thermal preferences that match present day (but not future) conditions. While we used a watershed in California's Sierra Nevada as a model system, our quantitative approach and inferences may transfer to other montane watersheds in the vulnerable rain-snow transition zone (Null et al. 2013). Understanding variation in thermal vulnerability over space and time may help protect these fragile ecosystems into warmer futures.

Time-varying water temperature sensitivity

Our results indicate that Bull Creek, and potentially other montane watersheds, are vulnerable to climate change-induced increases in air temperature due to positive thermal sensitivity throughout the year. Despite conventional wisdom that deeper pools may generally buffer against warming (Hawkins et al. 1997), we found that riffles and pools had similar average temperatures and thermal sensitivities. Some differences existed in paired riffle-pool thermal sensitivities in headwaters, but those were rare and seasonal. The high amount of variation in water temperature and thermal sensitivity within and among headwaters is likely due

to their shorter lengths of upstream influence and lower thermal buffering relative to mainstem or intermediate reaches.

The two headwater reaches in our study with the lowest water velocities (H-1 and H-3) had the highest early summer thermal sensitivities, possibly due to increased residence time enabling long wave radiation and sensible heat transfer to have a stronger effect. These two sites were also located in meadows with low baseflow and a high likelihood of being covered by snow during the winter, so spring increases in air temperature melting the snow could expose reaches and the surrounding landscape to radiation that was previously blocked. This could sharply increase thermal sensitivity during snowmelt, as observed. Similar results have been found in models of watersheds near Vancouver, Canada (Leach and Moore 2019).

A strength of the multivariate DLM is its ability to estimate meaningful thermal sensitivity fluctuations over fine temporal scales—capturing the scales of variation of many temperature drivers (e.g. snowmelt, storms, and wildfires; Hunsaker et al. 2012). The short timescales at which thermal sensitivity fluctuated during snowmelt (e.g. daily) suggests that using temporally aggregated data (e.g. monthly mean or max; NorWeST) could be insufficient for capturing fine temporal scale dynamics, although this may be irrelevant for processes controlled by long-term average conditions (Turschwell et al. 2016). Seasonal declines in thermal sensitivity during the winter for some intermediate and mainstem reaches were possibly due to adjacent air temperatures dropping below 0°C, where the relationship between water and air temperature breaks down.

Our study could not directly test how interannual hydroclimatic variation may affect thermal sensitivity. Sierra Nevada watersheds experience up to an order of magnitude in interannual variation in snowpack, affecting snowmelt duration, discharge, and residence time— all of which alter thermal sensitivity (Smits et al. 2020). We predict that summer thermal sensitivity values would be lower in Bull Creek in high-snowpack years because the influence of cold snowmelt would be stronger and last longer.

Spatial scales and drivers of thermal vulnerability

The reach scale best explained temporal variation in water temperature for all metrics. In agreement, local conditions that best explained spatial variation (i.e. conductivity, elevation, and discharge) also varied at the reach scale. These results suggest that studies may miss important variation occurring within watersheds if stream temperatures are considered homogenous over longer distances (e.g. 1 km). Although the microhabitat scale did not perform as well, differences of 2°C to 4°C in maximum temperature often existed among microhabitats within the same reach. Even if these differences were relatively small compared to between-reach differences, this variation should not be neglected as it could matter for species that live close to or above their thermal optima. Because other studies have reported that the best spatial scale explaining water temperature variation may change seasonally (Imholt et al. 2013), our results may only apply to the summer.

Thermal regimes of headwaters are critical to watershed health, as propagation of water temperature downstream was the paramount driver of local temperature in our study. Roon et al.

(2021) similarly found that reach-level water temperature propagated downstream, with local temperature magnitude influencing the distance of propagation. The strong ability of water temperature to propagate downstream suggests that increases in temperature in highly-vulnerable headwaters may warm up downstream sections, even if downstream sections are buffered against local air temperature effects by high discharge levels.

The environmental covariates that explained spatial variation in summer stream temperature illustrate how mountain stream vulnerability to climate change can be highly connected to snowmelt processes. Elevation drives maximum water temperature along hillslopes, and at high elevations it controls the rain-to-snow transition (Klos et al. 2014; Turschwell et al. 2016). In turn, the positive association observed between conductivity and maximum water temperature is likely due to low conductivity values in Sierra Nevada streams not varying with discharge (i.e. chemostatic behavior) and being associated with fast, shallow groundwater inputs from snowmelt (Miller et al. 2014; Ackerer et al. 2020). Consistent with this observation, discharge in Bull Creek was previously shown to not have a relationship with conductivity at I-1 and I-2, likely because the physical structure of their groundwater flow paths generate higher velocities of shallow groundwater (Ackerer et al. 2020). This relationship is further supported by H-2 having the lowest maximum water temperature and the lowest conductivity. Similar to our study, Wissler et al. (2022) found that in the Cascade Range (North of the Sierra Nevada) thermal regimes were heavily influenced by groundwater and potentially snowmelt. Wissler et al. (2022) also found that the rain-dominated Coast Range had warmer water temperatures despite cooler air temperatures and more riparian cover, possibly because of reduced groundwater influence. The observed negative relationship between discharge and maximum temperature supports the notion that reduced thermal buffering in smaller streams could leave some headwaters especially vulnerable to climate-change induced low flows. However, groundwater influence may be greater in streams that reach baseflow due to a higher proportion of flow originating from groundwater, which may dampen summer warming depending on local geomorphology (Ward et al. 2011). Capturing reach-scale variation in temperature and local hydrogeomorphic conditions may lead to more accurate predictions of thermal refugia, increasing precision when quantifying aquatic species vulnerability to future climate (Steel et al. 2016).

Implications for conservation

Although the distribution of macroinvertebrate thermal preferences matched the current availability of thermal habitat, we predicted a thermal mismatch by the end of the century that may threaten or locally extirpate up to 27.2% of macroinvertebrate taxa. Local extirpation may already be happening, as other studies across the world have found macroinvertebrates tolerant of warm conditions are replacing sensitive taxa over decadal timescales (Daufresne et al. 2007; Chessman 2009). Aquatic insects are often assumed to easily disperse to suitable habitat (e.g. higher elevations with greater snowmelt influence), but many cold-water taxa are poor dispersers and are thus prone to local extirpation (Dohet et al. 2015).

More extensive sampling in mountain regions is needed to determine realized rather than potential vulnerability of aquatic insect communities (Birrell et al. 2020). Realized vulnerability should be based on exposure (i.e. current distribution, life histories, and warming exposure),

sensitivity (i.e. physiological, behavioral, and demographic changes in response to warming exposure), and adaptive capacity of organisms (i.e. plasticity and dispersal potential), as suggested by Kovach et al. (2019). Thus, assessing and acting upon realized vulnerability requires considering heterogeneity in temperature exposure within watersheds, as well as understanding how organisms may take advantage of that heterogeneity over their lifespan (Fausch et al. 2002). Our results support that thermal vulnerability in montane stream networks may be highly variable over space and time. Climate change will continue to alter stream water temperatures over the forthcoming decades via changes in air temperature, rain, snowfall, and snowmelt in ways that propagate downstream. Thus, it is crucial to understand how stream ecosystems will respond.

Acknowledgements

References

Abatzoglou, J. T., and T. J. Brown. 2012. A comparison of statistical downscaling methods suited for wildfire applications. Int. J. Climatol. 32: 772–780. doi:10.1002/joc.2312

Ackerer, J., C. Steefel, F. Liu, R. Bart, M. Safeeq, A. O'Geen, C. Hunsaker, and R. Bales. 2020. Determining How Critical Zone Structure Constrains Hydrogeochemical Behavior of Watersheds: Learning From an Elevation Gradient in California's Sierra Nevada. Front. Water 2: 23. doi:10.3389/frwa.2020.00023

Arismendi, I., M. Safeeq, S. L. Johnson, J. B. Dunham, and R. Haggerty. 2013. Increasing synchrony of high temperature and low flow in western North American streams: Double trouble for coldwater biota? Hydrobiologia 712: 61–70. doi:10.1007/s10750-012-1327-2

Birrell, J. H., A. A. Shah, S. Hotaling, J. J. Giersch, C. E. Williamson, D. Jacobsen, and H. A. Woods. 2020. Insects in high-elevation streams: life in extreme environments imperiled by climate change. Glob. Change Biol. 26: 6667–6684. doi:10.1111/gcb.15356

Brown, L. E., and D. M. Hannah. 2007. Alpine stream temperature response to storm events. J. Hydrometeorol. 8: 952–967. doi:10.1175/JHM597.1

Caissie, D. 2006. The thermal regime of rivers: A review. Freshw. Biol. 51: 1389–1406. doi:10.1111/j.1365-2427.2006.01597.x

Chessman, B. C. 2009. Climatic changes and 13-year trends in stream macroinvertebrate

assemblages in New South Wales, Australia. Glob. Change Biol. 15: 2791–2802. doi:10.1111/j.1365-2486.2008.01840.x

Clusella-Trullas, S., R. A. Garcia, J. S. Terblanche, and A. A. Hoffmann. 2021. How useful are thermal vulnerability indices? Trends Ecol. Evol. 36: 1000–1010. doi:10.1016/j.tree.2021.07.001

Daufresne, M., P. Bady, and J. F. Fruget. 2007. Impacts of global changes and extreme hydroclimatic events on macroinvertebrate community structures in the French Rhône River. Oecologia 151: 544–559. doi:10.1007/s00442-006-0655-1

Dewson, Z. S., A. B. W. James, and R. G. Death. 2007. A review of the consequences of decreased flow for instream habitat and macroinvertebrates. J. North Am. Benthol. Soc. 26: 401–415.

Dohet, A., D. Hlúbiková, C. E. Wetzel, L. L'Hoste, J. F. Iffly, L. Hoffmann, and L. Ector. 2015. Influence of thermal regime and land use on benthic invertebrate communities inhabiting headwater streams exposed to contrasted shading. Sci. Total Environ. 505: 1112–1126. doi:10.1016/j.scitotenv.2014.10.077

Elliott, J. M. 2000. Pools as refugia for brown trout during two summer droughts: Trout responses to thermal and oxygen stress. J. Fish Biol. 56: 938–948. doi:10.1006/jfbi.1999.1220

Fausch, K. D., C. E. Torgersen, C. V. Baxter, and H. W. Li. 2002. Landscapes to Riverscapes: Bridging the Gap between Research and Conservation of Stream Fishes. BioScience 52: 483. doi:10.1641/0006-3568(2002)052[0483:LTRBTG]2.0.CO;2

Ficklin, D. L., I. T. Stewart, and E. P. Maurer. 2013. Effects of climate change on stream temperature, dissolved oxygen, and sediment concentration in the Sierra Nevada in California. Water Resour. Res. 49: 2765–2782. doi:10.1002/wrcr.20248

FitzGerald, A. M., S. N. John, T. M. Apgar, N. J. Mantua, and B. T. Martin. 2021. Quantifying thermal exposure for migratory riverine species: Phenology of Chinook salmon populations predicts thermal stress. Glob. Change Biol. 27: 536–549. doi:10.1111/gcb.15450

Hare, D. K., A. M. Helton, Z. C. Johnson, J. W. Lane, and M. A. Briggs. 2021. Continental-scale analysis of shallow and deep groundwater contributions to streams. Nat. Commun. 12: 1450. doi:10.1038/s41467-021-21651-0

Hawkins, C. P., J. N. Hogue, L. M. Decker, and J. W. Feminella. 1997. Channel Morphology, Water Temperature, and Assemblage Structure of Stream Insects. J. North Am. Benthol. Soc. 16: 728–749.

Herbst, D. B., S. D. Cooper, R. B. Medhurst, S. W. Wiseman, and C. T. Hunsaker. 2018. A

comparison of the taxonomic and trait structure of macroinvertebrate communities between the riffles and pools of montane headwater streams. Hydrobiologia 820: 115–133. doi:10.1007/s10750-018-3646-4

Hogg, I. D., and D. D. Williams. 1996. Response of stream invertebrates to a global-warming thermal regime: an ecosystem-level manipulation. Ecology 77: 395–407. doi:10.2307/2265617

Holmes, E. E., E. J. Ward, and K. Wills. 2012. MARSS: Multivariate autoregressive state-space models for analyzing time-series data. R J. 4: 11–19. doi:10.32614/rj-2012-002

Hunsaker, C. T., T. W. Whitaker, and R. C. Bales. 2012. Snowmelt Runoff and Water Yield Along Elevation and Temperature Gradients in California's Southern Sierra Nevada. J. Am. Water Resour. Assoc. 48: 667–678. doi:10.1111/j.1752-1688.2012.00641.x

Imholt, C., C. Soulsby, I. A. Malcolm, M. Hrachowitz, C. N. Gibbins, S. Langan, and D. Tetzlaff. 2013. Influence of scale on thermal characteristics in a large montane river basin. River Res. Appl. 29: 403–419. doi:10.1002/rra.1608

Isaak, D. J., D. L. Horan, and S. P. Wollrab. 2013. A simple protocol using underwater epoxy to install annual temperature monitoring sites in rivers and streams. USDA For. Serv. - Gen. Tech. Rep. RMRS-GTR 1–21. doi:10.2737/RMRS-GTR-314

Isaak, D. J., and W. A. Hubert. 2001. A hypothesis about factors that affect maximum stream temperatures across montane landscapes. J. Am. Water Resour. Assoc. 37: 351–366. doi:10.1111/j.1752-1688.2001.tb00974.x

Isaak, D. J., S. J. Wenger, E. E. Peterson, and others. 2017. The NorWeST Summer Stream Temperature Model and Scenarios for the Western U.S.: A Crowd-Sourced Database and New Geospatial Tools Foster a User Community and Predict Broad Climate Warming of Rivers and Streams. Water Resour. Res. 53: 9181–9205. doi:10.1002/2017WR020969

Isaak, D. J., M. K. Young, D. E. Nagel, D. L. Horan, and M. C. Groce. 2015. The cold-water climate shield: delineating refugia for preserving salmonid fishes through the 21st century. Glob. Change Biol. 21: 2540–2553. doi:10.1111/gcb.12879

Klos, P. Z., T. E. Link, and J. T. Abatzoglou. 2014. Extent of the rain-snow transition zone in the western U.S. under historic and projected climate. Geophys. Res. Lett. 41: 4560–4568. doi:10.1002/2014GL060500

Kobayashi, D., Y. Ishii, and Y. Kodama. 1999. Stream temperature, specific conductance and runoff process in mountain watersheds. Hydrol. Process. 13: 865–876. doi:10.1002/(SICI)1099-1085(19990430)13:6<865::AID-HYP761>3.0.CO;2-O

Kovach, R. P., J. B. Dunham, R. Al-Chokhachy, and others. 2019. An Integrated Framework for Ecological Drought across Riverscapes of North America. BioScience 69: 418–431.

doi:10.1093/biosci/biz040

Larson, R. P., J. M. Byrne, D. L. Johnson, S. W. Kienzle, and M. G. Letts. 2011. Modelling climate change impacts on Spring Runoff for the Rocky Mountains of Montana and Alberta II: Runoff change projections using future scenarios. Can. Water Resour. J. 36: 35–52. doi:10.4296/cwrj3601035

Leach, J. A., and R. D. Moore. 2019. Empirical Stream Thermal Sensitivities May Underestimate Stream Temperature Response to Climate Warming. Water Resour. Res. 55: 5453–5467. doi:10.1029/2018WR024236

Leathers, K. 2022. Data for: Thermal vulnerability in a mountain stream network: Temporal, spatial, and biological data. 10664527 bytes. doi:10.6078/D14D92

Ledger, M. E., L. E. Brown, F. K. Edwards, L. N. Hudson, A. M. Milner, and G. Woodward. 2013. Extreme Climatic Events Alter Aquatic Food Webs. A Synthesis of Evidence from a Mesocosm Drought Experiment. Adv. Ecol. Res. 48: 343–395. doi:10.1016/B978-0-12-417199-2.00006

Letcher, B. H., D. J. Hocking, K. O'Neil, A. R. Whiteley, K. H. Nislow, and M. J. O'Donnell. 2016. A hierarchical model of daily stream temperature using air-water temperature synchronization, autocorrelation, and time lags. PeerJ 4: e1727. doi:10.7717/peerj.1727

Levin, S. A. 1992. The problem of pattern and scale in ecology. Ecology 73: 1943–1967. doi:10.2307/1941447

Li, H., X. Deng, D.-Y. Kim, and E. P. Smith. 2014. Modeling maximum daily temperature using a varying coefficient regression model. Water Resour. Res. 50: 3073–3087. doi:10.1002/2013WR014243

Lisi, P. J., D. E. Schindler, T. J. Cline, M. D. Scheuerell, and P. B. Walsh. 2015. Watershed geomorphology and snowmelt control stream thermal sensitivity to air temperature. Geophys. Res. Lett. 42: 3380–3388. doi:10.1002/2015GL064083

Mayer, T. D. 2012. Controls of summer stream temperature in the Pacific Northwest. J. Hydrol. 475: 323–335. doi:10.1016/j.jhydrol.2012.10.012

McManus, M. G., E. D'amico, E. M. Smith, R. Polinsky, J. Ackerman, and K. Tyler. 2020. Variation in stream network relationships and geospatial predictions of watershed conductivity. Freshw. Sci. 39: 704–721. doi:10.1086/710340

Miller, M. P., D. D. Susong, C. L. Shope, V. M. Heilweil, and B. J. Stolp. 2014. Continuous estimation of baseflow in snowmelt-dominated streams and rivers in the Upper Colorado River Basin: A chemical hydrograph separation approach. Water Resour. Res. 50: 6986–6999. doi:10.1002/2013WR014939

Mohseni, O., H. G. Stefan, and T. R. Erickson. 1998. A nonlinear regression model for weekly stream temperatures. Water Resour. Res. 34: 2685–2692. doi:10.1029/98WR01877

Null, S. E., J. H. Viers, M. L. Deas, S. K. Tanaka, and J. F. Mount. 2013. Stream temperature sensitivity to climate warming in California's Sierra Nevada: Impacts to coldwater habitat. Clim. Change 116: 149–170. doi:10.1007/s10584-012-0459-8

Null, S. E., J. H. Viers, and J. F. Mount. 2010. Hydrologic response and watershed sensitivity to climate warming in California's Sierra Nevada. PLoS ONE 5. doi:10.1371/journal.pone.0009932

Ode, P. R., E. A. Fetscher, and L. B. Busse. 2016. Standard Operating Procedures (Sop) for the Collection of Field Data for Bioassessments of California Wadeable Streams: Benthic Macroinvertebrates, Algae, and Physical Habitat. SWAMP Bioassessment Proced.

Pepin, N., R. S. Bradley, H. F. Diaz, and others. 2015. Elevation-dependent warming in mountain regions of the world. Nat. Clim. Change 5: 424–430. doi:10.1038/nclimate2563

Poff, N. L. 1997. Landscape Filters and Species Traits : Towards Mechanistic Understanding and Prediction in Stream Ecology. North Am. Benthol. Soc. 16: 391–409.

Pyne, M. I., and N. L. R. Poff. 2017. Vulnerability of stream community composition and function to projected thermal warming and hydrologic change across ecoregions in the western United States. Glob. Change Biol. 23: 77–93. doi:10.1111/gcb.13437

R Core Team. 2020. R: A Language and Environment for Statistical Computing. R Foundation for Statistical Computing.

Reich, K., N. Berg, D. Walton, M. Schwartz, F. Sun, X. Huang, and A. Hall. 2018. Climate Change in the Sierra Nevada: California's Water Future. UCLA Cent. Clim. Sci.

Rolls, R. J., C. Leigh, and F. Sheldon. 2012. Mechanistic effects of low-flow hydrology on riverine ecosystems: ecological principles and consequences of alteration. Freshw. Sci. 31: 1163–1186. doi:10.1899/12-002.1

Roon, D. A., J. B. Dunham, and C. E. Torgersen. 2021. A riverscape approach reveals downstream propagation of stream thermal responses to riparian thinning at multiple scales. Ecosphere 12. doi:10.1002/ecs2.3775

Roos, M. 2004. California's Cooperative Snow Surveys Program. ICID 2nd Asian Reg. Conf.

Sardina, P., J. Beardall, J. Beringer, M. Grace, and R. M. Thompson. 2017. Consequences of altered temperature regimes for emerging freshwater invertebrates. Aquat. Sci. 79: 265–276. doi:10.1007/s00027-016-0495-y

Scheuerell, M. D., and J. G. Williams. 2005. Forecasting climate-induced changes in the survival

of Snake River spring/summer chinook salmon (Oncorhynchus tshawytscha). Fish. Oceanogr. 14: 448–457. doi:10.1111/j.1365-2419.2005.00346.x

Selwood, K. E., and H. C. Zimmer. 2020. Refuges for biodiversity conservation: A review of the evidence. Biol. Conserv. 245: 108502. doi:10.1016/j.biocon.2020.108502

Siirila-Woodburn, E. R., A. M. Rhoades, B. J. Hatchett, and others. 2021. A low-to-no snow future and its impacts on water resources in the western United States. Nat. Rev. Earth Environ. 2: 800–819. doi:10.1038/s43017-021-00219-y

Simmons, J. A., M. Anderson, W. Dress, and others. 2015. A Comparison of the Temperature Regime of Short Stream Segments under Forested and Non-Forested Riparian Zones at Eleven Sites Across North America. River Res. Appl. 31: 964–974. doi:10.1002/rra.2796

Smits, A. P., S. MacIntyre, and S. Sadro. 2020. Snowpack determines relative importance of climate factors driving summer lake warming. Limnol. Oceanogr. Lett. 5: 271–279. doi:10.1002/lol2.10147

Steel, E. A., T. J. Beechie, C. E. Torgersen, and A. H. Fullerton. 2017. Envisioning, Quantifying, and Managing Thermal Regimes on River Networks. BioScience 67: 506–522. doi:10.1093/biosci/bix047

Steel, E. A., C. Sowder, and E. E. Peterson. 2016. Spatial and Temporal Variation of Water Temperature Regimes on the Snoqualmie River Network. J. Am. Water Resour. Assoc. 52: 769–787. doi:10.1111/1752-1688.12423

Stefan, H. G., and E. B. Preud'homme. 1993. Stream Temperature Estimation From Air Temperature. J. Am. Water Resour. Assoc. 29: 27–45. doi:10.1111/j.1752-1688.1993.tb01502.x

Trimmel, H., P. Weihs, D. Leidinger, H. Formayer, G. Kalny, and A. Melcher. 2018. Can riparian vegetation shade mitigate the expected rise in stream temperatures due to climate change during heat waves in a human-impacted pre-alpine river? Hydrol. Earth Syst. Sci. 22: 437–461. doi:10.5194/hess-22-437-2018

Turschwell, M. P., E. E. Peterson, S. R. Balcombe, and F. Sheldon. 2016. To aggregate or not? Capturing the spatio-temporal complexity of the thermal regime. Ecol. Indic. 67: 39–48. doi:10.1016/j.ecolind.2016.02.014

U.S. Geological Survey. 2017. 1/3rd arc-second Digital Elevation Models (DEMs).

Ver Hoef, J. M., E. E. Peterson, D. Clifford, and R. Shah. 2014. SSN: An R Package for Spatial Statistical Modeling on Stream Networks. J. Stat. Softw. 56. doi:10.18637/jss.v056.i03

Vieira, N. K. M., N. L. Poff, D. M. Carlisle, S. R. Moulton, M. L. Koski, and B. C. Kondratieff. 2006. A Database of Lotic Invertebrate Traits for North America.doi:10.1899/0887-3593

Vlach, V., O. Ledvinka, and M. Matouskova. 2020. Changing low flow and streamflow drought seasonality in central european headwaters. Water 12: 3575. doi:10.3390/w12123575

Ward, A. S., M. N. Gooseff, and P. A. Johnson. 2011. How can subsurface modifications to hydraulic conductivity be designed as stream restoration structures? Analysis of Vaux's conceptual models to enhance hyporheic exchange. Water Resour. Res. 47. doi:10.1029/2010WR010028

Webb, B. W., and F. Nobilis. 1997. Long-term perspective on the nature of the air–water temperature relationship: a case study. Hydrol. Process. 11: 137–147. doi:10.1002/(sici)1099-1085(199702)11:2<137::aid-hyp405>3.3.co;2-u

Wissler, A. D., C. Segura, and K. D. Bladon. 2022. Comparing headwater stream thermal sensitivity across two distinct regions in Northern California. Hydrol. Process. 36. doi:10.1002/hyp.14517

Woodward, G., D. M. Perkins, and L. E. Brown. 2010. Climate change and freshwater ecosystems: Impacts across multiple levels of organization. Philos. Trans. R. Soc. B Biol. Sci. 365: 2093–2106. doi:10.1098/rstb.2010.0055

Yarnell, S. M., J. H. Viers, and J. F. Mount. 2010. Ecology and Management of the Spring Snowmelt Recession. BioScience 60: 114–127. doi:10.1525/bio.2010.60.2.6

Yuan, L. L. 2006. Estimation and Application of Macroinvertebrate Tolerance Values. US EPA ORD Natl. Cent. Environ. Assess.

Supplementary Materials

Table S1. Matrices, dimensions, and parameters for the multivariate Dynamic Linear Model (question 1). Process errors (w_t) were modeled as a multivariate normal distribution with a mean of 0 and covariance matrix Q, which captured site-specific intercepts and slopes. In this case, each site was allowed to have different diagonal values in Q, as we expected state variances to potentially differ across sites. Observation error (v_t) was also modeled as a multivariate normal distribution with a mean of 0 and covariance matrix R, but this matrix was set to diagonal and equal, as all sites were instrumented with the same sensor type and were assumed to have similar precision. The model converged via the BFGS optimization algorithm. The time-varying states (x_t) were examined against a null hypothesis of no sensitivity (i.e. bootstrapped 95% confidence intervals including zero).

Matrix	Dimensions	Parameters within matrix
y_t	52x345 matrix	Data values were water temperature in Celsius. Each row was a site, and each column was a timestep (i.e. day)
Z_t	52x104x345 matrix	Data values were air temperature in Celsius. Each row was a site. The diagonal values of the first 52 columns represented the individual intercept process error of each site and the last 52 diagonal values represented the individual slope process error in the air-water temperature relationship of each site. The 345 pages of the matrix each represented a day.
x_t	104x1 list	Thermal sensitivity (x_t) initial values were a 104 x 1 list set to 0 for the regression intercept and slope for each site, as we had no prior expectation for these values.
R	52x52 matrix	R was set to diagonal and equal, so a single observation error value was calculated for all sites.
Q	104x104 matrix	The first 52 diagonal values represented the individual intercept process error of each site, and the last 52 diagonal values represented the individual slope process error in the air-water temperature relationship of each site.

Table S2. Matrices, dimensions, and parameters for the Multivariate Autoregressive model (question 2). The process error variance-covariance matrix (Q) always had the same dimensions (52 rows x 52 columns), but its diagonal structure reflected the number of thermal regimes. For example, the watershed-scale matrix had the same process error for all states, while variances were allowed to vary at the site level in the microhabitat-scale matrix. In the covariance matrix (C) rows were sites and columns reflected the spatial grouping (or number of thermal regimes). For the covariate data (c_t), rows represented the spatial grouping (air temperature data at different spatial scales), and columns were the total number of time steps (i.e. days) considered over the summer period (a total of 40). Individual site water temperature was always used, but air temperature was averaged according to spatial scale tested (i.e. c_t varied from a single average time series based on all sensors to test the watershed scale to 52 site specific time series to test the microhabitat scale). We ran an additional set of models without air temperature as a covariate. Water and air temperature were log-transformed to achieve normally distributed model residuals. We assessed model support via the Akaike Information Criteria corrected for small sample size (AICc). The second-best spatial scale for maximum water temperature and diel range was pool-riffle within each reach (20 regimes), while the simplified pool-riffle scale (2 regimes) was second-best for minimum and mean water temperature. Inclusion of air temperature was only supported for mean and minimum temperature.

Matrix	Spatial Scale				
	Watershed	Pool-Riffle	Reach	Pool-Riffle within Reach	Microhabitat
Q matrix ('stochastic' variation in water temperature)	52x52 (watershed level process error variance, i.e. single Q parameter)	52x52 (pool vs. riffle level process error variance, i.e. 2 Q parameters)	52x52 (reach level process error variance, i.e. 10 Q parameters)	52x52 (pool-riffle within reach level process error variance, i.e. 20 Q parameters)	52x52 (microhabitat process error variance, i.e. 52 Q parameters)
C matrix (air temperature effects)	52x1 (Same effect for all sites)	52x2 (different effect for pools vs. riffles)	52x10 (different effect for each reach)	52x20 (different effect for pools and riffles within each reach)	52x52 (different effect for each site)
c_t matrix (air temperature data)	1x40 (single covariate, mean values across the watershed)	2x40 (2 covariates, mean values for pools and riffles)	10x40 (10 covariates, mean values within reaches)	20x40 (20 covariates, mean values for pools and riffles within each reach)	52x40 (52 covariates, one per site)

Table S3. Environmental characteristics of the study reaches across Bull Creek watershed in the summer (question 3). Stream channel and discharge measurements were taken in August 2020. Average air temperature and water temperature values were calculated based on the summer period of peak thermal temperatures from 7/11/2020 to 8/20/2020. Elevation, conductivity, and discharge varied mostly at the reach scale.

Reach	H-1	H-2	H-3	H-4	I-1	I-2	I-3	M-1	M-2	M-3
Maximum Water Temperature (°C)	19.1	12.2	14.6	12.9	16.1	15.4	14.5	16.6	17.2	16.9
Mean Water Temperature (°C)	14.3	9.6	12	11.3	12.9	11.9	12.2	13.3	13.5	12.7
Minimum Water Temperature (°C)	11.9	8.2	10.1	9.9	11.1	9.5	10.5	10.5	10.8	10.4
Diel Water Temperature Range (°C)	7.2	4	4.5	3	5	5.9	3.9	6.1	6.5	6.5
Conductivity (µS/cm)	22.3	9.1	33.5	25.9	15.5	17.8	17.1	24.1	20.6	15.5
Canopy Cover (%)	73	91.9	55	78.2	82.6	83.3	92.9	66.8	79.4	88.8
Stream Width (cm)	94.3	59.9	69.6	83.7	117.8	96.6	120.5	316.8	244.6	202.2
Elevation (m)	2161	2306	2332	2395	2211	2217	2287	2097	2120	2158
Depth (cm)	8.7	5.8	15.9	12.6	13.9	14.3	15.6	15.6	12.7	17.7
Velocity (cm/s)	4.1	9.9	0.6	4.8	1.7	7.9	4.9	11.2	10.5	8.3
Average Air Temperature (°C)	14.3	9.6	12.1	11.3	12.9	12	12.2	13.3	13.6	12.8
Q (L/s)	0.5	0.4	0.2	0.7	1.0	3.6	11.7	16	12.5	11.7

Table S4. Best autocovariance model chosen, range, and parsill values for SSN models (question 3). Upstream metric is the shape of the semivariogram that performed best (i.e. the one with the lowest RMSPE). Parsill (i.e. partial sill) is the variance of the distance covariance function at distance 0. Range is the maximum distance away from a location that spatial autocorrelation will explain variation.

	Parameter	Mean	Minimum	Maximum	Diel
Autocovariance model	*Upstream Metric*	Exponential	Spherical	Spherical	Mariah
	Range (km)	4.693	5.583	0.306	8.894
	Parsill Upstream	2.386	1.691	1.971	1.513
	Parsill Nugget	<0.001	0.002	<0.001	<0.001
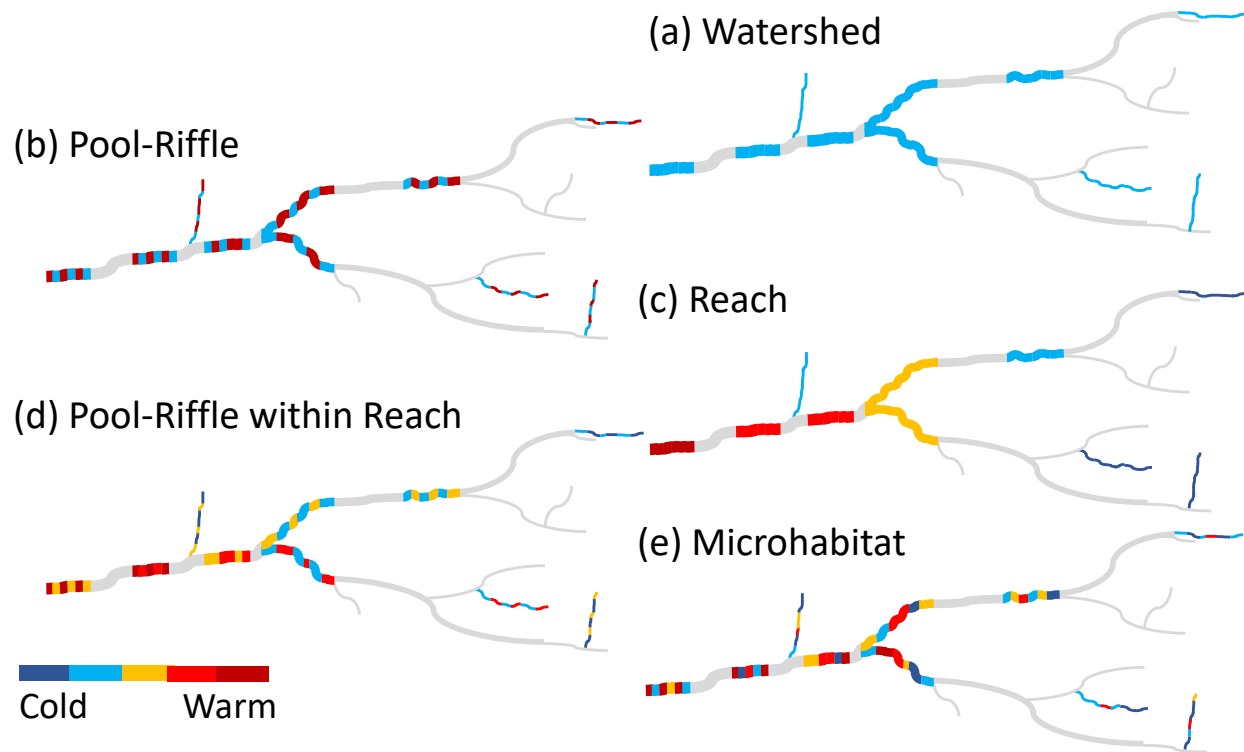
Figure S1. Hypothesized spatial scales of temperature variation across the watershed, as tested in question 2. The ten reaches are colored according to temperature at a given time step, to demonstrate possible scales of variation: (a) *Watershed,* where all water temperature sites are similar throughout the watershed (1 regime); (b) *Pool-Riffle*, where water temperature differs between pools and riffles throughout the watershed (2 regimes); (c) *Reach,* where variation in water temperature is mainly explained by differences between reaches (~50 stretches of stream; 10 regimes); (d) *Pool-Riffle within Reach,* where variation in water temperature is mainly explained by differences between the pools and riffles within each reach (20 regimes); and (e) *Microhabitat*, where variation in water temperature is unique to each site (52 regimes). We defined summer thermal regimes as the characteristic patterns of variation in temperature during the summer—both the unexplained or 'stochastic' portion (in Q of the Multivariate Autoregressive model), and the portion that is explained by fluctuations in air temperature (in C). See Methods for details.
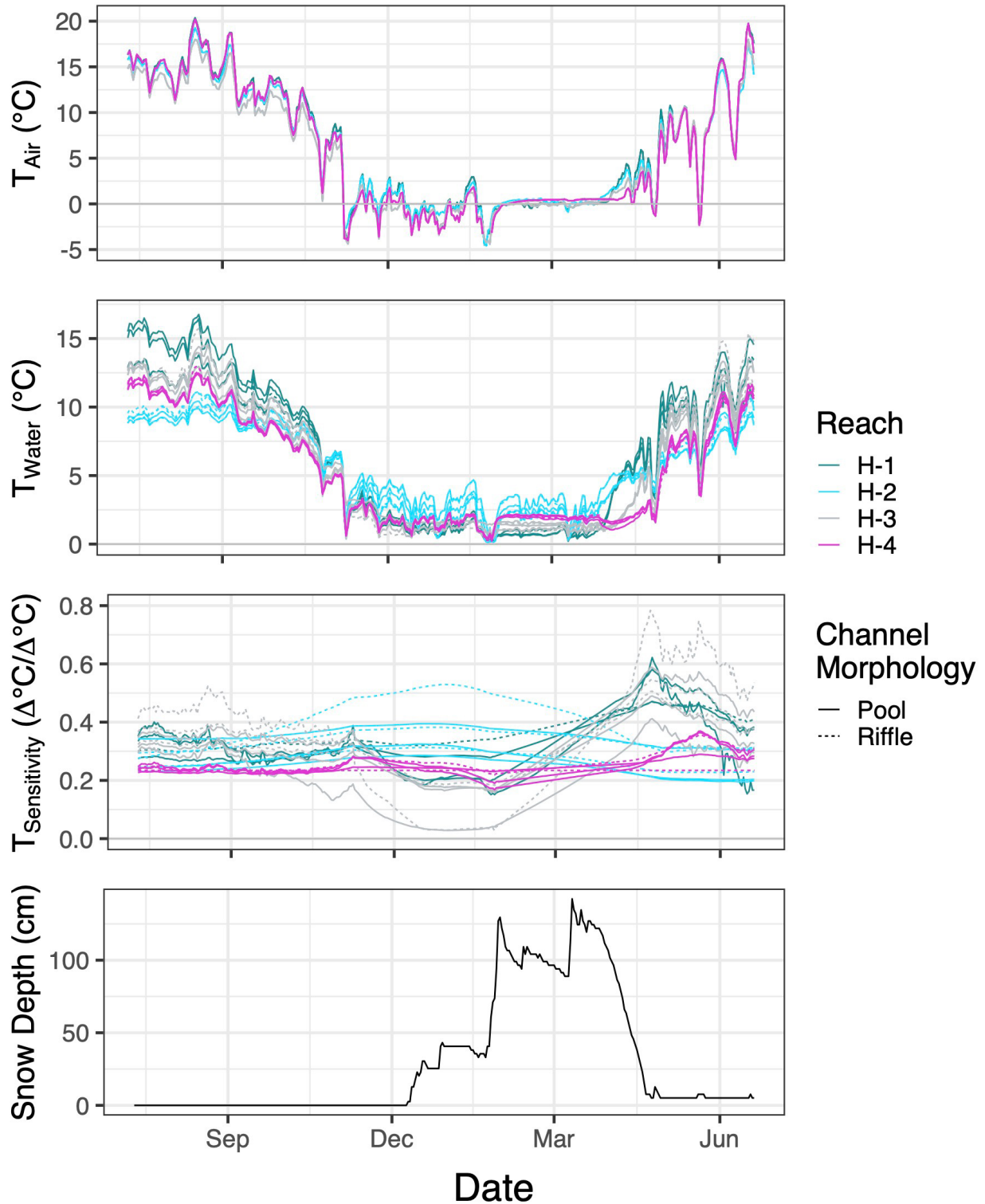
Figure S2. Temporal patterns of snow depth from the upper Bull Creek watershed with associated fluctuations in mean air temperature, water temperature, and time-varying thermal sensitivity at the microhabitat scale (i.e. sensor-specific). Snow depth data was accessed from the California Data Exchange Center for the Upper Bull (KUB) monitoring site.
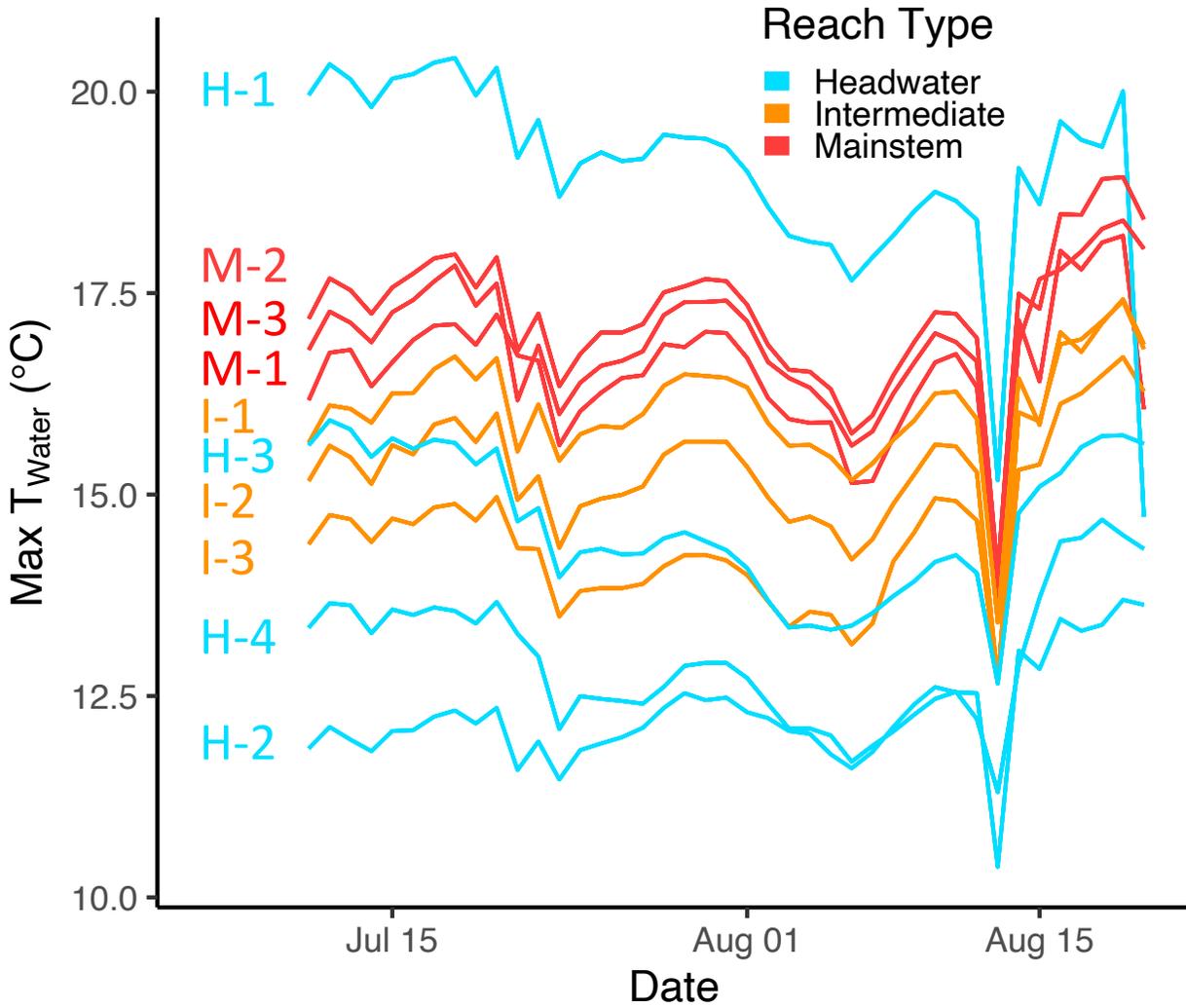
Figure S3. Average of reach maximum daily water temperature over the critical summer period. The maximum water temperature of every sensor within a reach was averaged at a daily scale to produce the average reach maximum water temperature. Reach locations are shown in Figure 2. On August 13, strong smoke from a nearby wildfire caused a synchronous, pronounced dip in water temperature. Site names reflect the position of each reach within the stream network (H = headwater reaches, I = intermediate reaches, M = Mainstem reaches).

Figure S4. Spatial ... which included elevation, d... ...vation and discharge residual are ...ectively. Positive values of discharge ...ould be expected at that elevation gi... ...charge. Point colors represent av... ...t of the map displays the relative am... ...re, and the nugget (i.e. residual variation that is unexplained or occurs on scales smaller than the two closest sensors in this study). Sensor site locations are jittered from their actual locations, shown in Figure 2, for visibility.
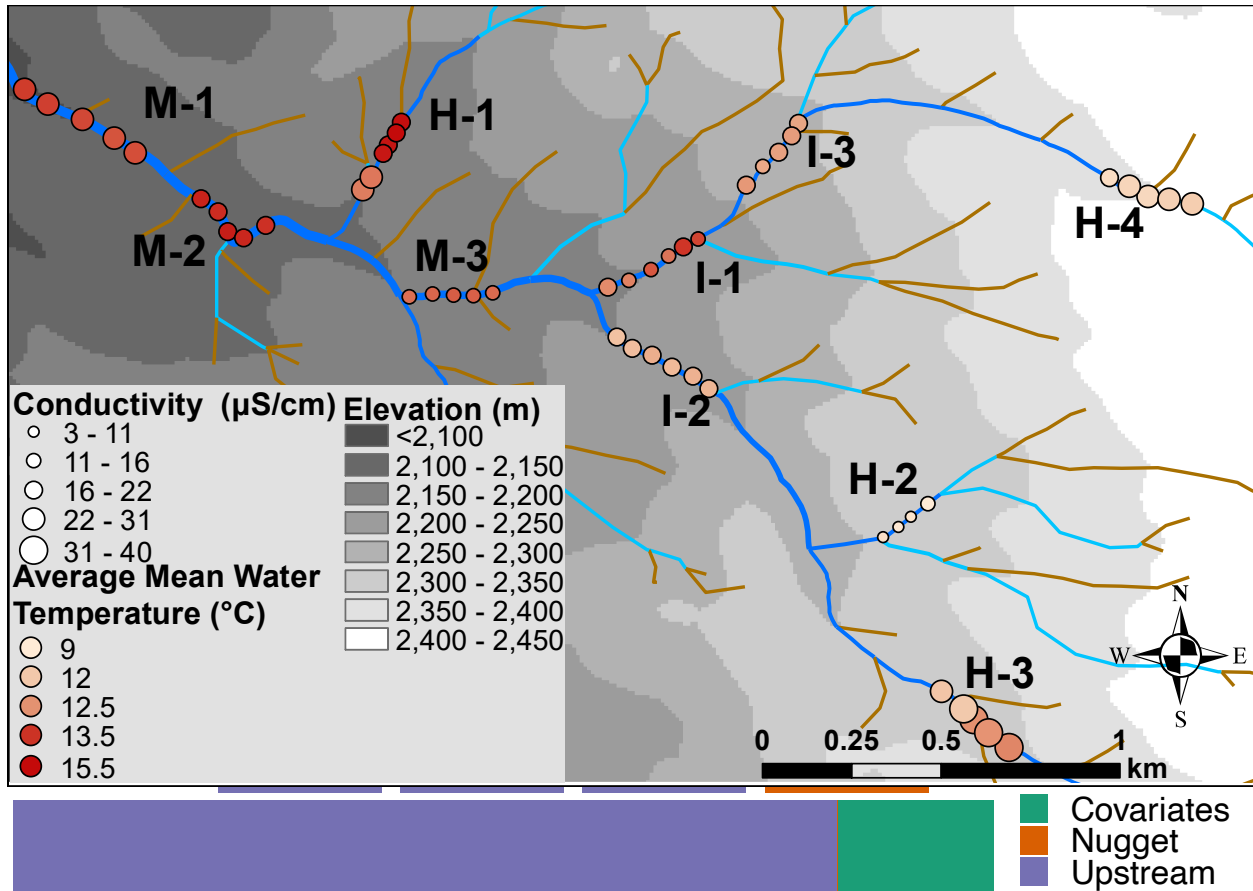
Figure S5. SS[...]n includes elevation, conductivity, a[...]uctivity are displayed on the map via[...]epresent average mean water tempera[...]ve amount of variation explained by c[...]al variation that is unexplained o[...]s study). Sensor site locations are ji[...]ered from their actual locations, shown in Figure 2, for visibility.

Figure S6. SSN map of the best model for min [...] cluded elevation, discharge residual, conductivity, and [...]s. Selected covariates discharge residual (a) and conductiv[...] in the best model and are displayed on the maps. Positive values of discharge residual represent sites where the discharge is higher than would be expected at that elevation given the positive linear relationship between elevation and discharge. Point colors represent average minimum water temperature. The bar along the bottom of the map displays the relative amount of variation explained by covariates, upstream temperature, and the nugget (i.e. residual variation that is unexplained or occurs on scales smaller than the two closest sensors in this study). Sensor site locations are jittered from their actual locations, shown in Figure 2, for visibility.
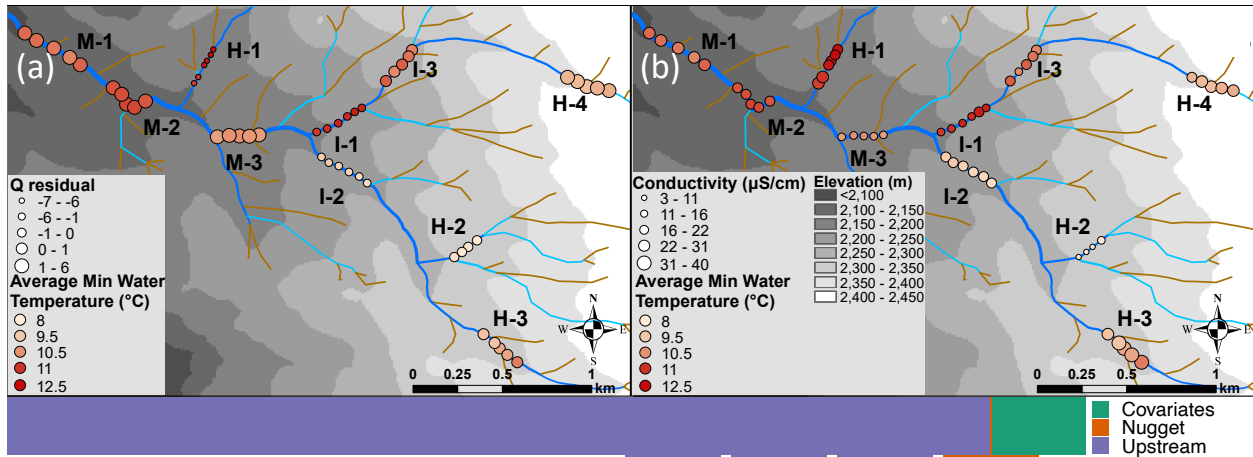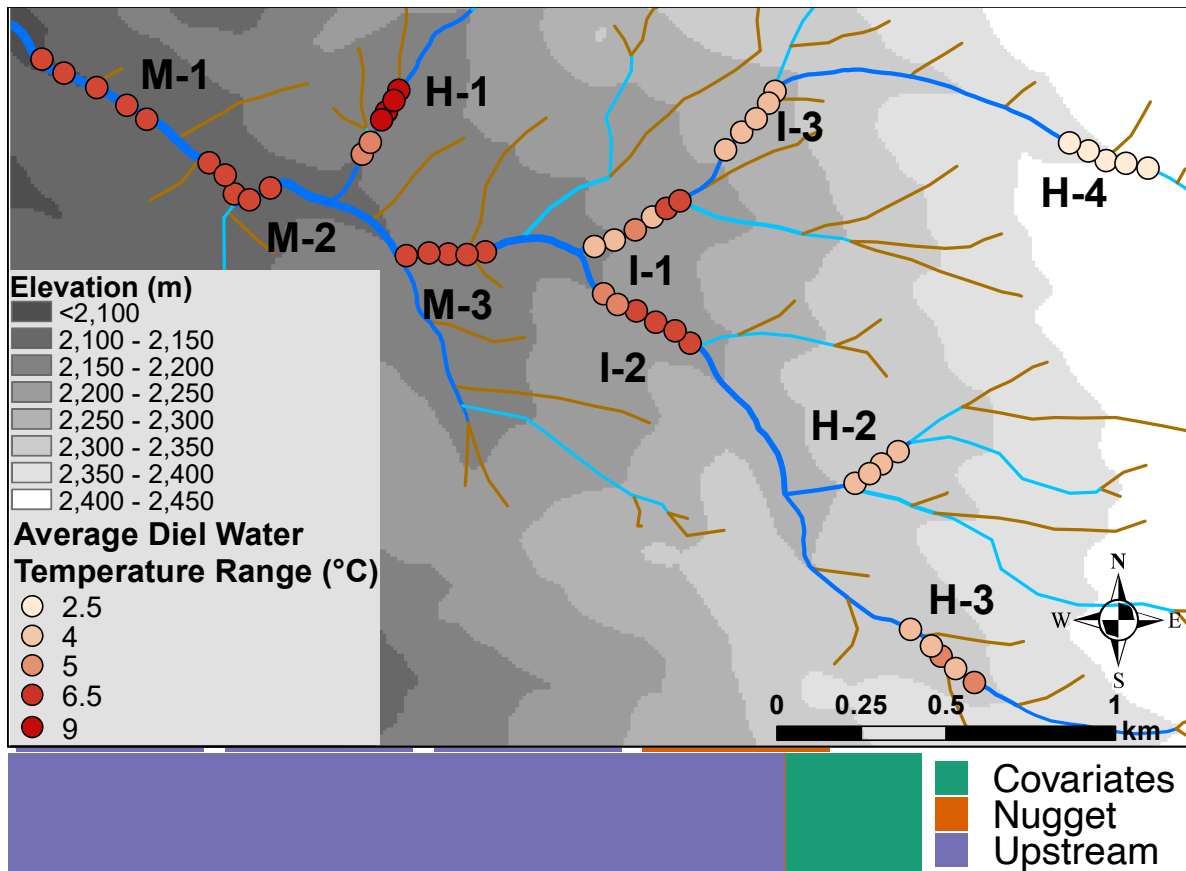
...ture, which included elevation
... the best model and displayed
... water temperature range. The
...riation explained by
...on that is unexplained or
... Sensor site locations are
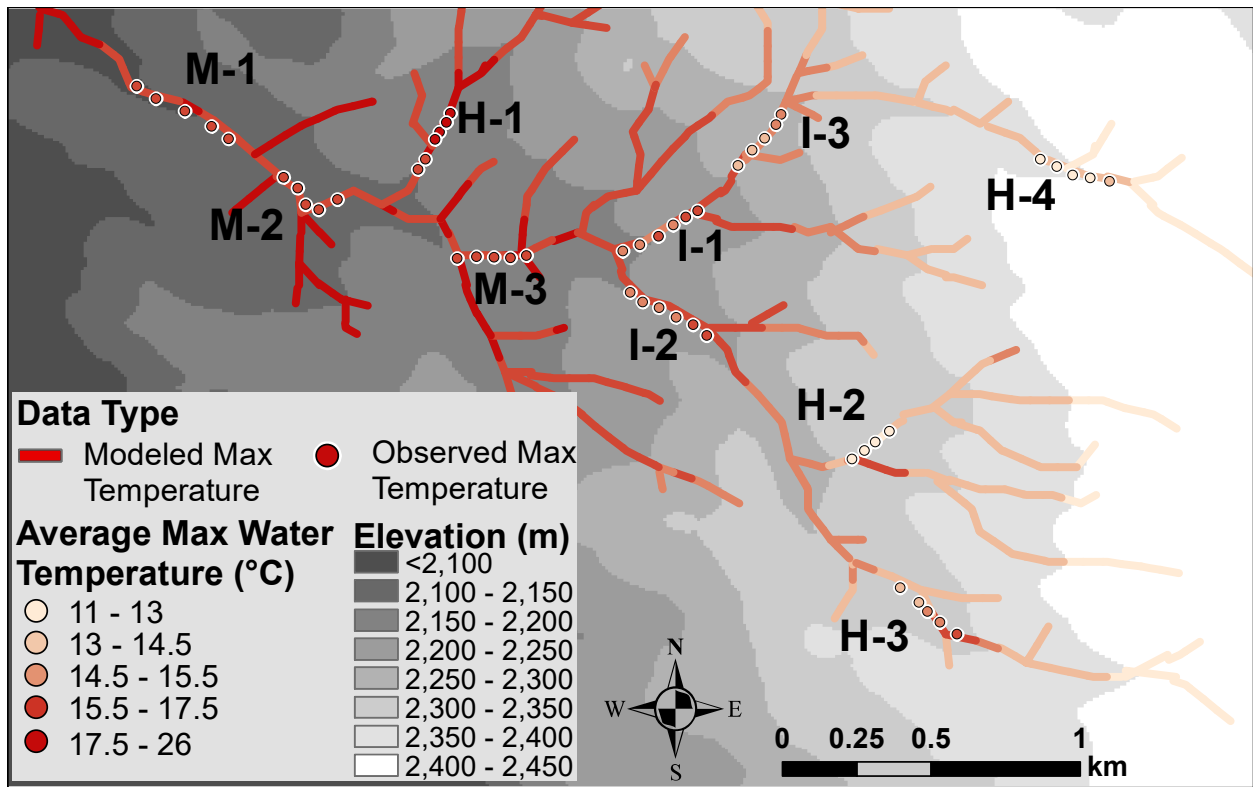...

Figure S8. Map of forecasted maximum water temperature by the end of century under a RCP 4.5 emissions scenario, in which maximum water temperature is expected to increase by 0.5°C. See Methods for details. Current observed maximum water temperature is displayed with points. Sensor site locations are jittered from their actual locations, shown in Figure 2, for visibility.

Transition from Chapters 3 to 4

Chapter 3 suggested that increased air temperatures from climate change would threaten many coldwater taxa in a Sierra Nevada watershed. However, modeled expectations are not always realized in complex ecosystems, and low flows could affect macroinvertebrate communities via other abiotic mechanisms like reduced water velocity and increased fine sediment deposition. Although stream low flows can alter communities via multiple environmental and biological mechanisms, their relative importance is uncertain (Hawkins et al. 1997, Waddle and Holmquist 2013, Herbst et al. 2019). Further, it is unclear whether drought-induced community change across space and over time are realized through similar processes (Angert 2024). This is assumed when scientists use space-for-time substitution approaches, where, for example, a warm site at the base of a mountain is understood to 'preview' the community at higher elevations if temperatures increase. Addressing the accuracy of space-for-time approaches is critical, as they underpin much of the literature on climate change ecology (Lovell et al. 2023). In Chapter 4, I sought to investigate the abiotic and biotic pathways whereby droughts may alter invertebrate community composition and structure in the same Sierra Nevada watershed as in Chapter 3. This approach adds realism to my previous findings on how invertebrate communities are likely to respond to climate change-induced low flows in Sierra Nevada streams.

References

Angert, A. L. 2024. The space-for-time gambit fails a robust test. Proceedings of the National Academy of Sciences 121:e2320424121.

Hawkins, C. P., J. N. Hogue, L. M. Decker, and J. W. Feminella. 1997. Channel Morphology, Water Temperature, and Assemblage Structure of Stream Insects. Journal of the North American Benthological Society 16:728–749.

Herbst, D. B., S. D. Cooper, R. B. Medhurst, S. W. Wiseman, and C. T. Hunsaker. 2019. Drought ecohydrology alters the structure and function of benthic invertebrate communities in mountain streams. Freshwater Biology 64:886–902.

Lovell, R. S. L., S. Collins, S. H. Martin, A. L. Pigot, and A. B. Phillimore. 2023. Space-for-time substitutions in climate change ecology and evolution. Biological Reviews 98:2243–2270.

Waddle, T. J., and J. G. Holmquist. 2013. Macroinvertebrate response to flow changes in a subalpine stream: Predictions from two-dimensional hydrodynamic models. River Research and Applications 29:366–379.

4

Ecological Pathways Connecting Drought to Stream Invertebrate Community Shifts across Space and Time

Abstract

Climate change is intensifying seasonal and interannual droughts in high mountains across the globe, with ramifications on the structure and dynamics of snow-dependent river ecosystems. Low flows can alter communities via multiple environmental (abiotic) and biological (biotic) mechanisms. However, it remains challenging to understand the relative importance of each mechanism, and whether they operate similarly across space and over time. Here, we investigated the abiotic and biotic mechanisms whereby drought alters stream invertebrate community composition and structure in high-mountain streams across space and over time. To this end, we monitored a river network in California's Sierra Nevada (Bull Creek watershed) using a highly-replicated, nested design. The spatial design encompassed 60 sites following a nested structure that captured microhabitat and reach-level variation within the watershed. The temporal design benefitted from long-term data in four reaches that were sampled repeatedly over two decades (11 times from 2002 to 2023). We used Spatial Stream Network (SSN) models to explain the spatial variance and autoregressive (AR) models for the temporal variance. Temperature, water velocity, and fine sediment all explained variation in a similar percentage of taxa in the community (36.8% - 47.4%), but fine sediment had eight times more negative relationships than positive ones. Notably, the effects of abiotic mechanisms differed across space and time: only ~13% of taxa had their variance explained by the same abiotic mechanism across space and time, and total spatial variance explained by abiotic mechanisms for each species had no relationship with its temporal counterpart. With regards to biological mechanisms, we found that community dissimilarity across space was driven by differences in fine sediment causing species *turnover* (i.e., sensitive species being replaced by tolerant ones), while temporal dissimilarity was driven by differences in temperature and water velocity causing *reordering* (i.e., shifts in relative abundance). Our results challenge the key assumption of 'space-for-time' substitution that underpins abundant research on climate change ecology. We contend that space-for-time substitution approaches may be inappropriate in mountain river studies because of their hierarchical structure, high temporal variability, and mechanisms operating distinctly across space and time.

Introduction

Climate change is intensifying seasonal and interannual droughts in high mountain streams across the globe, with ramifications on the structure and dynamics of ecosystems. Future droughts are expected to reduce flow magnitude and prolong low flow duration due to increased air temperature, reduced snowpack, and more frequent extreme dry seasons (Swain et al. 2018, Siirila-Woodburn et al. 2021). These projections matter to ecosystem health because recent experiments have shown that future drought conditions can alter species phenology, community composition, and ecosystem processes (Leathers et al. 2024). Low flows are simultaneously becoming more common and extreme from other anthropogenic activities like water abstraction for agriculture, flow regulation from dams, and land use change (Rolls et al. 2012). Intensifying low flows are ecologically impactful, even if intermittency is not reached, because flow is a 'master variable' that controls a wide range of physical conditions (Poff et al. 1997, Lake 2003). Specifically, low flows cause or are associated with increased water temperature, reduced water velocity, and increased sedimentation, hereafter referred to as *abiotic mechanisms* of drought (Dewson et al. 2007). However, disentangling the relative effects of these mechanisms, and whether their influence varies over space and time, remains a challenge.

Drought can manifest in the physical environment in multiple ways that act either directly or indirectly (via interactions and 'second-order' effects). For example, droughts reduce thermal buffering, which can increase maximum water temperature up to 10°C in some cases (Elliott 2000, Rolls et al. 2012) Increased maximum temperatures can in turn deplete dissolved oxygen and ultimately impact biota even if thermal maxima are not surpassed (Croijmans et al. 2021). Although past work has extensively examined the effects of warming and drying on stream ecosystems, examining these effects alone is inadequate to understand the proximate mechanisms of community change–that is, *how* change is realized (Dewson et al. 2007, Aspin et al. 2018, Nelson et al. 2021). Water velocity also declines during drought, altering species' ability to avoid predators and harming filter feeders that rely on high water velocities for food, among other impacts (Malmqvist and Sackmann 1996). Water velocity reduction in turn reduces the transport capacity of substrate, increasing the deposition of fine sediment. Sedimentation homogenizes habitats by covering large substrates with silt, which can stifle exchange with the hyporheic zone. This can be critical, as the hyporheic zone provides refuge for invertebrates and is the location through which groundwater influences water temperature and dissolved oxygen (Rolls et al. 2012). As a result, sedimentation can reduce macroinvertebrate abundance and species richness in streams (Dewson et al. 2007). Although these three abiotic mechanisms have been shown to affect stream communities and ecosystems, their relative importance and causal relationships are uncertain. For example, reduced flow can increase the cooling influence of groundwater (Dewson et al. 2007, Wawrzyniak et al. 2017). Conversely, water temperature may rise in a pool habitat as thermal buffering declines even if water velocity does not change. Understanding the abiotic mechanisms of drought is not only central to basic ecology, but could also inform conservation and management actions aimed at increasing climate resilience of mountain stream ecosystems.

Efforts to understand how projected climate change is poised to affect aquatic communities often depend on space-for-time substitution approaches that lack verification. Space-for-time substitution argues that differences seen over a spatial range encompassing

varying environmental conditions mirror temporal differences that would occur in a single location undergoing a similar change in environmental conditions. This approach is commonly used in freshwater ecology (Meerhoff et al. 2012); however, the assumption that spatial climate-biotic relationships are transferable to temporal relationships is rarely validated (Lovell et al. 2023). When transferability has been tested, studies in terrestrial systems have found mixed or no support for the magnitude (and even direction) of climate effects being preserved across space and time (Elmendorf et al. 2015, Gaüzère et al. 2020, Angert 2024). Support for space-for-time substitution is also mixed in freshwater studies, but few studies have attempted a robust validation (but see Phillimore et al. 2010, Frauendorf et al. 2019). It is therefore critical to understand whether spatial effects of climate-induced droughts are different from temporal effects, either systematically or otherwise, to better project ecological impacts into the future.

One reason why environmental covariate effects may differ between space and time is autocorrelation (i.e., observations made in close proximity over space or time are more similar than those far apart, for reasons other than the environment). On the spatial side, communities close in space may be similar to each other due to organismal dispersal among nearby patches, regardless of environmental similarity (Leibold et al. 2004). In turn, temporal autocorrelation may arise from populations in one time step affecting those in the following time step (e.g. via intergenerational effects). Spatial and temporal autocorrelation are critical in spatial and temporal modeling techniques, respectively, but it remains uncertain whether the two are related. Species with low dispersal ability can produce strong spatial autocorrelation patterns, which could be tied to expectations of low temporal variability if dispersal-limited populations have high abundances in the same locations year after year. Autocorrelation unrelated across space and time, or unrelated to environmental predictive power, could reflect species specific and abiotic reasons that communities have different spatial and temporal drivers.

A final source of uncertainty connecting drought to community shifts is the multiple ways in which communities can change. Studies have often examined how drought can change species richness (Vellend et al. 2013), but species richness change does not reflect change in relative abundances, or replacement of sensitive taxa with tolerant taxa (Avolio et al. 2015). Alternatively, examining community dissimilarity differences account for all of these changes, but interpretation is abstract and does not reveal the pathways through which communities differ (Collins et al. 2008). One solution is to examine the components of rank abundance curves (RAC) that in aggregate contain the information used in dissimilarity indices (Avolio et al. 2019). When comparing two rank abundance curves, differences can be seen in the identity of the species present (*turnover*), the relative abundance of each species in the community (*reordering*), the total number of species in the community (*richness*), and the slope of the RAC (*evenness*). Drought can alter community composition and structure through these pathways, but the relative importance of these mechanisms, and how they operate over space and time, remains a critical knowledge gap (Figure 1).
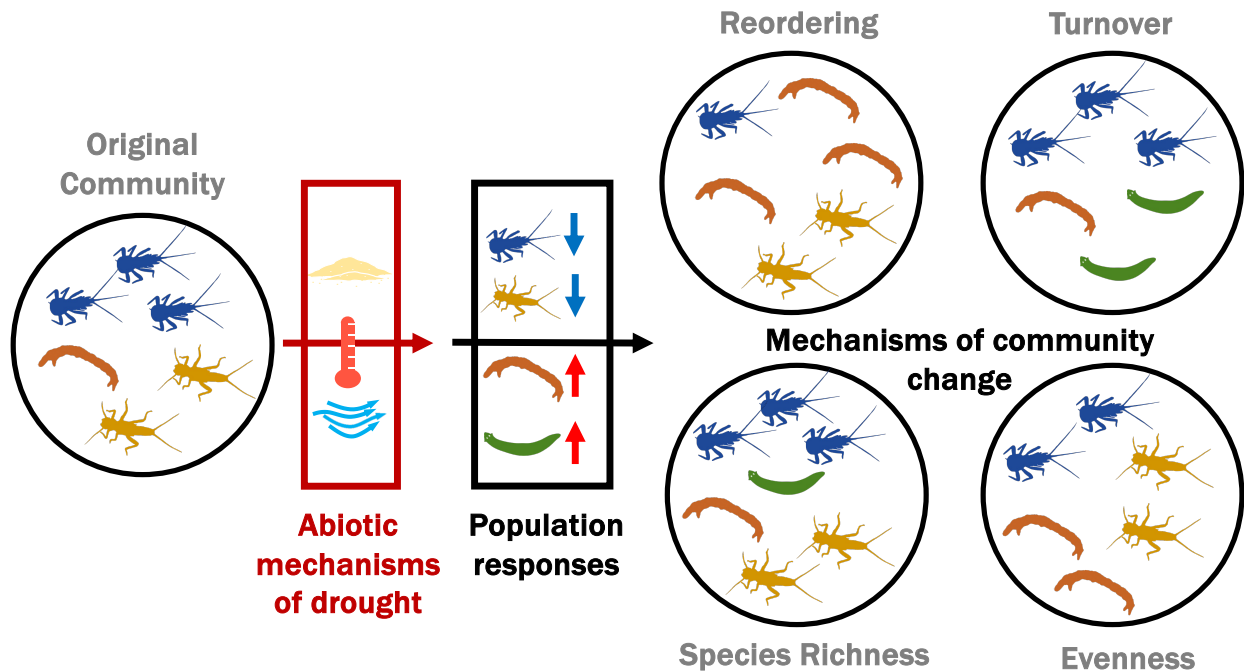
Figure 1. Conceptual diagram of the ways drought can affect community composition via rank abundance curves. Abiotic mechanisms of drought (e.g., increased fine sediment, increased water temperature, and reduced water velocity) can affect communities by *reordering* which species are most abundant, causing *turnover* in which species are present, altering *species richness*, and shifting the *evenness* in abundance among taxa. The combination of these mechanisms explain variation between two communities. In this theoretical example, Ephemeroptera (blue) and Plecoptera (yellow) both decline in abundance due to drought, while Chironomidae (orange) and Turbellaria (green) both experience population growth. Figure inspired by Avolio et al. 2019.

Here we investigated the abiotic and biotic pathways whereby drought alters invertebrate community composition and structure in a long-studied watershed in California's Sierra Nevada. Specifically, we asked: 1) How do species respond to the different abiotic facets of drought (i.e., increased water temperature, reduced water velocity, and increased fine sediment), and is there one particular mechanism that is most impactful?; 2) Do species respond the same way to spatial and temporal variation in each of these abiotic mechanisms (e.g., warming over time *vs.* warming across the river network)?; 3) What are the main mechanisms of biotic change (i.e., community *reordering, turnover, evenness, richness*), and do they similarly explain community change across space and over time?; and finally, 4) What is the whole chain of causality, or ecological pathway (i.e., sequence of abiotic and biotic mechanisms), ultimately connecting drought to community shifts over space and time?

We predicted that: 1) Temperature, water velocity, and fine sediment would all explain variation in taxa abundance across space and time because of response diversity among Sierra Nevada macroinvertebrates (Hawkins et al. 1997, Waddle and Holmquist 2013, Herbst et al. 2019); 2) Although space-for-time substitutions are common in ecology, including in freshwater studies (Meerhoff et al. 2012, Amundrud and Srivastava 2019), we expected that abiotic

mechanisms of drought would affect species differently across space and time. In high mountain streams, summer water temperature and water velocity have high interannual variation depending on snowmelt magnitude, which could result in stronger temporal than spatial effects; 3) The amount and nature of community change may be unequal between space and time, due to different abiotic mechanisms driving change and autocorrelation having different signatures across space *vs.* over time (as in Gumpertz et al. 2000); and finally, 4) Community reordering and species turnover would be the most important proximal causes of community change across space and over time, respectively (as suggested by Bruno et al. 2019, Avolio et al. 2019). Assessing these predictions would help reveal the ecological pathways connecting drought to stream community change–an important goal given that climate change is projected to increase drought intensity and duration in high-mountain ecosystems globally (Barnett et al. 2005).

Methods

Study site and experimental design

This study took place in Bull Creek, California within Sierra National Forest. Bull Creek consists mostly of Sierra mixed-conifer forest with a number of meadows surrounding headwaters (Hunsaker et al. 2012). The watershed falls within the rain-snow transition elevation zone (1500–2500 m), but over 75% of precipitation falls as snow (Hunsaker et al. 2012). However, climate change is predicted to increase the proportion of rainfall going forward (Null et al. 2013). Bull Creek is part of the Kings River Experimental Watersheds (KREW), which have been rigorously monitored for their hydrologic conditions since 2002 (Wagenbrenner et al. 2021).

To answer our research questions, we used samples from four reaches in Bull Creek that were sampled 11 times from 2002-2023, encapsulating a range of low and high precipitation years and associated streamflow levels during the summer (Figure 2). These samples include those previously taken at the reach scale (i.e., ~50-100 m) between 2002 and 2015 (discussed in Herbst et al. 2019), and those we sampled from the same four long-term reaches every year from 2020 to 2023. All samples were collected in the summer after snowmelt allowed access to sample, between June and August. We tested spatial effects by comparing four reach samples taken within the same year. Temporal effects were determined by comparing the community from a year to every other year in the same reach. We also tested for space-time effects where a reach's community was compared to every other reach community regardless of year or location.
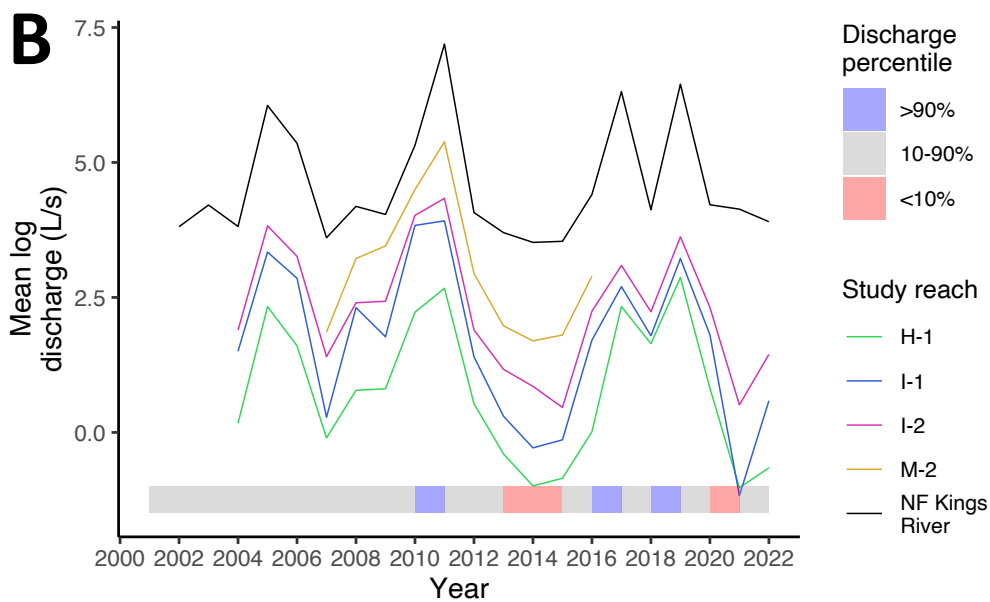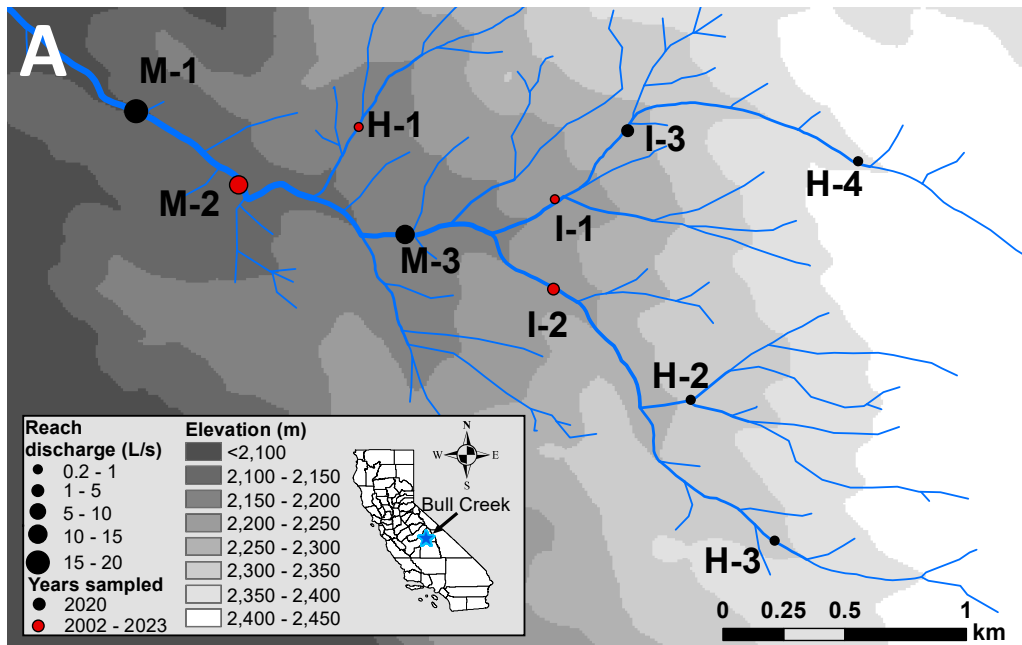
Figure 2. Map of Bull Creek study reaches and variation in discharge over space and time. (A) Map of the measured discharge in 2020 and the years that each reach was sampled. Reaches H-1, M-2, I-1, and I-2 were sampled eleven times between 2002 and 2023 and were included in temporal and spatial analyses. The six other reaches were only sampled in 2020 and only used in spatial comparisons at the microhabitat scale, including species spatial responses. Reach names reflect the stream network position (H = headwater reaches; I = intermediate reaches; M = mainstem reaches). (B) The time series of average July discharge from the four reaches that were studied from 2002 - 2023. Bull Creek reach time series come from hydrologic stations maintained by the USDA Pacific Southwest Research Station. The average water year discharge of the North Fork Kings River, to which Bull Creek is a tributary, is also plotted for context.

North Fork Kings River data comes from site 11218400 which had over 80 years of data. This was used to classify water years by the percentile of discharge in the time series using shaded rectangles at the bottom of the figure.

Additionally, we examined if abiotic mechanisms of drought effects and community assembly differed spatially at the microhabitat scale. To test this, we took fine scale microhabitat samples in 2020 using a nested spatial design. Ten reaches within Bull Creek (including the four long term reaches) were sampled in 2020 with six microhabitat samples taken from each reach. Microhabitat samples came from three paired pool-riffles, so that each reach had three pool and three riffle samples. Microhabitat sites were chosen to capture natural, intra-reach variation in abiotic mechanisms. We expected greater differences in RAC components within the microhabitat compared to the reach scale, as past work has found that most variation in macroinvertebrate communities occurs within the reach (Heino et al. 2004). In all samples across years, abiotic mechanisms were measured, and the macroinvertebrate community was sampled as described below.

Environmental data collection

Abiotic mechanisms of drought were measured during macroinvertebrate collection every year. We calculated water temperature in our study as the average temperature 30 days before the sampling date of a year. We estimated water temperature before 2020 using historic air temperature records beginning in 2004 within the Bull Creek watershed. We found a strong linear relationship (i.e., $R^2 > 0.95$) between air and water temperature averaged over the 30 days before sampling in our data from 2020-2023, so we estimated past water temperature using the resulting regression equation from the relationship. Air temperature records were not available from 2002-2003, so we used Parameter-elevation Relationships on Independent Slopes Model (PRISM) downscaled air temperature daily estimates for the 30 days prior to sampling for those years (PRISM Climate Group 2024). We corrected for overestimation in PRISM air temperature estimates relative to recorded Bull Creek air temperature using a linear regression that had strong support. High frequency water temperature sensors were deployed prior to sampling in 2020 to capture average thermal conditions leading up to sampling. An MX2202 temperature sensor (Onset Computer Corporation) was placed in each microhabitat site at approximately July 11, over a month before invertebrate sampling. Multiple STIC (Stream Temperature, Intermittency, and Conductivity) loggers were placed in long term reaches from 2021-2023 (Chapin et al. 2014). Other abiotic mechanisms were measured at the time of sampling, including water velocity, the percent of fine sediment substrate, and discharge. Water velocity was estimated from 2002-2015 with a Global Water flow probe FP111 at the 50 transect sites. Water velocity in 2020 was measured five times in each microhabitat using a USGS pygmy flow meter connected to an Aqua CMD Current meter digitizer. After 2020, water velocity was estimated using a combination of the USGS pygmy flow meter and measuring the velocity of a floating leaf at five points in a cross-stream transect for each reach. Measurements were averaged for tests done at the reach scale. Prior to 2021, reach estimates of velocity and sediment were a weighted average of pool and riffle values based on the proportion of pool and riffle habitat. The proportion of fine substrate particles (i.e., <0.1 mm diameter) was estimated in every reach. Prior to 2020, visual estimates of fine sediment coverage were made 50 times in each reach divided among 10 cross-stream transects. A square foot grid with 25 equally spaced points was used in 2020 to estimate

the substrate size under each point in the microhabitat prior to sampling. Substrate coverage was visually estimated from 2021-2023 prior to sampling; observations were taken every 10 m in the 100 m reach at each of the 11 sampling locations. Finally, we measured discharge in every reach using the velocity cross-sectional area method (Ode et al. 2016). Microhabitat discharge was assumed to be equal within a reach.

Biological data collection

Stream invertebrates were sampled using a 250 µm D-frame net until 2020 and a 500 µm D-frame net beginning in 2021. This sampling difference likely did not affect our results; past work in streams has found that community samples collected with a 250 µm and 500 µm mesh are generally comparable (Herbst and Silldorff 2006, Buss and Borges 2008). All samples were stored in ~70% ethanol. We used a rotating-drum splitter on samples in the laboratory to split the sample into smaller fractions before sorting and identifying at least 500 individuals from each sample under a stereomicroscope. Subsamples were completely processed to avoid bias regarding the size of individuals picked and identified. Invertebrates were identified to the highest resolution possible, typically genus or species level. Total taxa abundance was corrected by multiplying the counted abundance by the inverse of the fraction of the sample identified. All samples at the reach scale were made comparable by correcting density estimates to 1 m2 and ensuring all aggregate reach samples contained a number of subsamples from riffle or pool habitats proportional to the prevalence of those habitats. The 2021-2023 samples consisted of 11 evenly spaced surber samples throughout a 150 m reach; sampling alternated between the right, center, and left of the channel. In other years, samples were taken and identified from pools and rifles separately, but the proportion of riffle:pool habitat area in the reach was recorded from 2002-2015. We used this proportion to calculate a weighted average of the aggregate reach community. Abundance was corrected in the same manner in 2020; the riffle pool ratio was approximated by matching discharge in 2020 with the historic year from 2002-2015 that had the closest discharge for each reach. The riffle pool ratio of the selected historic year at the same location could then be used to correct abundance records.

Taxa responses to drought across space and time

In order to answer our first and second research questions, we first examined how taxa responded to abiotic mechanisms of drought across space at the microhabitat scale using a Spatial Stream Network (SSN) model. In an SSN model, environmental covariates and watercourse distances both explain variation in dependent variables within stream networks (Isaak et al. 2017). We used a SSN model for the most common taxa in the study (i.e., 19 taxa present in at least half the microhabitat sites and half of the reach samples taken over time) to test how much variation in taxa abundance was explained by spatial autocorrelation, abiotic mechanisms, or was left unexplained. We also examined how community abundance was explained by space and abiotic mechanisms using SSN models. We used ArcGIS (ESRI) to create the SSN object containing all sites, variables, site connectivity, and site environmental distances from one another. Using the *SSN* package in R, we used upstream distance to determine spatial autocorrelation along with mean water temperature, water velocity, and percent fine sediment as covariates. The exponential semivariogram covariance structure was used to explain how covariance changes with distance. A poisson distribution was used in taxa-specific

models, given the prevalence of low or zero abundance observations for many taxa. Covariate effect sizes were standardized by standard error for comparability. SSN model results include variance partitioned to spatial autocorrelation, covariates, and variance left unexplained.

To test the importance of temporal autocorrelation and covariate effects across time, we used generalized least squares (gls) models explaining variation in taxa abundance at the reach scale with abiotic mechanisms as explanatory variables and first order autoregression [AR(1)]. We took the log abundance of each taxa used previously in the spatial analysis for our time series models. We standardized resulting effect sizes by standard error and recorded AR1 ϕ (phi) as an estimate of temporal autocorrelation. Model R^2 was calculated from the aggregate variance explained by all the abiotic mechanisms. Total community abundance was also assessed in spatial and temporal models to see if abiotic mechanisms have similar importance over space and time.

Standardized effects for each abiotic mechanism of drought from our SSN and gls results were compared using linear regression to determine if abiotic mechanisms have a consistent effect across space and time. We also compared spatial autocorrelation (i.e., upstream distance autocorrelation) and temporal autocorrelation (ϕ) of all taxa based on model results. In order to determine if the aggregate influence of abiotic mechanisms on taxa abundance is the same spatially and temporally, we compared the total proportion of variance attributed to abiotic mechanisms across space and time. Lastly, we tested if there was a relationship between taxa variance explained by abiotic mechanisms and autocorrelation for both spatial and temporal comparisons.

Drivers and mechanisms of community change

We compared community composition components across space, time, space-time, and different scales, in order to answer our third research question. Spatial differences were examined at the reach and microhabitat scale. Comparisons were made between all 60 samples collected for the microhabitat spatial comparison (n = 1,770 comparisons). Spatial comparison at the reach scale was done by comparing the four long term reach samples taken within the same year (n = 66 comparisons). We made comparisons across time at the reach scale by comparing the community from every year to every other year for the same reach (n = 220 comparisons). Lastly, comparisons across space-time at the reach scale compared every reach community against every other reach community without grouping by year or site (n = 946 comparisons).

We used the *codyn* R package to examine change in turnover, reordering, richness, and evenness between communities across space, time, and space-time (Avolio et al. 2019). We always used the RAC_difference function, even for temporal comparisons to ensure comparability and because we wanted temporal comparisons to include samples more than one time step away. Turnover difference (i.e., species difference) was calculated by:

$$Turnover\ difference\ = 2*\frac{min(b,c)}{a+b+c} \qquad (1)$$

where *a* is the number of species present in both samples, *b* is the number of species unique to the first sample, and *c* is the number of species unique to the second sample. Reordering

difference (i.e., rank difference) was calculated by:

$$Reordering\ difference\ = \frac{\Sigma_i^N(|R_{i,x} - R_{i,y}|)}{(S_{tot})^2} \qquad (2)$$

where $R_{i,x}$ is the rank of species R_i in sample x, $R_{i,y}$ is the rank of species R_i in sample y, and S_{tot} is the total number of unique species in both samples. We calculated richness difference as the difference in the alpha diversity of two samples divided by the alpha diversity of the two samples combined. Evenness was measured using the variance of abundance values to ensure that it is independent of species richness (Smith and Wilson 1996). Evenness difference is simply the difference between the evenness values of communities. Because we are interested in the magnitude of the RAC components rather than which community has greater evenness or species richness, we took the absolute value of evenness and species richness comparisons. We used one-way ANOVA tests to determine if RAC components differed among comparisons made across space, time, and space-time. If comparison was significant, then we ran a Tukey's Honest Significant Difference post-hoc test to determine pairwise differences. We also estimated RAC components for microhabitat samples in 2020 to compare to reach scale spatial differences.

Causal pathways connecting drought to community change

For our final question, on the causal pathways ultimately connecting drought to community dissimilarity across space and time, we used piecewise structural equation models (pSEM). We did this with the psem function in the piecewiseSEM R package to mechanistically test the relationships between abiotic mechanisms, RAC components, and community dissimilarity all at once (Lefcheck 2016). Each pSEM was composed of five linear models; four models predicted each RAC component by abiotic mechanism differences between communities, and one model explained community dissimilarity between communities with the RAC components. We made pSEMs comparing communities across space, time, and space and time at the reach scale, along with a pSEM for microhabitat comparisons across space. We calculated the absolute difference in mean water temperature, water velocity, and percent of fine sediment between two samples to use the delta as covariates in models. We used generalized linear models to determine which differences in abiotic mechanisms best explained differences in RAC components for each space, time, or space-time comparison at the reach scale. The same tests were repeated with microhabitat spatial community comparisons to determine the importance of scale. Effect sizes of abiotic mechanisms were standardized by dividing by the standard error, for comparability between the abiotic mechanisms within and between models. We used ANOVA models to determine which RAC components best explained Bray Curtis dissimilarity for each space, time, or space-time comparison at the reach scale and microhabitat communities across space. We calculated partial eta squared (ηp2) of RAC components for comparability within models.

Results

Drought and the mosaic of environmental conditions

Environmental conditions fluctuated strongly across space and over the years, largely driven by high variability in snowpack (and snowmelt-driven discharge) over the two study

decades. Temporally, summer discharge varied by two orders of magnitude over the course of the study in every reach of Bull Creek (Figure S1). Discharge was exceptionally high in water years 2011, 2017, and 2019, but fell below the 10th percentile of historic discharge records in 2014, 2015, and 2021 (Figure 2). Spatially, discharge among the ten reaches of Bull Creek ranged from 0.2 - 16 L/s in the moderate drought year of 2020, when the microhabitat sampling took place (Figure 2).

The strong temporal and spatial variation in discharge drove variation in the abiotic mechanisms of drought we considered: water temperature, water velocity, and fine sediment. Average water temperature showed similar spatial (9.2 - 15.2°C) and temporal (6.5 - 15.6°C) variation in our study, where the interannual range of temperature in each reach was approximately 6°C (Figure S1; Figure S2). Water velocity at the reach scale varied 1-2 orders of magnitude over time with greater variation in smaller reaches (Figure S1; Figure S3). Spatially, water velocity was typically lowest in the headwater reach, while the mainstem reach water velocity was 9.7 times higher on average across all years. Fine sediment cover was low at the reach scale (7.5%) and standard deviation was similar across space (7.4%) and time (9.5%). Temporally, high discharge could cause large erosion events that increased silt cover, but low discharge years could also increase sedimentation by increasing the settlement of silt (Figure S1; Figure S4). In a moderate drought year, the microhabitat scale had higher average fine sediment cover (33.7%) and standard deviation (39.8%) than that seen on average at the reach scale. Multicollinearity of abiotic mechanisms was not supported by variance inflation factor tests (less than 2 in all cases at both microhabitat and reach scales), supporting that they could independently explain variation in our study. These results suggest that variables associated with low flow exist in a diverse environmental mosaic across the watershed, supported by fine scale sampling and extended repeated sampling.

Effects of drought on common taxa

Among the 19 taxa retained to examine drought effects, all abiotic mechanisms were influential and had a similar percentage of significant relationships among common taxa (36.8% - 47.4%; Figure 3). At least one of the abiotic mechanisms was supported as an explanatory driver in 78.9% of taxa when combining spatial and temporal results. Water temperature had a positive relationship roughly as often as a negative one (four *vs.* three times, respectively). This suggests high response diversity in the community, as increased water temperatures may benefit and harm a similar number of species. Increased water velocity had a negative relationship six times and only one positive relationship, suggesting that reduced flow may benefit more species than are harmed in the watershed. Lastly, increased fine sediment showed eight negative relationships and a single positive one, suggesting that sedimentation may threaten most taxa. Collectively, these results support that drought may simultaneously improve and worsen habitat quality for certain species via different abiotic mechanisms, and illustrate that variation in effect direction and magnitude confer response diversity at the community level.
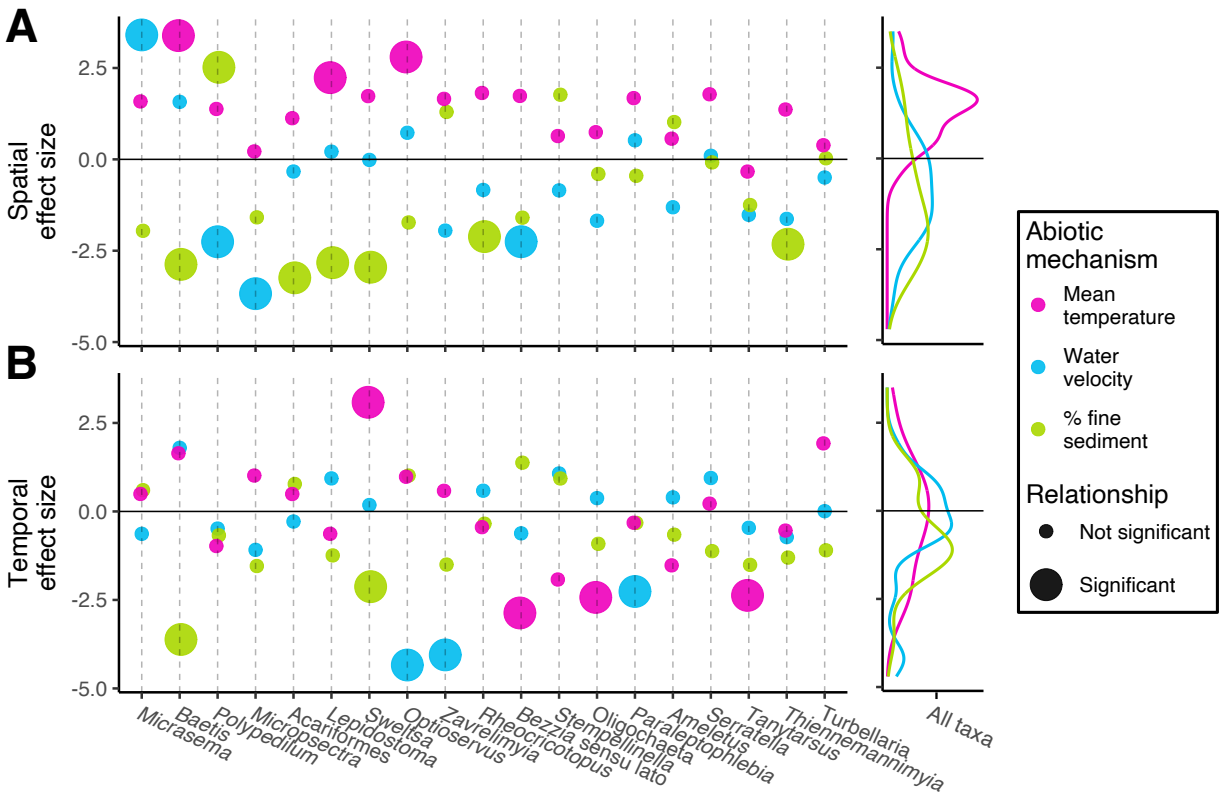
Figure 3. Abiotic mechanism effect sizes explaining spatial and temporal variation in the abundance of taxa. Taxa are ordered by the amount of spatial variation in abundance explained by abiotic mechanisms in aggregate. (A) Spatially, mean temperature has a positive association with species abundance, whereas higher proportions of fine sediment substrate tend to have a negative association with abundance. (B) Temporally, all abiotic mechanisms have significant relationships in at least one taxa. Species were more likely to have significant associations with species abundance across space rather than across time. Density plots display the distribution of species effect sizes for all taxa included in the plot.

Spatial vs. temporal importance of drought

Spatial and temporal drought effects varied within species, failing to support that spatial relationships are transferable to temporal studies. The lack of a space-for-time relationship was apparent in the rarity of abiotic mechanisms being significant in the same taxa across space and time. Of the 15 taxa that showed a significant effect, only two (*Sweltsa* and *Baetis*) had significant relationships with the same covariate in spatial and temporal tests (negative fine sediment relationships in both cases).

When examining responses across species, the number of taxa for which water temperature was a significant covariate was similar for space *vs.* time. However, water temperature almost always had a positive effect in spatial comparisons (median = 1.6), but when measured over time, the community-wide average effect size was negligible (median = -0.3; Figure 3). Water velocity had negative relationships with an equal number of taxa (three)

spatially and temporally, but only had a negative relationship with community abundance spatially (Figure 4). Fine sediment was supported as a covariate in seven taxa spatially, but only two taxa temporally. Despite more taxa having a negative relationship with fine sediment spatially, fine sediment had a negative relationship with community abundance in temporal but not spatial comparisons. Linear regressions of spatial and temporal abiotic mechanism effect sizes found nonsignificant positive slopes with weak predictive power (Figure 5).
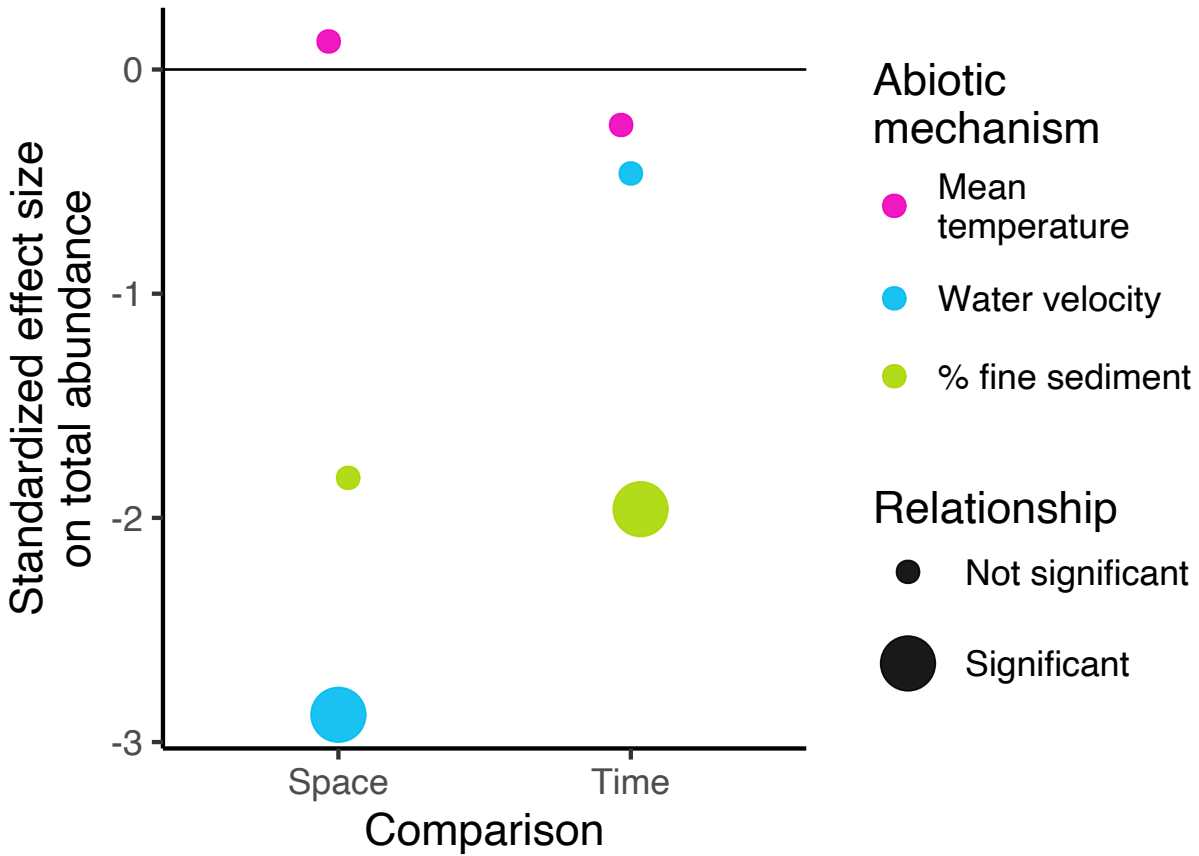

Figure 4. The standardized effect sizes of abiotic mechanisms explaining community abundance differences across space and time. Fine sediment coverage has a negative relationship with community abundance across time, but water velocity has a negative relationship with abundance across space. Spatial autocorrelation (i.e., variance explained by upstream distance) is 77.1%, while temporal autocorrelation (i.e., phi) is 0.72. Abiotic mechanisms explain 13.9% variation across space and 9.6% variation across time.
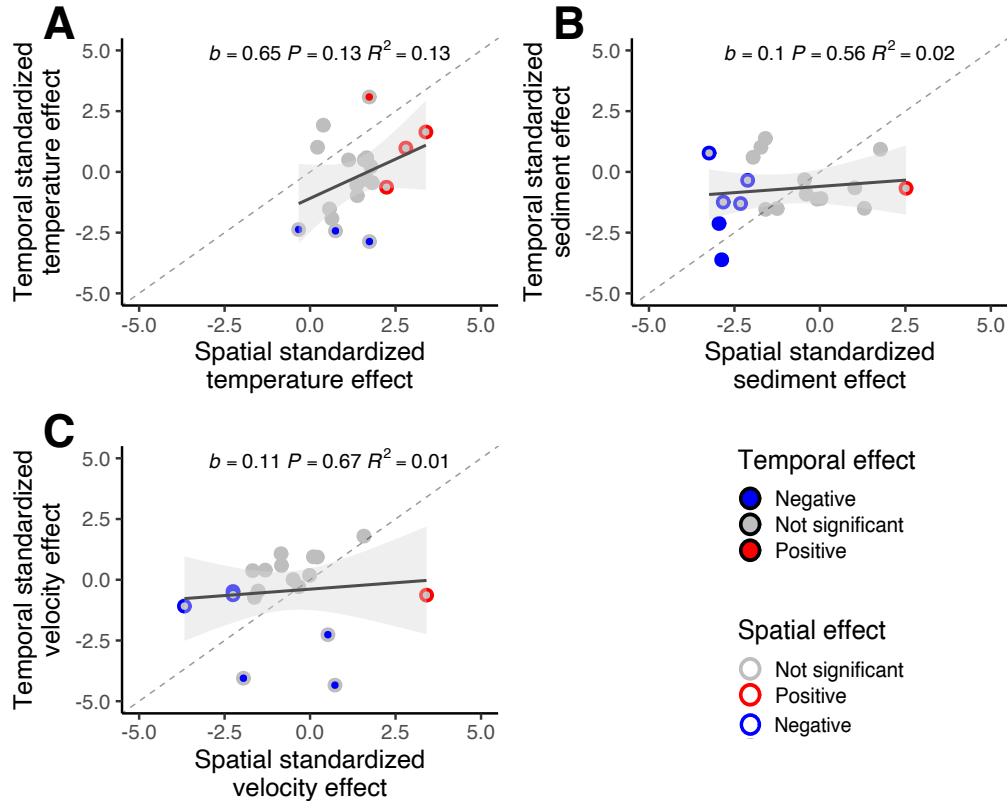
Figure 5. Species responses due to spatial differences do not provide reliable information on how species respond across time. (A) Water temperature displays both positive and negative relationships with species abundance, but only one taxon displayed the same significant relationship across space and time. (B) Taxa respond to increased fine sediment substrate coverage mostly negatively, but spatial effect sizes do not explain temporal effect sizes. (C) The most common taxa typically respond negatively to increased water velocity, but spatial effect sizes do not explain temporal effect sizes. The gray dashed line represents a hypothetical case where spatial and temporal effects and autocorrelation are the same. The black line is the line of best fit with a shaded error region for each regression.

Space-for-time substitution was not supported, neither for the environmental drivers (i.e., the aggregate importance of the three abiotic mechanisms) nor for autocorrelation (Figure 6; Table S1). Specifically, the spatial variance explained by abiotic mechanisms in aggregate for each species had no relationship with temporal variance ($F_{1,17} = 0.136$, $P > 0.05$). Similarly, the degree of spatial autocorrelation observed for a species was not related to its temporal autocorrelation ($F_{1,17} = 0.214$, $P > 0.05$). There was also no relationship between the amount of variance explained by abiotic mechanisms and autocorrelation for either spatial ($F_{1,17} = 0.075$, $P > 0.05$) or temporal tests ($F_{1,17} = 0.066$, $P > 0.05$). This suggests that neither an increase in spatiotemporal processes nor an increase in environmental filtering causes a decline in the other, possibly due to high unexplained variance.
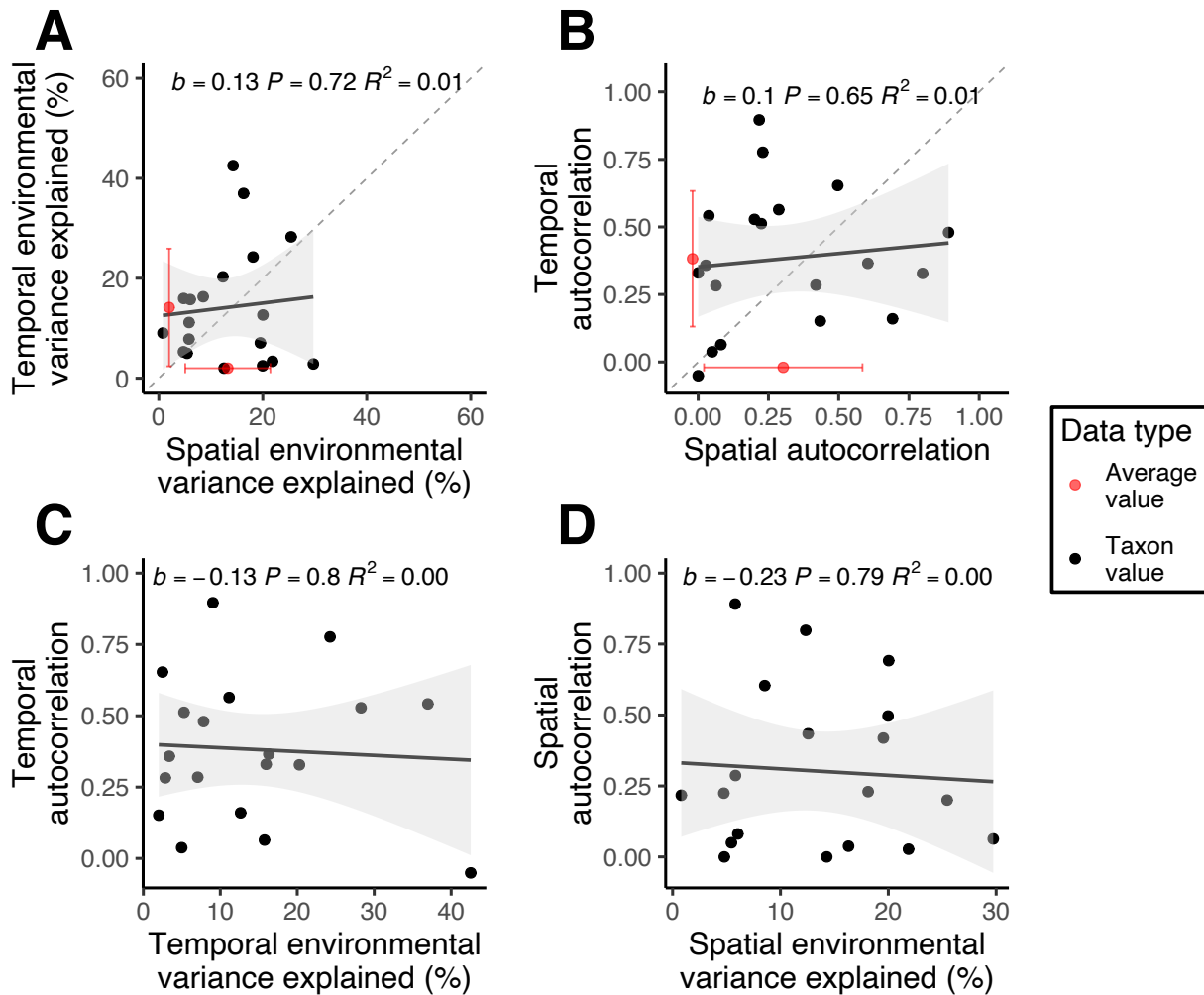
Figure 6. (A) Explanatory power of abiotic mechanisms of drought in aggregate explaining spatial variation in taxa abundance is not related to the ability of abiotic mechanisms to explain temporal variation. (B) Increased species spatial autocorrelation is not associated with increased temporal autocorrelation. (C) The amount of temporal variance explained by abiotic mechanisms is not related to a species' temporal autocorrelation. (D) The amount of spatial variance explained by abiotic mechanisms is not related to a species' spatial autocorrelation. The gray dashed line represents a hypothetical case where spatial and temporal drought effects and autocorrelation are the same. The black line is the line of best fit with a shaded 95% confidence interval for each regression. Black points are values for individual taxons and red points are the mean value for the corresponding axis with ∓ 1 SD error bars.

These results support our prediction that neither the amount of variation explained by drought-related drivers (individually or in aggregate), nor variation explained by biological autocorrelation (i.e., by virtue of communities closer in time or space being more similar than those further apart) can be transferred between space and time.

Community change components across space and time

Community dissimilarity and its biological components had the smallest differences when reaches were compared across space rather than across time or across space and time simultaneously at the reach scale (Figure 7). Median community dissimilarity was lower in spatial comparisons (0.582) than both temporal (0.724) and space-time (0.727) comparisons ($F_{2,1229} = 30.180$, $P < 0.001$). The same pattern was seen when comparing differences in species richness ($F_{2,1229} = 8.915$, $P < 0.001$) and reordering ($F_{1,17} = 39.800$, $P < 0.001$). The median species richness difference was 0.066 when comparing across space, but 0.115 and 0.116 when comparing across time and space-time respectively. In the case of reordering, the median difference across space (0.209) was again lower than that of time (0.230) and space-time (0.236). However, turnover difference across time had a lower median value (0.402) than comparisons across space (0.409) and space-time (0.426; $F_{2,1229} = 9.642$, $P < 0.001$). We did not find significant evenness differences among comparisons ($F_{2,1229} = 2.705$, $P = 0.067$). Evenness and richness differences were relatively low, while reordering and turnover were moderately high. These results support our prediction that the biotic mechanisms of community change differ across space and time.
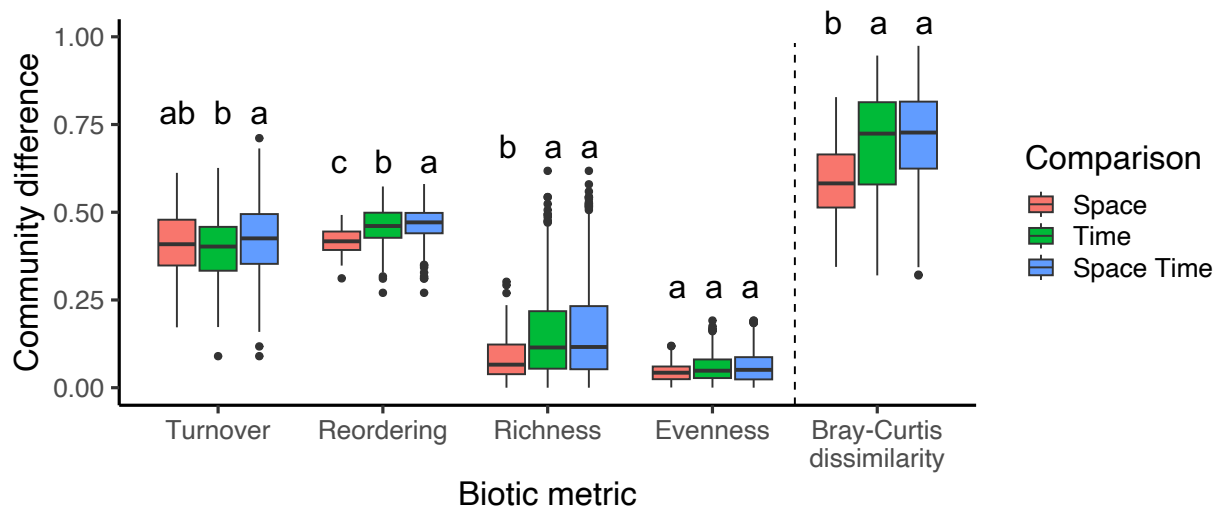

Figure 7. Boxplots for RAC pathways (left of the dashed line) and Bray-curtis dissimilarity across space, time, and space-time at the reach scale. Reordering values are multiplied by 2 to make the range of possible values 0-1 like for all metrics. Different letters indicate pairwise significant differences based on Tukey's honestly significant difference post-hoc tests. For the boxplot, the central band is the median, the box is the interquartile range, whiskers are 1.5 times the interquartile range, and circles are outliers.

Causal pathways connecting drought to community change

Abiotic mechanisms of drought controlled biological pathways, and ultimately community dissimilarity, differently across space and time. Temperature, water velocity, and sediment all explained biological pathways in space-time comparisons (Figure 8; Table S2). However, sediment was the only significant abiotic mechanism in spatial tests. Temporal comparisons had the opposite pattern; sediment did not explain biotic pathways, but temperature and water velocity did. Turnover was significantly explained by differences in abiotic

mechanisms across space, time, and space-time comparisons, but the abiotic mechanisms that were significant depended on the type of comparison. Reordering was explained by temperature across time and space-time, but was unexplained in space comparisons. Lastly, evenness was explained by abiotic mechanisms in space and space-time comparisons, but the specific abiotic mechanisms varied. Although every abiotic mechanism explained biotic pathways in space-time comparisons, the effect size was typically smaller than when comparing across space or time individually.

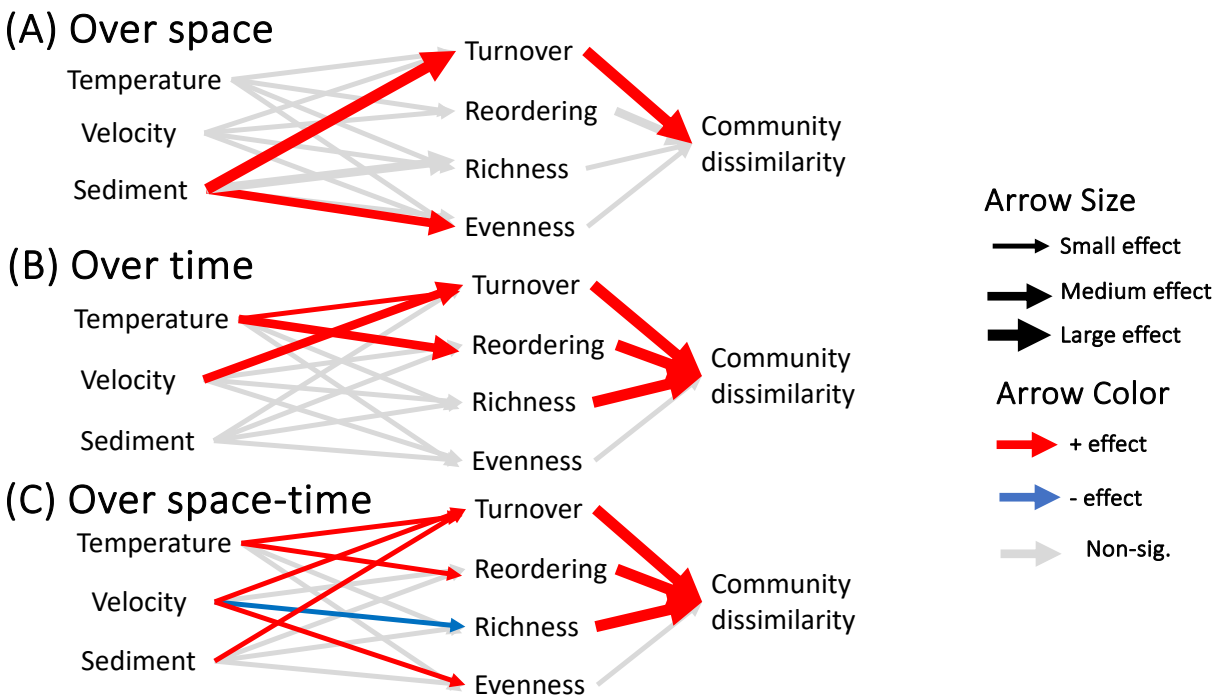## Ecological pathways connecting drought to community change

Figure 8. Abiotic mechanism differences affect community composition through different pathways depending on if communities are compared over (A) space, (B) time, or (C) space-time. Piecewise structural equation models visualize the relationship between abiotic mechanisms and rank abundance curve components that explain Bray-curtis dissimilarity. Arrow size is determined by standardized effect sizes where 0-0.2 is a small effect, 0.2-3 is a medium effect, and values greater than 0.3 are large effects. Arrow color is red if there is a significant positive relationship, blue if there is a significant negative relationship, and gray if there is no significant relationship.

Turnover and reordering were the main biotic pathways that explained community dissimilarity across space and time. η_p^2 values supported that these biotic mechanisms were the most impactful drivers of community dissimilarity, and both were significant regardless of space-time, space, or time comparison (Table S3). Reordering explained the most variation in temporal dissimilarity ($\eta_p^2 = 0.180$, $P < 0.001$) and space-time dissimilarity ($\eta_p^2 = 0.174$, $P < 0.001$) comparisons, but turnover had the highest eta squared value when comparing across space ($\eta_p^2 = 0.080$, $P = 0.025$). Differences in richness significantly explained dissimilarity across time

($\eta_p^2 = 0.038$, $P < 0.001$) and space-time ($\eta_p^2 = 0.050$, $P < 0.001$), but not space alone. When richness was significant, it had a much lower eta squared value compared to turnover and reordering. Additionally, spatial scale (reach *vs.* microhabitat) affected our results. The abiotic and biotic pathways of drought were stronger and more diverse at the microhabitat scale with every abiotic and biotic mechanism possessing a significant link to explain community dissimilarity (Figure S5).These findings support our prediction that reordering and turnover are the biological pathways that best explain community dissimilarity associated with drought, although the relative importance of each biological pathway varied from our prediction at some spatial scales.

Discussion

Understanding drought impacts on high-mountain ecosystems is critical given climate change projections and increased anthropogenic alteration to watersheds (Siirila-Woodburn et al. 2021). Despite this need, the interplay of drought-induced processes–both abiotic and biotic–that lead to altered stream communities remains uncertain, limiting our ability to predict where and when droughts are most ecologically harmful. Here we investigated the ecological pathways whereby droughts altered invertebrate communities in a Sierra Nevada watershed across space and time. We leveraged an experimental design that simultaneously maximized environmental and biological variation across nested spatial scales (60 microhabitats within 10 reaches) and over time (by visiting a subset of sites over two decades). We found that 1) Temperature, water velocity, and fine sediment all explained variation in a similar proportion of the community taxa; 2) Abiotic mechanism effects differed across space and time, as spatial effects were generally unrelated to temporal effects; 3) Biotic community differences across space and time were unequal; and 4) The overall ecological pathway of drought differed across space and time. Our work adds to past research finding that drought alters river communities in complex ways (Rolls et al. 2012, Aspin et al. 2018), showing that temporal and spatial relationships (and thus pathways of ecological change) can differ widely. Although space-for-time substitution approaches are widespread in ecology (Lovell et al. 2023), we contend they may be inappropriate for the study of climate change on high-mountain stream ecosystems because of the hierarchical structure of watersheds and high temporal variability of the systems.

Unequal drought effects across space and time

Space-for-time substitution was not supported in our study and may be inappropriate in lotic research generally. Space-for-time substitution assumes that succession occurs equivalently across a landscape and that habitat patches, in combination, contain a myriad of points along the chronosequence (Pickett 1989). The hierarchical nature of rivers runs counter to this assumption. River environments and communities gradually change longitudinally, in line with the river continuum concept, resulting in different steady state communities with changes in stream size and network position (Vannote et al. 1980). Furthermore, spate disturbances from snowmelt in high mountain streams can affect the majority of the stream network synchronously, frequently resetting the community and promoting stochastic processes like priority effects (i.e., the effect of a species on another is determined by the arrival order at a site). Even in situations where space-for-time substitution is touted as valid, the environmental drivers explaining variation differed greatly between spatial and temporal models (Blois et al. 2013). Space-for-time

substitution performs best when spatial and temporal heterogeneity are similar, but we found temporal differences in community composition to be higher than spatial differences. This may be due to temporal heterogeneity increasing in communities with subannual lifespans like many macroinvertebrates, as work has shown that species lifespan is a better predictor of temporal heterogeneity than spatial heterogeneity (Collins et al. 2018). Finally, space-for-time substitution has the best support at large spatial and temporal scales, but the scales that individuals live within and environmental variation acts upon are much finer (Blois et al. 2013). For these reasons, space-for-time substitution is especially ill suited to assess mechanistic processes in streams.

Understanding drought effects across space-time requires understanding both spatial and temporal ecological pathways individually. All abiotic mechanisms of drought and nearly all biotic mechanisms of change explained community dissimilarity across space-time, but drought affected communities through unequal, narrower subsets of these pathways when spatial or temporal comparisons were made alone. Our results differ from a previous macroinvertebrate study in Hawaii streams that found space-for-time substitution generally held true, however, support is mixed in validations of other taxonomic groups (e.g., birds, butterflies, and plants; White and Kerr 2006, Adler and Levine 2007, La Sorte et al. 2009, Elmendorf et al. 2015, Frauendorf et al. 2019). We found that, spatially, fine sediment was more likely to have a significant negative relationship with individual taxa and it drove regional community dissimilarity by causing turnover in community composition (i.e., taxa sensitive to silt like *Baetis* and *Sweltsa* were replaced by tolerant taxa like *Polypedilum*). One reason for fine sediment having a spatial but not temporal effect could be that reach scale spatial variation in substrate reflects more meaningful environmental differences than temporal sediment variation. For example, a small headwater reach like H-1 in our study consistently has a greater proportion of silt and small substrate sizes than a larger mainstem reach. Fairly consistent spatial differences in fine sediment could be a reason that reordering of existing taxa was more important temporally than spatially. If environmental conditions within a reach are more similar year-to-year than the difference between reaches, then the same taxa may consistently use the same habitat patches even if their relative abundance can change. Alternatively, legacy effects could occur where taxa that were present in large numbers the prior year lead to a large number of local progeny, even if environmental conditions are no longer favorable and their relative abundance declines.

Overall variance explained by abiotic mechanisms and autocorrelation were both unrelated across space and time, despite mean values being similar. Spatial and temporal autocorrelation might be expected to both be high for taxa that are poor dispersers in environments that are relatively stable, as these conditions promote local autocorrelation over time. This was seen with Acariformes and Turbellaria, but other taxa with poor mobility like Oligochaeta had low spatiotemporal autocorrelation. Oligochaeta might be undersampled because a substantial fraction of their populations are located in the hyporheic zone, limiting our ability to accurately assess their population (Malard et al. 2001). However other taxa that are strong dispersers may break down the positive relationship between spatial and temporal autocorrelation. *Baetis* and *Sweltsa* had high variation explained by local environmental conditions and high temporal autocorrelation, suggesting they can disperse well and the environment they inhabit is similar year to year. These taxa are mobile and can emigrate out of adjacent, unsuitable microhabitats, reducing spatial autocorrelation. Examinations of

invertebrates elsewhere have seen that species models accounting for temporal and spatial autocorrelation are better supported than temporal autocorrelation alone and species autocorrelations may differ from one watershed to another (Gumpertz et al. 2000, Nally et al. 2006). These results support that spatio-temporal models require both spatial and temporal processes to be examined independently, due to the lack of correlation observed. Previous work also supports that spatial or temporal analysis alone can result in biased results (Wiley et al. 1997), so independent spatial and temporal processes must be integrated to understand ecological phenomena.

Diversity of responses to drought-driven abiotic changes

The different abiotic facets, or mechanisms of drought all influenced taxa and communities. While increased fine sediment from drought may harm most taxa, increased temperatures and reduced water velocity could counteract this in high elevation streams. Increased fine sediment tended to have a negative effect size on taxa abundance over both space and time, consistent with experimental studies' results describing fine sediment as a 'master stressor' (Blöcher et al. 2020). Fine sediment substrate indirectly harms macroinvertebrates via oxygen depletion and directly harms them by covering refugia, clogging gills, and causing abrasion (Jones et al. 2012). Warming water temperatures, on the other hand, were associated with increased taxa abundance, based on positive bias in covariate effects. Climate change could therefore improve thermal conditions for warm eurythermal species at high elevations. Past work has shown that taxa abundance peaks at the center of their elevation range, with densities that follow a normal distribution (Richard Hauer et al. 2000). Elevation differences reflect thermal variation driving species abundance, so the most prevalent species seen in our watershed may be at higher elevations and colder water temperatures than they prefer. An alternative explanation is that the coldest reaches of Bull Creek are small headwaters that may be food limited due to low productivity in smaller streams and colder water. Lastly, taxa were more likely to benefit from low flows than high flows over both space and time, so climate change may benefit the most prevalent taxa that prefer pool habitat, such as Chironomidae. Summer water temperature and water velocity reflect preceding snowpack, making watersheds that could lose snow precipitation with warming particularly susceptible to habitat shifts that could favor low-elevation taxa due to climate change. However, the high response diversity seen for taxa in the community suggests that ecosystem processes like aquatic-terrestrial subsidies will likely be maintained.

Given our observations that only one of our common taxa had multiple significant abiotic mechanisms of drought explaining temporal variation, this study's findings suggest that climate change impacts will occur through individual mechanisms of drought rather than the interaction between multiple parameters. In our study, Sweltsa had a negative relationship with fine sediment and a positive relationship with water temperature, suggesting an antagonistic relationship between these parameters. However, all other taxa either had one or no significant abiotic mechanism for temporal variation. Our results contrast with mesocosm experiments finding that 54% of studied invertebrate families were significantly affected by water velocity and sedimentation in one case, and 46% of taxa were affected by both temperature and fine sediment in another (Piggott et al. 2015, Beermann et al. 2018). Mesocosm experiments may find stronger effects due to simplified environments that often preclude natural factors such as spatial habitat heterogeneity, variance in prior year community composition, and the hyporheic zone.

Although the abiotic mechanisms in our study were not found to be multicollinear, they could interact in complex ways once certain thresholds are reached or they could interact with other environmental variables not assessed here. Increased fine sediment can reduce groundwater influence and promote macrophyte growth, which could increase water temperature and reduce water velocity respectively.

Importance of spatiotemporal scales

The use of the microhabitat rather than reach scale samples greatly enhanced our ability to explain community differences, suggesting that the scale we consider to be a community can influence our findings. The largest effect sizes and partial eta squared occurred at microhabitat scale, suggesting that drought affects communities most strongly at the microhabitat scale. One reason for this could be that the gradient of abiotic mechanisms of drought was larger at the microhabitat scale for fine sediment and water velocity without reach scale averaging of microhabitat conditions. Previous work has similarly found that local environmental conditions and biotic communities varied most at the microhabitat spatial scale rather than the reach scale, leading to community metrics like richness and evenness having the strongest relationships with environmental factors at the microhabitat scale (Boyero 2003, Herbst et al. 2018). Although temperature varied little within reaches at the microhabitat scale (as seen in Leathers et al. 2023), our microhabitat analyses included additional reaches in cold headwaters that increased the gradient of water temperature differences and may have led to stronger relationships. Although many studies take multiple samples within stream reaches and combine them to identify a representative community, this approach may be better suited for capturing total biodiversity rather than understanding the mechanisms of community change. In the same way that grouping spatial and temporal pathways of drought effects together muddles our ability to predict their individual pathways, grouping microhabitats together at the reach scale can be inappropriate to understand what drives fine scale variation in communities. This has nuance, however, as intra-reach differences in environment conditions can decline as river size increases, and both extreme floods and droughts can homogenize reaches (Herbst et al. 2018). If reaches are comprised of more consistent microhabitats, then assemblage similarity can increase and conglomerate reach scale samples may be suitable to test drivers of change (Heino et al. 2004). Lastly, relationships between the environment and a biotic response found at the reach scale can still be informative to microhabitat relationships, as past work has found them to be positively correlated (Lamouroux et al. 2004). Similarly to our findings, the environment-biotic relationship was stronger at the microhabitat rather than reach scale in this case.

Examining communities at the appropriate temporal scale is also important, although this was not a focus of our manuscript. Communities change over time due to seasonal change and the life histories of the species present. When comparing communities across space, care should be taken that sampling is conducted in a time period short enough that seasonal differences or variations in emergence do not conflate spatial and temporal differences between locations. Community composition can shift at the scale of days in periods of flash flood events (Leung et al. 2012), but streams with less extreme disturbance have been seen to shift in community composition roughly monthly (Warwick 2018). Although sampling date varied up to roughly a month interannually in our study, the beginning of our sampling period was typically determined by road access due to annual snowpack. Variation in community composition over time is partly

due to environmental shifts related to discharge (Fierro et al. 2021), so our corrected sampling date may have improved year to year comparability of macroinvertebrate communities.

Limitations and future directions

Follow-up studies may build off our findings to better understand how drought, and environmental stressors generally, affect stream communities. We did not test for causality of abiotic mechanisms of drought on biotic responses using methods such as reciprocal transplants or common gardens (Lovell et al. 2023). However, given that space-for-time was not supported, a more accurate method of predicting temporal effects in a short term study could be experiments using natural, manipulatable systems (Elmendorf et al. 2015). Even though we found that water temperature, water velocity, and sediment were uncorrelated, it is uncertain how they may interact in their effects on taxa and communities. Past work in agricultural areas found that sedimentation and water velocity had additive effects (Elbrecht et al. 2016), but a meta-analysis of multiple stressors in freshwater systems observed that water temperature most often had antagonistic interactions with other stressors (Jackson et al. 2016). We found that turnover and reordering were the primary biotic pathways of community dissimilarity, but future work could investigate if these findings differ at the regional scale. In a regional rather than small watershed study, species are more likely to differ across space, so turnover and richness differences may become more influential and reordering could decline in importance. Additionally, the relative importance of reordering may depend on the taxonomic resolution of communities. Studies with fine taxonomic resolution would likely have lower reordering between communities. However, our finding that reordering and turnover are dominant biotic mechanisms of change is supported elsewhere. Analysis of 66 communities found that the largest composition differences were due to reordering (Avolio et al. 2019), and another study observed turnover of thermophilic alpine stream macroinvertebrates replacing cold-adapted taxa with warming drive shifts in community composition (Bruno et al. 2019). In our study, spatial comparisons occurred at the microhabitat scale, but temporal comparisons took place at the reach scale when modeling individual taxon responses. This was done because only ten reaches were sampled spatially–an insufficient sample size for an SSN model–requiring the use of microhabitat-scale samples. However, our finding that drought effects differ across spatial and temporal comparisons was consistently observed, including when communities were compared at the reach scale in both cases. Future studies could build on our work by systematically changing the spatial and temporal resolution of sampling, and examining whether the space-for-time relationships that we did not detect emerges at some combination of scales.

Concluding remarks

Our study shows that predicting biotic responses to drought requires a precise understanding of ecological context and a broad range of studies across space and time to succeed. We found that space-for-time substitution approaches may be inappropriate in the study of drought effects in mountain streams, possibly due to the hierarchical physical structure of streams and the high temporal variability they experience in abiotic conditions and communities. Unequal spatial and temporal dynamics in streams could also be due to variability caused by the relatively short lifespans of most macroinvertebrate groups and frequent spate disturbances that trigger community succession in river ecosystems (Power et al. 2008, Collins et al. 2018). The

use of space-for-time substitution in our study would have overestimated the effect of fine sediment on future communities due to climate change, but would have underestimated the impact of temperature and water velocity shifts. Studies hoping to use space-for-time should both validate the transferability of spatial relationships and, ideally, corroborate that spatial effects are real (Lovell et al. 2023). Models predicting future communities will need to account for both the temporal and spatial drivers of variation, as accurate temporal models alone will fail to account for influence from the surrounding metacommunity and landscape. Research assessing how drought affects stream communities should also consider a variety of abiotic mechanisms of drought, as many species may only respond to a single aspect of low flow. Lastly, biotic responses should be assessed at the spatial and temporal scale that best suits the taxa and question. The spatial scale assessed should reflect the area that taxa perceive as their habitat (Boyero 2003), and the sampling date should be chosen when disturbance and invertebrate emergence are unlikely to shift community composition during the sampling period for a single timestep (Warwick 2018). There is a need to continue carefully-designed monitoring programs that capture both spatial and temporal dimensions of environmental change, as these datasets are needed to accurately assess causal pathways and provide necessary knowledge to design effective future studies. Considering spatial and temporal variation in the appropriate context is necessary in the quest to learn how climate change will alter mountain streams.

Acknowledgements

References

Adler, P. B., and J. M. Levine. 2007. Contrasting relationships between precipitation and species richness in space and time. Oikos 116:221–232.

Amundrud, S. L., and D. S. Srivastava. 2019. Disentangling how climate change can affect an aquatic food web by combining multiple experimental approaches. Global Change Biology 25:3528–3538.

Angert, A. L. 2024. The space-for-time gambit fails a robust test. Proceedings of the National Academy of Sciences 121:e2320424121.

Aspin, T. W. H., T. J. Matthews, K. Khamis, A. M. Milner, Z. Wang, M. J. O'Callaghan, and M. E. Ledger. 2018. Drought intensification drives turnover of structure and function in stream invertebrate communities. Ecography 41:1992–2004.

Avolio, M. L., I. T. Carroll, S. L. Collins, G. R. Houseman, L. M. Hallett, F. Isbell, S. E. Koerner, K. J. Komatsu, M. D. Smith, and K. R. Wilcox. 2019. A comprehensive approach to analyzing community dynamics using rank abundance curves. Ecosphere 10:e02881.

Avolio, M. L., K. J. L. Pierre, G. R. Houseman, S. E. Koerner, E. Grman, F. Isbell, D. S. Johnson, and K. R. Wilcox. 2015. A framework for quantifying the magnitude and variability of community responses to global change drivers. Ecosphere 6:1–14.

Barnett, T. P., J. C. Adam, and D. P. Lettenmaier. 2005. Potential impacts of a warming climate on water availability in snow-dominated regions. Nature 438:303–309.

Beermann, A. J., V. Elbrecht, S. Karnatz, L. Ma, C. D. Matthaei, J. J. Piggott, and F. Leese. 2018. Multiple-stressor effects on stream macroinvertebrate communities: A mesocosm experiment manipulating salinity, fine sediment and flow velocity. Science of the Total Environment 610–611:961–971.

Blöcher, J. R., M. R. Ward, C. D. Matthaei, and J. J. Piggott. 2020. Multiple stressors and stream macroinvertebrate community dynamics: Interactions between fine sediment grain size and flow velocity. Science of the Total Environment 717:137070.

Blois, J. L., J. W. Williams, M. C. Fitzpatrick, S. T. Jackson, and S. Ferrier. 2013. Space can substitute for time in predicting climate-change effects on biodiversity. Proceedings of the National Academy of Sciences 110:9374–9379.

Boyero, L. 2003. Multiscale patterns of spatial variation in stream macroinvertebrate communities. Ecological Research 18:365–379.

Bruno, D., O. Belmar, A. Maire, A. Morel, B. Dumont, and T. Datry. 2019. Structural and functional responses of invertebrate communities to climate change and flow regulation in alpine catchments. Global Change Biology 25:1612–1628.

Buss, D. F., and E. L. Borges. 2008. Application of rapid bioassessment protocols (RBP) for benthic macroinvertebrates in Brazil: comparison between sampling techniques and mesh sizes. Neotropical Entomology 37:288–295.

Chapin, T. P., A. S. Todd, and M. P. Zeigler. 2014. Robust, low-cost data loggers for stream temperature, flow intermittency, and relative conductivity monitoring. Water Resources Research 50:6542–6548.

Collins, S. L., M. L. Avolio, C. Gries, L. M. Hallett, S. E. Koerner, K. J. La Pierre, A. L. Rypel, E. R. Sokol, S. B. Fey, D. F. B. Flynn, S. K. Jones, L. M. Ladwig, J. Ripplinger, and M.

B. Jones. 2018. Temporal heterogeneity increases with spatial heterogeneity in ecological communities. Ecology 99:858–865.

Collins, S. L., K. N. Suding, E. E. Cleland, M. Batty, S. C. Pennings, K. L. Gross, J. B. Grace, L. Gough, J. E. Fargione, and C. M. Clark. 2008. RANK CLOCKS AND PLANT COMMUNITY DYNAMICS. Ecology 89:3534–3541.

Croijmans, L., J. F. De Jong, and H. H. T. Prins. 2021. Oxygen is a better predictor of macroinvertebrate richness than temperature—a systematic review. Environmental Research Letters 16:023002.

Dewson, Z. S., A. B. W. James, and R. G. Death. 2007. A review of the consequences of decreased flow for instream habitat and macroinvertebrates. Journal of the North American Benthological Society 26:401–415.

Elbrecht, V., A. J. Beermann, G. Goessler, J. Neumann, R. Tollrian, R. Wagner, A. Wlecklik, J. J. Piggott, C. D. Matthaei, and F. Leese. 2016. Multiple-stressor effects on stream invertebrates: A mesocosm experiment manipulating nutrients, fine sediment and flow velocity. Freshwater Biology 61:362–375.

Elliott, J. M. 2000. Pools as refugia for brown trout during two summer droughts: Trout responses to thermal and oxygen stress. Journal of Fish Biology 56:938–948.

Elmendorf, S. C., G. H. R. Henry, R. D. Hollister, A. M. Fosaa, W. A. Gould, L. Hermanutz, A. Hofgaard, I. S. Jónsdóttir, J. C. Jorgenson, E. Lévesque, B. Magnusson, U. Molau, I. H. Myers-Smith, S. F. Oberbauer, C. Rixen, C. E. Tweedie, and M. D. Walker. 2015. Experiment, monitoring, and gradient methods used to infer climate change effects on plant communities yield consistent patterns. Proceedings of the National Academy of Sciences 112:448–452.

Fierro, P., R. M. Hughes, and C. Valdovinos. 2021. Temporal Variability of Macroinvertebrate Assemblages in a Mediterranean Coastal Stream: Implications for Bioassessment. Neotropical Entomology 50:873–885.

Frauendorf, T. C., R. A. MacKenzie, R. W. Tingley, A. G. Frazier, M. H. Riney, and R. W. El-Sabaawi. 2019. Evaluating ecosystem effects of climate change on tropical island streams using high spatial and temporal resolution sampling regimes. Global Change Biology 25:1344–1357.

Gaüzère, P., L. L. Iversen, A. W. R. Seddon, C. Violle, and B. Blonder. 2020. Equilibrium in plant functional trait responses to warming is stronger under higher climate variability during the Holocene. Global Ecology and Biogeography 29:2052–2066.

Gumpertz, M. L., C. Wu, and J. M. Pye. 2000. Logistic Regression for Southern Pine Beetle Outbreaks with Spatial and Temporal Autocorrelation. Forest Science 46:95–107.

Hawkins, C. P., J. N. Hogue, L. M. Decker, and J. W. Feminella. 1997. Channel Morphology, Water Temperature, and Assemblage Structure of Stream Insects. Journal of the North American Benthological Society 16:728–749.

Heino, J., P. Louhi, and T. Muotka. 2004. Identifying the scales of variability in stream macroinvertebrate abundance, functional composition and assemblage structure. Freshwater Biology 49:1230–1239.

Herbst, D. B., S. D. Cooper, R. B. Medhurst, S. W. Wiseman, and C. T. Hunsaker. 2018. A comparison of the taxonomic and trait structure of macroinvertebrate communities between the riffles and pools of montane headwater streams. Hydrobiologia 820:115–133.

Herbst, D. B., S. D. Cooper, R. B. Medhurst, S. W. Wiseman, and C. T. Hunsaker. 2019. Drought ecohydrology alters the structure and function of benthic invertebrate communities in mountain streams. Freshwater Biology 64:886–902.

Herbst, D. B., and E. L. Silldorff. 2006. Comparison of the performance of different bioassessment methods: similar evaluations of biotic integrity from separate programs and procedures. Journal of the North American Benthological Society 25:513–530.

Hunsaker, C. T., T. W. Whitaker, and R. C. Bales. 2012. Snowmelt Runoff and Water Yield Along Elevation and Temperature Gradients in California's Southern Sierra Nevada. Journal of the American Water Resources Association 48:667–678.

Isaak, D. J., J. M. Ver Hoef, E. E. Peterson, D. L. Horan, and D. E. Nagel. 2017. Scalable population estimates using spatial-stream-network (SSN) models, fish density surveys, and national geospatial database frameworks for streams. Canadian Journal of Fisheries and Aquatic Sciences 74:147–156.

Jackson, M. C., C. J. G. Loewen, R. D. Vinebrooke, and C. T. Chimimba. 2016. Net effects of multiple stressors in freshwater ecosystems: A meta-analysis. Global Change Biology 22:180–189.

Jones, J. I., J. F. Murphy, A. L. Collins, D. A. Sear, P. S. Naden, and P. D. Armitage. 2012. THE IMPACT OF FINE SEDIMENT ON MACRO-INVERTEBRATES. River Research and Applications 28:1055–1071.

La Sorte, F. A., T. M. Lee, H. Wilman, and W. Jetz. 2009. Disparities between observed and predicted impacts of climate change on winter bird assemblages. Proceedings of the Royal Society B: Biological Sciences 276:3167–3174.

Lake, P. S. 2003. Ecological effects of perturbation by drought in flowing waters. Freshwater Biology 48:1161–1172.

Lamouroux, N., S. Dolédec, and S. Gayraud. 2004. Biological traits of stream macroinvertebrate

communities: Effects of microhabitat, reach, and basin filters. Journal of the North American Benthological Society 23:449–466.

Leathers, K., D. Herbst, G. De Mendoza, G. Doerschlag, and A. Ruhi. 2024. Climate change is poised to alter mountain stream ecosystem processes via organismal phenological shifts. Proceedings of the National Academy of Sciences 121:e2310513121.

Leathers, K., D. Herbst, M. Safeeq, and A. Ruhi. 2023. Dynamic, downstream-propagating thermal vulnerability in a mountain stream network: Implications for biodiversity in the face of climate change. Limnology and Oceanography 68.

Lefcheck, J. S. 2016. piecewiseSEM: Piecewise structural equation modelling in R for ecology, evolution, and systematics. Methods in Ecology and Evolution 7:573–579.

Leibold, M. A., M. Holyoak, N. Mouquet, P. Amarasekare, J. M. Chase, M. F. Hoopes, R. D. Holt, J. B. Shurin, R. Law, D. Tilman, M. Loreau, and A. Gonzalez. 2004. The metacommunity concept: A framework for multi-scale community ecology. Ecology Letters 7:601–613.

Leung, A. S. L., A. O. Y. Li, and D. Dudgeon. 2012. Scales of spatiotemporal variation in macroinvertebrate assemblage structure in monsoonal streams: the importance of season. Freshwater Biology 57:218–231.

Lovell, R. S. L., S. Collins, S. H. Martin, A. L. Pigot, and A. B. Phillimore. 2023. Space-for-time substitutions in climate change ecology and evolution. Biological Reviews 98:2243–2270.

Malard, F., M. Lafont, P. Burgherr, and J. V. Ward. 2001. A Comparison of Longitudinal Patterns in Hyporheic and Benthic Oligochaete Assemblages in a Glacial River. Arctic, Antarctic, and Alpine Research 33:457–466.

Malmqvist, B., and G. Sackmann. 1996. Changing risk of predation for a filter-feeding insect along a current velocity gradient. Oecologia 108:450–458.

Meerhoff, M., F. Teixeira-de Mello, C. Kruk, C. Alonso, I. González-Bergonzoni, J. P. Pacheco, G. Lacerot, M. Arim, M. Beklioğlu, S. Brucet, G. Goyenola, C. Iglesias, N. Mazzeo, S. Kosten, and E. Jeppesen. 2012. Environmental Warming in Shallow Lakes. Pages 259–349 Advances in Ecological Research. Elsevier.

Nally, R. M., N. J. Lloyd, and P. S. Lake. 2006. Comparing patterns of spatial autocorrelation of assemblages of benthic invertebrates in upland rivers in south-eastern Australia. Hydrobiologia 571:147–156.

Nelson, D., M. H. Busch, D. A. Kopp, and D. C. Allen. 2021. Energy pathways modulate the resilience of stream invertebrate communities to drought. Journal of Animal Ecology 90:2053–2064.

Null, S. E., J. H. Viers, M. L. Deas, S. K. Tanaka, and J. F. Mount. 2013. Stream temperature sensitivity to climate warming in California's Sierra Nevada: Impacts to coldwater habitat. Climatic Change 116:149–170.

Ode, P. R., E. A. Fetscher, and L. B. Busse. 2016. Standard Operating Procedures (Sop) for the Collection of Field Data for Bioassessments of California Wadeable Streams: Benthic Macroinvertebrates, Algae, and Physical Habitat. SWAMP Bioassessment Procedures.

Phillimore, A. B., J. D. Hadfield, O. R. Jones, and R. J. Smithers. 2010. Differences in spawning date between populations of common frog reveal local adaptation. Proceedings of the National Academy of Sciences 107:8292–8297.

Pickett, S. T. A. 1989. Space-for-Time Substitution as an Alternative to Long-Term Studies. Pages 110–135 *in* G. E. Likens, editor. Long-Term Studies in Ecology. Springer New York, New York, NY.

Piggott, J. J., C. R. Townsend, and C. D. Matthaei. 2015. Climate warming and agricultural stressors interact to determine stream macroinvertebrate community dynamics. Global Change Biology 21:1887–1906.

Poff, N. L., J. D. Allan, M. B. Bain, J. R. Karr, K. L. Prestegaard, B. D. Richter, R. E. Sparks, and J. C. Stromberg. 1997. The Natural Flow Regime: A Paradigm for River Conservation and Restoration. BioScience 47:769–784.

Power, M. E., M. S. Parker, and W. E. Dietrich. 2008. Seasonal Reassembly of a River Food Web: Floods, Droughts, and Impacts of Fish. Ecological Monographs 78:263–282.

PRISM Climate Group. 2024. PRISM gridded climate data. Oregon State University.

Richard Hauer, F., J. A. Stanford, J. Joseph Giersch, and W. H. Lowe. 2000. Distribution and abundance patterns of macroinvertebrates in a mountain stream: an analysis along multiple environmental gradients. SIL Proceedings, 1922-2010 27:1485–1488.

Rolls, R. J., C. Leigh, and F. Sheldon. 2012. Mechanistic effects of low-flow hydrology on riverine ecosystems: ecological principles and consequences of alteration. Freshwater Science 31:1163–1186.

Siirila-Woodburn, E. R., A. M. Rhoades, B. J. Hatchett, L. S. Huning, J. Szinai, C. Tague, P. S. Nico, D. R. Feldman, A. D. Jones, W. D. Collins, and L. Kaatz. 2021. A low-to-no snow future and its impacts on water resources in the western United States. Nature Reviews Earth & Environment 2:800–819.

Smith, B., and J. B. Wilson. 1996. A Consumer's Guide to Evenness Indices. Oikos 76:70.

Swain, D. L., B. Langenbrunner, J. D. Neelin, and A. Hall. 2018. Increasing precipitation

volatility in twenty-first-century California. Nature Climate Change 8:427–433.

Vannote, R. L., W. G. Minshall, K. W. Cummins, J. R. Sedell, and C. E. Cushing. 1980. The River Continuum Concpet. Canadian Journal of Fisheries and Aquatic Sciences 37:130–137.

Vellend, M., L. Baeten, I. H. Myers-Smith, S. C. Elmendorf, R. Beauséjour, C. D. Brown, P. De Frenne, K. Verheyen, and S. Wipf. 2013. Global meta-analysis reveals no net change in local-scale plant biodiversity over time. Proceedings of the National Academy of Sciences 110:19456–19459.

Waddle, T. J., and J. G. Holmquist. 2013. Macroinvertebrate response to flow changes in a subalpine stream: Predictions from two-dimensional hydrodynamic models. River Research and Applications 29:366–379.

Wagenbrenner, J. W., D. N. Dralle, M. Safeeq, and C. T. Hunsaker. 2021. The Kings River Experimental Watersheds: Infrastructure and data. Hydrological Processes 35:e14142.

Warwick, J. M. 2018, May. Prairie stream ecology : temporal and spatial patterns of macroinvertebrates. Ph. D., University of Missouri--Columbia.

Wawrzyniak, V., P. Allemand, S. Bailly, J. Lejot, and H. Piégay. 2017. Coupling LiDAR and thermal imagery to model the effects of riparian vegetation shade and groundwater inputs on summer river temperature. Science of The Total Environment 592:616–626.

White, P., and J. T. Kerr. 2006. Contrasting spatial and temporal global change impacts on butterfly species richness during the 20th century. Ecography 29:908–918.

Wiley, M. J., S. L. Kohler, and P. W. Seelbach. 1997. Reconciling landscape and local views of aquatic communities: Lessons from Michigan trout streams. Freshwater Biology 37:133–148.

Supplementary Materials
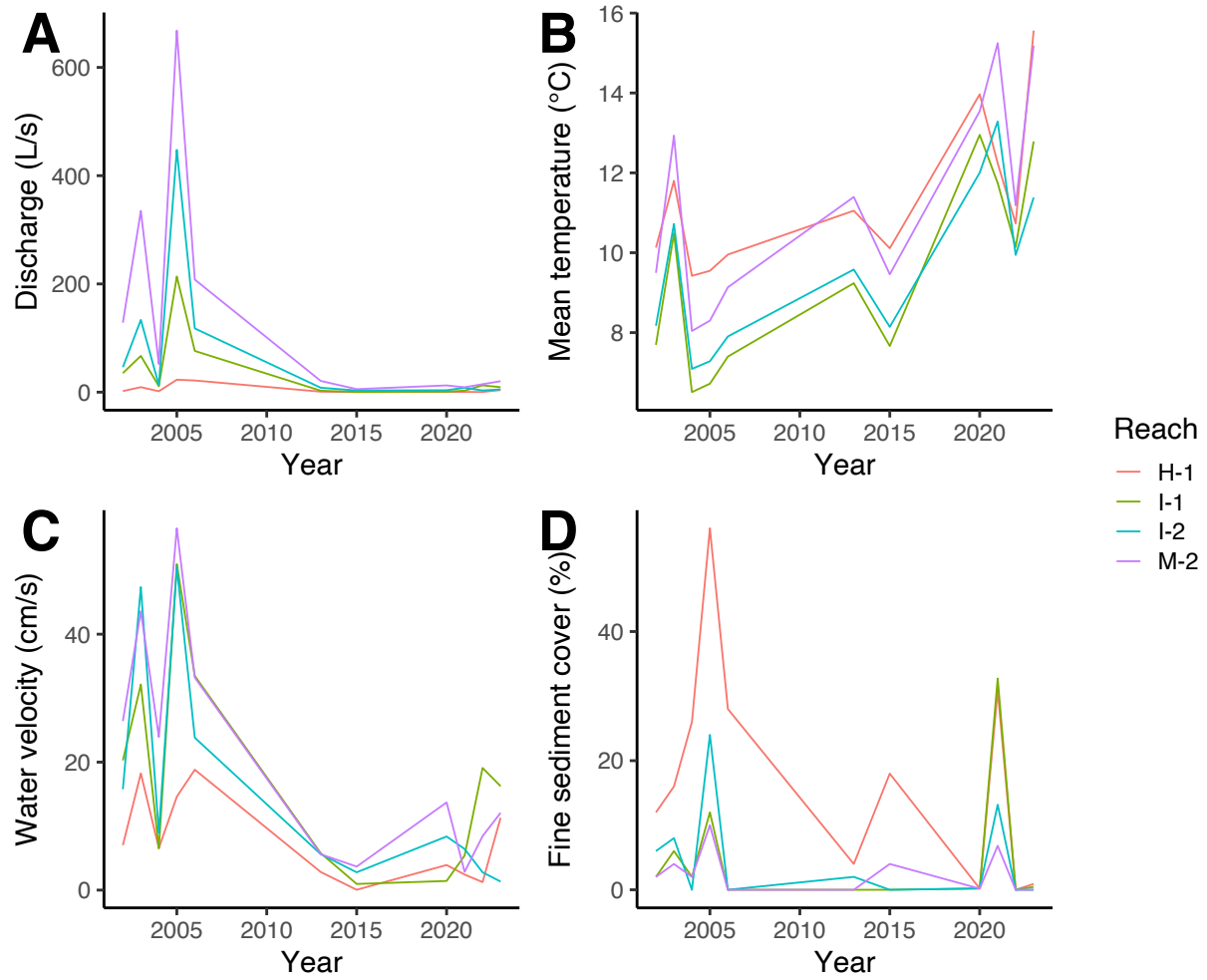
Figure S1. Variation in abiotic mechanisms of drought over time at the reach scale for (A) Discharge, (B) water temperature, (C) water velocity, and (D) fine sediment coverage.
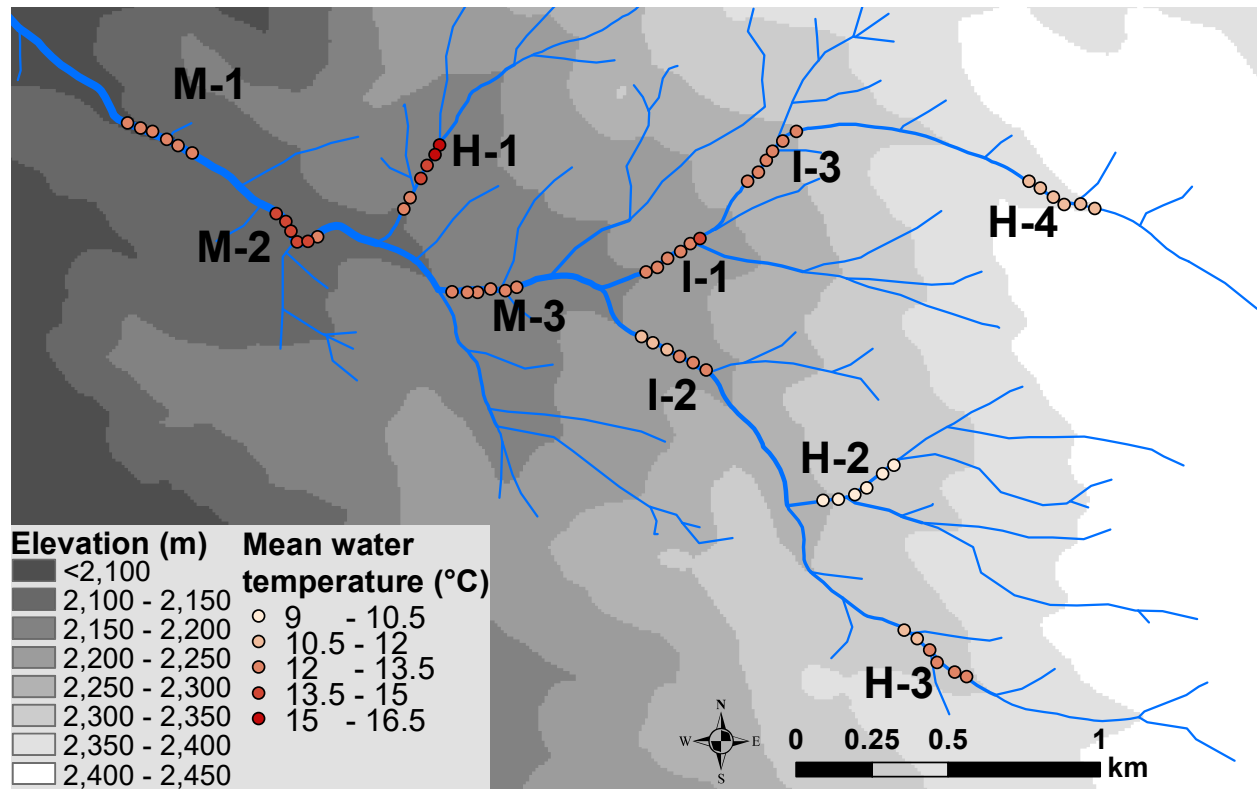
Figure S2. Map of microhabitat mean temperature in 60 sampled sites from 2020. Mean water temperature is the average temperature of the 30 days prior to sampling in 2020. Sites are moved slightly from their actual positions to avoid overlap; see Leathers et al. 2023 for actual map of locations.

Figure S3. Map of microhabitat water velocity in 60 sampled sites from 2020. Sites are moved slightly from their actual positions to avoid overlap; see Leathers et al. 2023 for actual map of locations.

Figure S4. Map of microhabitat fine sediment coverage in 60 sampled sites from 2020. Sites are moved slightly from their actual positions to avoid overlap; see Leathers et al. 2023 for actual map of locations.

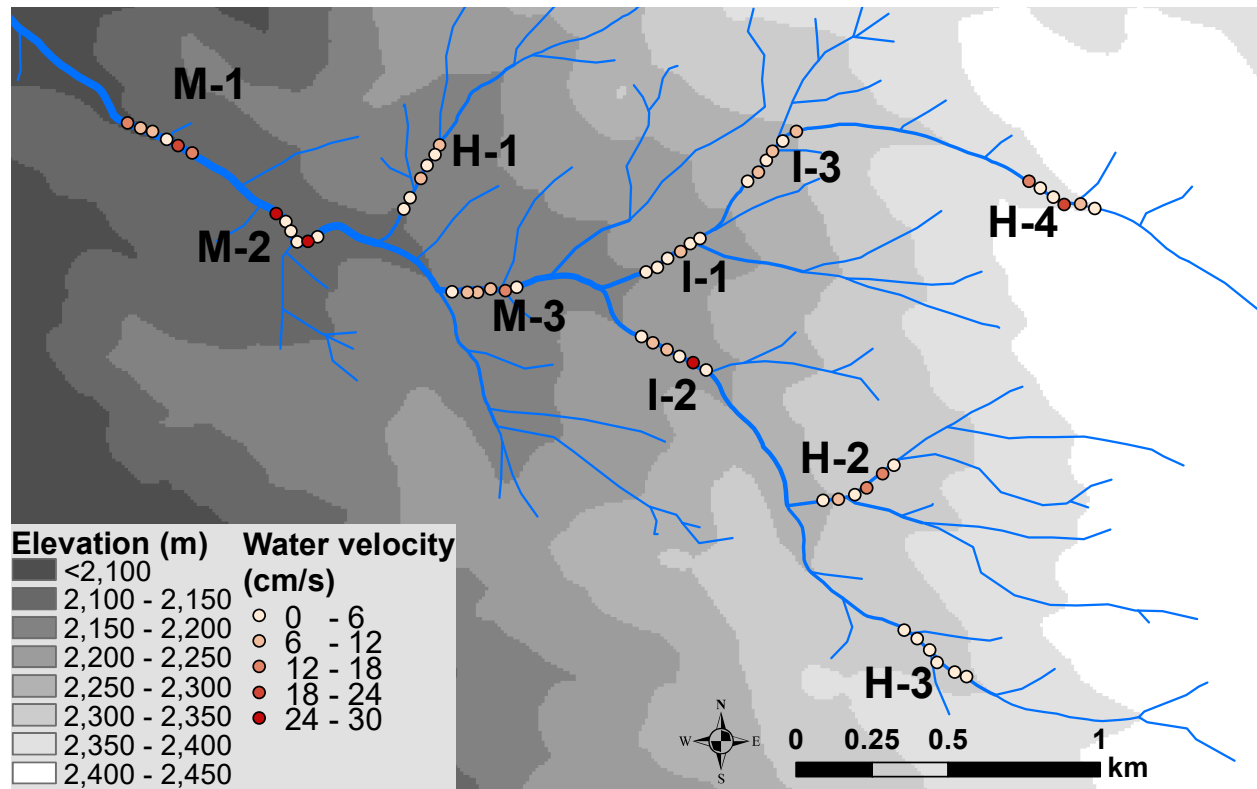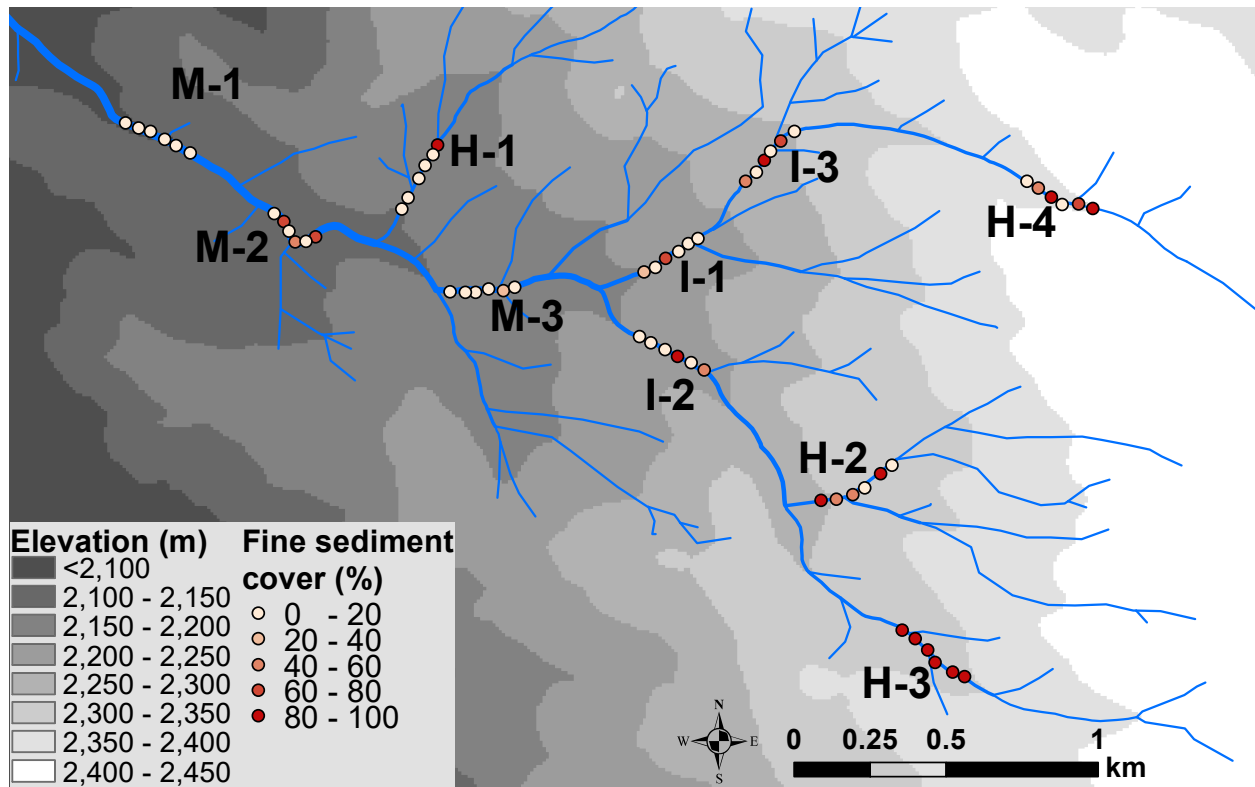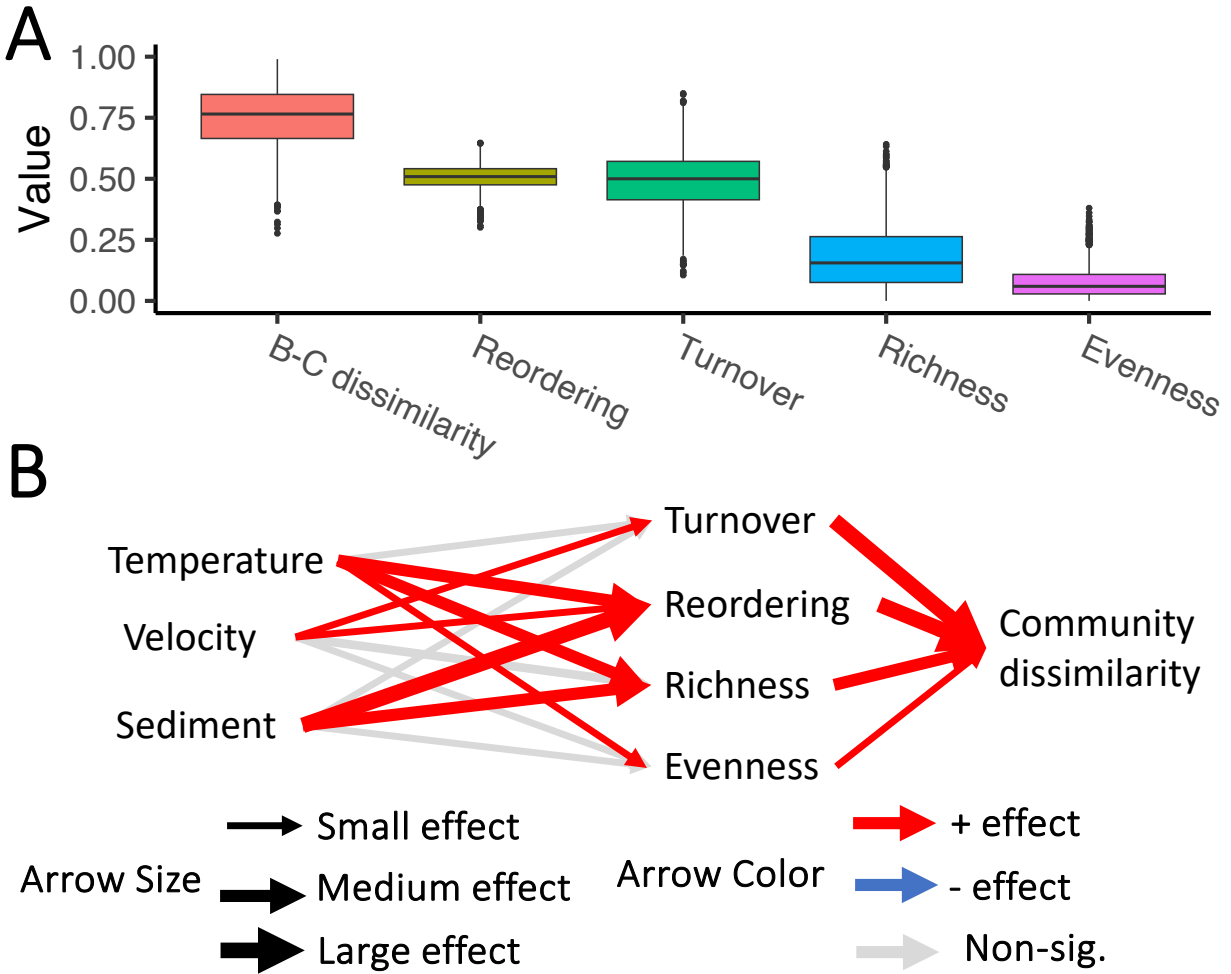**Figure S5.** (A) Microhabitat variance of rank abundance curve components and Bray-curtis dissimilarity. Reordering values are multiplied by 2 to make the range of possible values 0-1 like for all metrics. For the boxplot, the central band is the median, the box is the interquartile range, whiskers are 1.5 times the interquartile range, and circles are outliers. (B) We explained Bray-curtis community dissimilarity using a piecewise structural equation model with abiotic mechanisms and biotic mechanisms as explanatory variables. The model consisted of models that explained each rank abundance curve component by abiotic mechanisms and a model of Bray-curtis dissimilarity explained by rank abundance curve components. Differences in spatial scale (reach vs. microhabitat) affected our results, as abiotic mechanisms of drought explained community dissimilarity through more diverse pathways at the finer scale. At the microhabitat scale, water temperature, water velocity, and sediment affected all biotic pathways in aggregate, rather than only sediment being significant at the reach scale. Even looking specifically at sediment, it was a significant covariate for richness and reordering at the microhabitat scale, opposite of the reach scale model where it explained differences in turnover and evenness. All biotic pathways significantly explained community dissimilarity at the microhabitat scale contrary to only turnover at the reach scale.

Table S1. Spatial and temporal variance explained by abiotic mechanisms in aggregate and autocorrelation for the most common taxa of the study. Variance explained by abiotic mechanisms is the aggregate of all mechanisms. Spatial autocorrelation is based on upstream distance and temporal autocorrelation is phi.

Taxa	Spatial variance explained	Temporal variance explained	Spatial autocorrelation	Temporal autocorrelation
Baetis	25.456	28.286	0.200	0.528
Acariformes	19.977	2.480	0.497	0.653
Rheocricotopus	12.564	2.003	0.434	0.151
Zavrelimyia	14.290	42.542	0.000	-0.051
Tanytarsus	4.792	15.952	0.000	0.330
Micropsectra	20.031	12.641	0.692	0.160
Polypedilum	21.872	3.372	0.027	0.358
Thiennemannimyia	4.748	5.282	0.225	0.512
Stempellinella	8.542	16.301	0.604	0.365
Micrasema	29.731	2.849	0.063	0.282
Lepidostoma	19.538	7.064	0.419	0.285
Turbellaria	0.805	9.036	0.217	0.896
Paraleptophlebia	5.827	11.145	0.287	0.564
Oligochaeta	6.047	15.738	0.081	0.064
Serratella	5.451	4.981	0.050	0.038
Sweltsa	18.126	24.261	0.230	0.776
Ameletus	5.803	7.825	0.891	0.480
Optioservus	16.311	36.973	0.038	0.542
Bezzia sensu lato	12.340	20.285	0.798	0.328

Table S2. Abiotic mechanisms of drought as covariates of biotic mechanisms in generalized linear models. Values are standardized effect sizes. * indicates a significant effect at $P < 0.05$. The standardized effect size of microhabitat abiotic mechanisms on biotic pathways were typically much higher than that at the reach scale; the greatest standardized effect size at the microhabitat scale was eight times greater than the maximum reach scale effect size.

Scale	Comparison	Abiotic mechanism	Turnover	Reordering	Richness	Evenness
Reach	Space	Mean temperature	0.126	-0.022	0.687	0.196
Reach	Space	Water velocity	-0.584	-0.139	-0.741	0.656
Reach	Space	Fine sediment	2.341 *	1.632	-1.82	1.337
Reach	Time	Mean temperature	3.01 *	3.84 *	0.159	0.947
Reach	Time	Water velocity	3.236 *	1.769	-1.85	0.484
Reach	Time	Fine sediment	0.395	-1.539	-0.018	-0.774
Reach	Space-Time	Mean temperature	3.478 *	4.595 *	0.557	-0.007
Reach	Space-Time	Water velocity	5.385 *	0.509	-3.301 *	3.512 *
Reach	Space-Time	Fine sediment	2.979 *	0.567	-1.768	0.021
Micro habitat	Space	Mean temperature	0.973	10.818 *	10.899 *	2.36 *
Micro habitat	Space	Water velocity	7.234 *	6.876 *	-1.287	0.075
Micro habitat	Space	Fine sediment	0.609	16.612 *	9.604 *	-0.156

Table S3. Variation in community dissimilarity (Bray Curtis) explained by biotic mechanisms. Values are partial eta squared to determine which RAC components best explain dissimilarity. * indicates a significant effect at $P < 0.05$. Bolded values have the highest partial eta squared for their comparison group. Reordering ($\eta_p^2 = 0.218$, $P < 0.001$) had the greatest effect on community dissimilarity at the microhabitat scale. Tests in this table agreed with the findings of the pSEM models, with one exception; reordering did not explain community dissimilarity in spatial comparisons in the pSEM model, although it was significant in the simpler, individual model.

Scale	Comparison	RAC component	Partial eta squared
Reach	Space	Turnover	0.080 *
Reach	Space	Reordering	0.044 *
Reach	Space	Richness	0.009
Reach	Space	Evenness	0.00
Reach	Time	Turnover	0.134 *
Reach	Time	Reordering	0.180 *
Reach	Time	Richness	0.038 *
Reach	Time	Evenness	0.002
Reach	Space-Time	Turnover	0.137 *
Reach	Space-Time	Reordering	0.174 *
Reach	Space-Time	Richness	0.050 *
Reach	Space-Time	Evenness	0.002
Microhabitat	Space	Turnover	0.064 *
Microhabitat	Space	Reordering	0.218 *
Microhabitat	Space	Richness	0.046 *
Microhabitat	Space	Evenness	0.064 *

5

Conclusion

My dissertation supports that climate change effects on low flows in Sierra Nevada streams will be pervasive, but environmental context is critical to understand how ecological impacts arise. The new insights made here, via a combination of field experiments, modeling, and long-term observation, help identify which mechanisms connecting drought to stream ecosystem dynamics should be examined in more detail going forward. Although flow intermittency may have greater impacts on stream communities than changes in flow magnitude, the latter is projected to occur in mountain ranges globally. These shifts in flow magnitude are poised to alter ecosystem dynamics, community composition, phenology, and food-webs.

I began my dissertation by experimentally simulating future low flow patterns in mountain streams. I found that reduced thermal buffering can raise water temperatures drastically, with pervasive effects on primary production, benthic production, and aquatic-terrestrial subsidies. Resulting phenological shifts altered key ecosystem processes such as aquatic-terrestrial subsidies, ecosystem metabolism, and secondary production. Next, I combined high-frequency temperature sensors and advanced spatiotemporal models to estimate the thermal vulnerability of a Sierra Nevada watershed. Thermal sensitivity of water to air temperature varied at fine temporal scales and variation occurred spatially at the reach scale. Models of current thermal habitat, combined with measured thermal sensitivity and projected future air temperatures, enabled end-of-century thermal distribution estimates. These projections illustrate that coldwater habitat will decline substantially. Lastly, I conducted extensive observational sampling of a Sierra Nevada watershed and found that different abiotic mechanisms of drought were all influential on macroinvertebrate species, although their effects differed when compared across space vs. time. Biotic community differences across space and time also contrasted, leading to the overall ecological pathway connecting drought to community change to be separate between space and time. This challenges the space-for-time substitution approach that underlies much climate change ecology research

A major finding of my dissertation is that riverine ecosystems must be studied at appropriate spatiotemporal scales to obtain accurate and useful inferences about drought responses. In Chapter 2, I documented fine-scale temporal changes in phenology and secondary production. These changes would be missed if only two time periods were compared (e.g., before vs after surpassing a certain flow threshold), or if results were averaged across the season. Results from Chapter 3 support that the common aggregation of temperature data from months to seasons can miss daily fluctuations in thermal sensitivity that are short-lived but ecologically important (e.g., effects from transient, extreme events like storms and wildfires). Chapter 4 highlighted that low flow has stronger impacts on communities at the microhabitat spatial scale compared to the more commonly-used reach scale; additionally, space-for-time substitution was not supported so the effects of low flow should be examined separately over space and time. The discrepancy between the predicted loss in coldwater taxa due to warming from Chapter 3 and the observed positive effect of temperature spatially in Chapter 4 could also be due to differences in

scale. I used CD75 thermal thresholds derived from broad regional occurrence data in Chapter 3 that may suggest a thermal relationship that is absent at finer spatial scales, such as that in Chapter 4. Studying environmental responses at appropriate spatio-temporal scales has long been a quest in ecology (Levin 1992, Wiley et al. 1997) and river science (Dong et al. 2017, Palmer and Ruhi 2019); this work adds nuance and mechanism to its continued importance.

Although climate change is expected to increase the extinction risks of species, intensify extreme climate events, and threaten the livelihoods and health of people (Calvin et al. 2023), my dissertation suggests that some taxa and ecosystem processes may benefit from advanced low flows in Sierra Nevada streams. Chapter 2 found that cross-ecosystem subsidies may increase in pulse magnitude due to advanced Chironomini emergence and riparian predators gain access to benthic macroinvertebrates in climate change-altered low flows. Chapter 4 observed that taxa were more likely to benefit from low flows than high flows, and taxa abundance tended to have a positively biased relationship with water temperature, even if increased fine sediment could be harmful. However, coldwater specialist taxa are vulnerable to predicted climate change. Expected increased intermittency threatens taxa that require long hydroperiods, and permanent ice sources feeding alpine streams may melt completely to the detriment of coldwater specialist taxa (Tronstad et al. 2019). Predicted risk associated with climate change is also regularly associated with end of century conditions near 2100, but there is no guarantee that the global climate will stabilize after that policy horizon.

Sierra Nevada communities and ecosystem dynamics may have been more stable than initially anticipated, when exposed to climate change-induced low flows, thanks to species response diversity. Response diversity occurs when organismal responses to environmental change vary in magnitude and/or direction, stabilizing aggregate ecosystem processes (Elmqvist et al. 2003). Communities with high response diversity are more resistant to ecological change, which is of critical importance as anthropogenic environmental threats multiply. In Chapter 2, species varied in their phenological shifts in response to advanced low flow and the most common taxa had high response diversity to change in discharge. In Chapter 4, species had little consistency in how and whether they responded to the abiotic mechanisms of drought. This may have resulted in community shifts associated with low flow occurring primarily via reordering of the relative abundance of taxa rather than change in species richness. In aggregate, these results illustrate that ecosystem processes may often remain stable even if many individual species respond to changing flow regimes–and the physical conditions they control. The observed stability is dependent on maintaining current biodiversity, so other environmental threats must be considered that could threaten species and the response diversity they contribute to.

This dissertation leaves numerous doors open for future work. For example, Sierra Nevada streams face other anthropogenic alterations that may have interactive effects with low flow [e.g., dams (Carlisle et al. 2016), livestock use (Herbst et al. 2012, Holmquist et al. 2015), logging (Banks et al. 2007), and the introduction of fish at historically fishless high elevations (Herbst et al. 2009)]. Synergistic negative effects could occur when low flow and other anthropogenic alterations like livestock grazing both increase sedimentation, which my findings along with others suggest should be a restoration priority (Herbst et al. 2012). Restoration efforts and management decisions will be most effective when these interactions are understood and both the areas of greatest risk and habitat with the best likelihood of improvement can be

identified. One promising avenue to assess habitat is the increasing prevalence of LIDAR data in the Sierra Nevada (Hooshyar et al. 2015). Aircraft LIDAR data could reveal fine-scale channel morphology and how it changes over time, improving the accuracy of hydrologic models that are least accurate in small headwaters (Andualem et al. 2024). Satellite infrared technology may also improve to measure finer scales of water temperature in small streams and identify areas with groundwater influence (Fakhari et al. 2023). If macroinvertebrates are largely driven by conditions at fine scales, then models should capture microhabitat features. Even if physical habitat conditions are adequately captured, understanding biotic responses will require greater knowledge of aquatic macroinvertebrate life histories and traits to accurately predict not just their exposure but also their vulnerability and adaptive capacity.

Researchers can better understand the ecological impacts of climate change if effort is funneled towards (i) improving our knowledge of species dispersal, as current traits are often inaccurate (Lancaster et al. 2024); and (ii) learning the distributions of macroinvertebrates within the Sierra Nevada (but see Meyer and McCafferty 2008, Mendez et al. 2019). Both of these sources of information are needed for accurate metapopulation models that could anticipate if species can disperse to suitable habitat as climate change takes place. The advent of eDNA measurements may allow more extensive occurrence data to be collected in pursuit of determining distributions, but collaboration between taxonomists and geneticists is needed to ensure accuracy, as eDNA-based methods still require substantial improvement (Pfrender et al. 2010, Emmons et al. 2023). If eDNA-based identification from water samples becomes reliable for most taxa, then sufficient funding and collaboration with community organizations can promote voluntarily collected samples from citizens. These efforts can build off of existing programs like CALeDNA in California that freely provide eDNA samples to citizens to use and send for analysis (Meyer et al. 2021). Accurate distributions are especially needed for the endemic species of the Sierra Nevada, of which there are many, and coldwater specialists with limited distributions (Erman 1996). Understanding species resistance to low-flow conditions is also valuable at metapopulation scales. However, it is uncertain to what extent interpopulation variation exists in resistance traits, and whether that trait variation is inheritable or phenotypic (plastic). Obtaining locally-relevant information on these biological factors could greatly inform climate risk assessments (Stoks et al. 2014).

Climate change will continue to alter global air temperature and precipitation patterns, affecting stream flow regimes and the abiotic conditions they control (Calvin et al. 2023). My dissertation shows how longer, advanced low flows arising from climate change will alter mountain stream ecosystem structure and dynamics in complex and sometimes subtle ways. Carefully designed experiments and field studies, complemented by advancements in high-frequency sensing and time-series modeling methods, were used to uncover the ways and context in which river ecosystems change. This dissertation contributes to a larger literature of drought ecology that must be considered collectively to progress in understanding this global driver of ecological change.

References

Andualem, T. G., S. Peters, G. A. Hewa, B. R. Myers, J. Boland, and D. Pezzaniti. 2024. Channel morphological change monitoring using high-resolution LiDAR-derived DEM

and multi-temporal imageries. Science of The Total Environment 921:171104.

Banks, J. L., J. Li, and A. T. Herlihy. 2007. Influence of clearcut logging, flow duration, and season on emergent aquatic insects in headwater streams of the Central Oregon Coast Range. Journal of the North American Benthological Society 26:620–632.

Calvin, K., D. Dasgupta, G. Krinner, A. Mukherji, P. W. Thorne, C. Trisos, J. Romero, P. Aldunce, K. Barrett, G. Blanco, W. W. L. Cheung, S. Connors, F. Denton, A. Diongue-Niang, D. Dodman, M. Garschagen, O. Geden, B. Hayward, C. Jones, F. Jotzo, T. Krug, R. Lasco, Y.-Y. Lee, V. Masson-Delmotte, M. Meinshausen, K. Mintenbeck, A. Mokssit, F. E. L. Otto, M. Pathak, A. Pirani, E. Poloczanska, H.-O. Pörtner, A. Revi, D. C. Roberts, J. Roy, A. C. Ruane, J. Skea, P. R. Shukla, R. Slade, A. Slangen, Y. Sokona, A. A. Sörensson, M. Tignor, D. Van Vuuren, Y.-M. Wei, H. Winkler, P. Zhai, Z. Zommers, J.-C. Hourcade, F. X. Johnson, S. Pachauri, N. P. Simpson, C. Singh, A. Thomas, E. Totin, P. Arias, M. Bustamante, I. Elgizouli, G. Flato, M. Howden, C. Méndez-Vallejo, J. J. Pereira, R. Pichs-Madruga, S. K. Rose, Y. Saheb, R. Sánchez Rodríguez, D. Ürge-Vorsatz, C. Xiao, N. Yassaa, A. Alegría, K. Armour, B. Bednar-Friedl, K. Blok, G. Cissé, F. Dentener, S. Eriksen, E. Fischer, G. Garner, C. Guivarch, M. Haasnoot, G. Hansen, M. Hauser, E. Hawkins, T. Hermans, R. Kopp, N. Leprince-Ringuet, J. Lewis, D. Ley, C. Ludden, L. Niamir, Z. Nicholls, S. Some, S. Szopa, B. Trewin, K.-I. Van Der Wijst, G. Winter, M. Witting, A. Birt, M. Ha, J. Romero, J. Kim, E. F. Haites, Y. Jung, R. Stavins, A. Birt, M. Ha, D. J. A. Orendain, L. Ignon, S. Park, Y. Park, A. Reisinger, D. Cammaramo, A. Fischlin, J. S. Fuglestvedt, G. Hansen, C. Ludden, V. Masson-Delmotte, J. B. R. Matthews, K. Mintenbeck, A. Pirani, E. Poloczanska, N. Leprince-Ringuet, and C. Péan. 2023. IPCC, 2023: Climate Change 2023: Synthesis Report. Contribution of Working Groups I, II and III to the Sixth Assessment Report of the Intergovernmental Panel on Climate Change [Core Writing Team, H. Lee and J. Romero (eds.)]. IPCC, Geneva, Switzerland. First. Intergovernmental Panel on Climate Change (IPCC).

Carlisle, D. M., S. M. Nelson, and J. May. 2016. Associations of stream health with altered flow and water temperature in the Sierra Nevada, California. Ecohydrology 9:930–941.

Dong, X., A. Ruhí, and N. B. Grimm. 2017. Evidence for self-organization in determining spatial patterns of stream nutrients, despite primacy of the geomorphic template. Proceedings of the National Academy of Sciences of the United States of America 114:E4744–E4752.

Elmqvist, T., C. Folke, M. Nystrom, G. Peterson, J. Bengtsson, B. Walker, and J. Norberg. 2003. Response diversity, ecosystem change, and resilience. Frontiers in Ecology and the Environment 1:488–494.

Emmons, S. C., Z. G. Compson, M. C. Malish, M. H. Busch, V. Saenz, K. T. Higgins, and D. C. Allen. 2023. DNA metabarcoding captures different macroinvertebrate biodiversity than morphological identification approaches across a continental scale. Environmental DNA 5:1307–1320.

Erman, N. 1996. Status of aquatic invertebrates. Sierra Nevada ecosystem project: final report to

Congress 2:987–1008.

Fakhari, M., J. Raymond, R. Martel, J.-P. Drolet, S. J. Dugdale, and N. Bergeron. 2023. Analysis of Large-Scale Groundwater-Driven Cooling Zones in Rivers Using Thermal Infrared Imagery and Radon Measurements. Water 15:873.

Herbst, D. B., M. T. Bogan, S. K. Roll, and H. D. Safford. 2012. Effects of livestock exclusion on in-stream habitat and benthic invertebrate assemblages in montane streams: Stream recovery and livestock grazing exclusion. Freshwater Biology 57:204–217.

Herbst, D. B., E. L. Silldorff, and S. D. Cooper. 2009. The influence of introduced trout on the benthic communities of paired headwater streams in the Sierra Nevada of California. Freshwater Biology 54:1324–1342.

Holmquist, J. G., J. Schmidt-Gengenbach, and J. W. Roche. 2015. Stream Macroinvertebrates and Habitat Below and Above Two Wilderness Fords Used by Mules, Horses, and Hikers in Yosemite National Park. Western North American Naturalist 75:311–324.

Hooshyar, M., S. Kim, D. Wang, and S. C. Medeiros. 2015. Wet channel network extraction by integrating LiDAR intensity and elevation data. Water Resources Research 51:10029–10046.

Lancaster, J., B. J. Downes, and Z. J. Kayll. 2024. Bigger is not necessarily better: empirical tests show that dispersal proxies misrepresent actual dispersal ability. Proceedings of the Royal Society B: Biological Sciences 291:20240172.

Levin, S. A. 1992. The problem of pattern and scale in ecology. Ecology 73:1943–1967.

Mendez, P. K., M. J. Myers, J. E. Damerow, C. Lew, and V. H. Resh. 2019. Species occurrence and distribution of Trichoptera (caddisflies) in California. Zoosymposia 14:113–133.

Meyer, M. D., and W. P. McCafferty. 2008. Mayflies (Ephemeroptera) of the Far Western United States. Part 3: California. Transactions of the American Entomological Society 134:337–430.

Meyer, R. S., M. M. Ramos, M. Lin, T. M. Schweizer, Z. Gold, D. R. Ramos, S. Shirazi, G. Kandlikar, W.-Y. Kwan, E. E. Curd, A. Freise, J. M. Parker, J. P. Sexton, R. Wetzer, N. D. Pentcheff, A. R. Wall, L. Pipes, A. Garcia-Vedrenne, M. P. Mejia, T. Moore, C. Orland, K. M. Ballare, A. Worth, E. Beraut, E. L. Aronson, R. Nielsen, H. A. Lewin, P. H. Barber, J. Wall, N. Kraft, B. Shapiro, and R. K. Wayne. 2021. The CALeDNA program: Citizen scientists and researchers inventory California's biodiversity. California Agriculture 75:20–32.

Palmer, M., and A. Ruhi. 2019. Linkages between flow regime, biota, and ecosystem processes: Implications for river restoration. Science 365.

Pfrender, M. E., C. P. Hawkins, M. Bagley, G. W. Courtney, B. R. Creutzburg, J. H. Epler, S. Fend, L. C. Ferrington, P. L. Hartzell, S. Jackson, D. P. Larsen, C. A. Lévesque, J. C. Morse, M. J. Petersen, D. Ruiter, D. Schindel, and M. Whiting. 2010. Assessing Macroinvertebrate Biodiversity in Freshwater Ecosystems: Advances and Challenges in DNA-based Approaches. The Quarterly Review of Biology 85:319–340.

Stoks, R., A. N. Geerts, and L. De Meester. 2014. Evolutionary and plastic responses of freshwater invertebrates to climate change: Realized patterns and future potential. Evolutionary Applications 7:42–55.

Tronstad, L. M., S. Hotaling, J. Joseph Giersch, O. J. Wilmot, and D. S. Finn. 2019. Headwaters fed by subterranean ice: Potential climate refugia for mountain stream communities? bioRxiv 80:395–407.

Wiley, M. J., S. L. Kohler, and P. W. Seelbach. 1997. Reconciling landscape and local views of aquatic communities: Lessons from Michigan trout streams. Freshwater Biology 37:133–148.